

เอสเทอร์ฟิเคชันแบบวิวิธพันธุ์ของกรดไขมันอิสระโดยใช้ตัวเร่งปฏิกิริยา
เบสอีทีเอส-10 แลกเปลี่ยนไอออน



นางสาวศิริมา จินปฏิพัทธ์

สถาบันวิทยบริการ
จุฬาลงกรณ์มหาวิทยาลัย

วิทยานิพนธ์นี้เป็นส่วนหนึ่งของการศึกษาตามหลักสูตรปริญญาวิทยาศาสตรมหาบัณฑิต

สาขาวิชาปิโตรเคมี และวิทยาศาสตร์พอลิเมอร์

คณะวิทยาศาสตร์ จุฬาลงกรณ์มหาวิทยาลัย

ปีการศึกษา 2550

ลิขสิทธิ์ของจุฬาลงกรณ์มหาวิทยาลัย

HETEROGENEOUS ESTERIFICATION OF FREE FATTY ACIDS USING
ION EXCHANGED ETS-10 BASE CATALYST



Miss Sirima Jeenpatiphat

สถาบันวิทยบริการ
จุฬาลงกรณ์มหาวิทยาลัย

A Thesis Submitted in Partial Fulfillment of the Requirements
for the Degree of Master of Science Program in Petrochemistry and Polymer Science

Faculty of Science

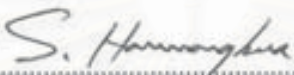
Chulalongkorn University

Academic Year 2007

Copyright of Chulalongkorn University

Thesis Title HETEROGENEOUS ESTERIFICATION OF FREE
 FATTY ACIDS USING ION EXCHANGED ETS-10
 BASE CATALYST
By Miss Sirima Jeenpatiphat
Field of Study Petrochemistry and Polymer Science
Thesis principal Advisor Duangamol Nuntasri, Ph.D.

Accepted by the Faculty of Science, Chulalongkorn University in Partial
Fulfillment of the Requirements for the Master's Degree


.....Dean of the Faculty of Science
(Professor Supot Hannongbua, Ph.D.)


THESIS COMMITTEE


.....Chairperson
(Professor Pattarapan Prasassarakich, Ph.D.)


.....Thesis principal Advisor
(Duangamol Nuntasri, Ph.D.)


.....Member
(Associate Professor Wimonrat Trakarnpruk, Ph.D.)


.....Member
(Assistant Professor Warinthorn Chavasiri, Ph.D.)


.....External member
(Kunn Kangvansaichol, Ph.D.)

ศิริมา จินปฏิพัทธ์ : เอสเทอร์ฟิเคชันแบบวิวิธพันธุ์ของกรดไขมันอิสระโดยใช้ตัวเร่งปฏิกิริยาเบสอีทีเอส-10 แลกเปลี่ยนไอออน. (HETEROGENEOUS ESTERIFICATION OF FREE FATTY ACIDS USING ION EXCHANGED ETS-10 BASE CATALYST) อ. ที่ปริกษาวิทยานิพนธ์หลัก: คร. ดวงกมล นันทศรี, 112 หน้า.

ได้สังเคราะห์ตัวเร่งปฏิกิริยาแอนแกลฮาร์ดทิทาโนซิลิเกต-10 (อีทีเอส-10) โดยการตกผลึกที่อุณหภูมิสูง และปราศจากสารคืนแบบอินทรีย์และสารก่อผลึก ได้ศึกษาผลของอัตราส่วนโดยโมลของซิลิกอนไดออกไซด์ต่อไททานเนียมไดออกไซด์ 0.5 ถึง 1.0 ในระบบ $5\text{SiO}_2 \cdot x\text{TiO}_2 \cdot 3\text{NaOH} \cdot \text{KF} \cdot 75\text{H}_2\text{O}$ นอกจากนั้นตัวเร่งปฏิกิริยาที่มีการปรับปรุงด้วยเบส สามารถเตรียมด้วยวิธีการแลกเปลี่ยนไอออนด้วยแอลคาไลน์แคทไอออนหลายชนิด เช่น โซเดียมไฮดรอกไซด์ โพแทสเซียมไฮดรอกไซด์ รูบิเดียมไฮดรอกไซด์และซีเซียมไฮดรอกไซด์โมโนไฮเดรต เพื่อเพิ่มความแรงและตำแหน่งของเบสของตัวเร่งปฏิกิริยา นำผลิตภัณฑ์ที่สังเคราะห์ได้มาตรวจสอบลักษณะเฉพาะด้วยเทคนิคการเลี้ยวเบนของรังสีเอกซ์ การดูดซับแก๊สไนโตรเจน ดิฟฟิวสิวิตีเฟล็กแทนซ์อัลตราไวโอเลต กล้องจุลทรรศน์แบบส่องกราด การคายรังสีจากอะตอมโดยใช้พลาสมาเหนี่ยวนำ และการดูดกลืนรังสีของอะตอม ตัวเร่งปฏิกิริยาที่สังเคราะห์ได้ประกอบด้วยอีทีเอส-10 ที่มีรูปร่างคล้ายสี่เหลี่ยม และขนาดโพรงประมาณ 0.6 นาโนเมตร ตัวเร่งปฏิกิริยาที่เตรียมได้ถูกนำไปประยุกต์กับปฏิกิริยาเอสเทอร์ฟิเคชันของกรดอิสระโอเลอิก ปาล์มติก และลิโนเลอิกกับเมทานอลเพื่อผลิตเมทิลเอสเทอร์ของกรดไขมันอิสระหรือไบโอดีเซล ได้ศึกษาผลของภาวะต่างๆเช่น ปริมาณของตัวเร่งปฏิกิริยา อัตราส่วนโดยโมลของเมทานอลต่อกรดไขมันอิสระ เวลาและอุณหภูมิในการเกิดปฏิกิริยา โดยรูบิเดียมอีทีเอส-10 สามารถเร่งปฏิกิริยาเอสเทอร์ฟิเคชันของทั้งกรดโอเลอิกและปาล์มติก ภาวะที่เหมาะสมในการทำปฏิกิริยา คือ อัตราส่วนโดยโมลของเมทานอลต่อกรดไขมันอิสระเท่ากับ 9 ต่อ 1 อุณหภูมิ 110 ถึง 120 องศาเซลเซียสใช้เวลา 18 ถึง 24 ชั่วโมง ปริมาณตัวเร่งปฏิกิริยาที่ใช้ 10 เปอร์เซ็นต์โดยน้ำหนักและใช้ความเร็วในการหมุน 220 รอบต่อนาที ได้ปริมาณผลิตภัณฑ์เมทิลเอสเทอร์สูงสุดที่ 100 เปอร์เซ็นต์ ได้ศึกษาความว่องไวในการเร่งปฏิกิริยาของตัวเร่งปฏิกิริยาที่ผ่านการใช้งานแล้วและที่ปรับสภาพเหมือนใหม่อีกด้วย

สาขาวิชา วิศวกรรมเคมีและวิทยาศาสตร์พอลิเมอร์ ถายมือชื่อ นิสิต ศิริมา จินปฏิพัทธ์

ปีการศึกษา 2550 ถายมือชื่ออาจารย์ที่ปริกษาวิทยานิพนธ์หลัก ดวงกมล นันทศรี

4972505423: MAJOR PETROCHEMISTRY AND POLYMER SCIENCE

KEY WORD: ETS-10 / HETEROGENEOUS / ESTERIFICATION / BIODIESEL

SIRIMA JEENPATIPHAT: HETROGENEOUS ESTERIFICATION OF FREE FATTY ACIDS USING ION EXCHANGED ETS-10 BASE CATALYST. THESIS PRINCIPAL ADVISOR: DUANGAMOL NUNTASRI, Ph.D., 112 pp.

Engelhard titanasilicate-10 (ETS-10) was synthesized *via* hydrothermal crystallization in the absence of organic template and seed. The influence of $\text{SiO}_2/\text{TiO}_2$ mole ratio of the initial gel on the formation of ETS-10 was examined in system $5\text{SiO}_2: x\text{TiO}_2: 3\text{NaOH}: \text{KF}: 75\text{H}_2\text{O}$, where x was varied between 0.5-1.0. In addition, base-modified ETS-10 could be prepared by ion-exchange method with various alkali cation i.e. NaOH, KOH, RbOH and CsOH·H₂O in order to increase basic site of catalyst. The synthesized materials were characterized by powder X-ray diffraction (XRD), N₂-adsorption/desorption, DR-UV spectroscopy, scanning electron microscopy (SEM), inductively coupled plasma-atomic emission spectroscopy (ICP-AES) and atomic absorption spectrophotometry (AAS) techniques. The synthetic materials are mainly cubic-like particle ETS-10 phase with pore size around 0.6 nm. All synthesized materials were tested their activities in esterification of oleic, palmitic and linoleic acid with methanol to produce fatty acid methyl ester (biodiesel). The various reaction conditions such as catalyst amount, methanol to oil mole ratio including reaction time and temperature were studied. From this study, Rb-ETS-10 was distinguishable in both oleic acid and palmitic acid esterification. The optimum condition is methanol to acid mole ratio 9 to 1, reaction temperature 110-120°C, reaction time 18-24 h, amount of catalyst 10 wt% with stirring speed 200 rpm. The maximum methyl ester yield reached 100% when reaction was carried out under the optimum condition. Moreover, catalytic activities of reused and regenerated Rb-ETS-10 catalysts were also investigated.

Field of Study: Petrochemistry and Polymer Science Student's Signature: Sirima Jeenpatiphat
 Academic year: 2007 Principal Advisor's Signature: Duangamol Nuntasri

ACKNOWLEDGEMENTS

The success of this thesis can be attributed to the extensive support, valuable suggestion and assistance from my thesis advisor, Dr. Duangamol Nuntasri. I deeply thank her for kindness throughout this study.

I would like to give my gratitude to the chairperson, Professor Dr. Pattarapan Prasassarakich and member of this thesis committee, Associate Professor Dr. Wimonrat Trakarnpruk, Assistant Professor Dr. Warinthorn Chavasiri and Dr. Kunn Kangvansaichol, respectively, for all of their kindness and useful advice in the research.

I would like to gratefully thank to the financial support from PTT Public Company Limited. Moreover, I am grateful to Program of Petrochemistry and Polymer Science, Faculty of Science, Chulalongkorn University for the valuable knowledge and experience. I also would like to thank the members of Materials Chemistry and Catalysis Research Unit and my friends for their encouragement and friendship.

Finally, I would like to express my deepest gratitude to my family for their entirely care, understanding and financial support.

สถาบันวิทยบริการ
จุฬาลงกรณ์มหาวิทยาลัย

CONTENTS

	Page
ABSTRACT (THAI).....	iv
ABSTRACT (ENGLISH).....	v
ACKNOWLEDGEMENTS.....	vi
CONTENTS.....	vii
LIST OF TABLES	xii
LIST OF FIGURES	xiv
LIST OF SCHEMES	xvii
LIST OF ABBREVIATIONS.....	xviii
CHAPTER I INTRODUCTION.....	1
1.1 Background.....	1
1.2 Literature review on the ETS-10 catalyst.....	3
1.2.1 Synthesis routes of ETS-10 catalyst.....	3
1.2.2 Modification and application of ETS-10 catalyst.....	6
1.3 Literature reviews on tranesterification and esterification reaction of vegetable oils and free fatty acids.....	8
1.3.1 Catalytic-free in tranesterification and esterification reactions.....	8
1.3.2 Transesterification and esterification over homogeneous catalysts.....	9
1.3.3 Transesterification and esterification over heterogeneous catalysts.....	9
1.4 Objectives.....	12
CHAPTER II THEORY.....	13
2.1 Catalysis.....	13
2.2 Type of catalysts.....	14
2.2.1 Homogeneous catalysts.....	14
2.2.2 Heterogeneous catalysts.....	14
2.3 Porous materials.....	15
2.4 Zeolites molecular sieves.....	16
2.4.1 Uses of zeolite.....	16

	Page
2.4.1.1 Commercial and domestic.....	16
2.4.1.2 Petrochemical industry.....	16
2.5 Titanosilicate materials.....	17
2.6 ETS-10 (Engelhard titanosilicate -10).....	18
2.6.1 Structures of ETS-10.....	18
2.6.2 Properties and application of ETS-10.....	20
2.6.3 Catalytic activity of ETS-10, Na-ETS-10, K-ETS-10, Rb-ETS-10 and Cs-ETS-10 catalysts.....	21
2.7 Modification of catalysts.....	21
2.7.1 Ion-exchange.....	21
2.7.2 Impregnation.....	22
2.8 Free fatty acids (FFAs)	23
2.8.1 Types of fatty acid.....	23
2.8.1.1 Saturated fatty acids.....	23
2.8.1.2 Unsaturated fatty acids.....	24
(a) <i>cis</i> Isomer.....	24
(b) <i>trans</i> Isomer.....	24
2.8.2 Palmitic acid.....	25
2.8.3 Oleic acid.....	26
2.8.4 Linoleic acid.....	26
2.8.5 Fatty acids composition of palm oil.....	26
2.9 Diesel Fuel.....	27
2.9.1 Petroleum diesel.....	27
2.9.1.1 Chemical composition.....	28
2.9.2 Synthetic diesel.....	28
2.9.3 Biodiesel.....	28
2.9.4 Properties of diesel fuels.....	29
2.10 The production of biodiesel.....	30
2.10.1 Direct use and blending.....	30
2.10.2 Thermal cracking (pyrolysis)	30
2.10.3 Transesterification (alcoholysis)	31

	Page
2.10.3.1 Transesterification kinetics and mechanism.....	31
2.10.4 Esterification.....	33
2.10.4.1 Esterification parameters.....	35
(a) Moisture and free fatty acid.....	35
(b) Molar ratio of alcohol to free fatty acid.....	35
(c) Catalyst type and concentration.....	35
(d) Reaction time.....	35
(e) Reaction temperature.....	36
2.11 Characterization of materials.....	36
2.11.1 Powder X-ray diffraction (XRD)	36
2.11.2 N ₂ adsorption-desorption technique.....	37
2.11.3 Diffuse reflectance-ultraviolet spectroscopy (DR-UV)	39
CHAPTER III EXPERIMENTAL.....	41
3.1 Instruments, apparatus and analytical techniques.....	41
3.1.1 Centrifuge.....	41
3.1.2 Oven and furnace.....	41
3.1.3 Powder X-ray diffraction (XRD)	42
3.1.4 Scanning electron microscopy (SEM)	42
3.1.5 Nitrogen adsorption-desorption technique.....	42
3.1.6 Diffuse-reflectance UV-Visible technique (DR-UV).....	42
3.1.7 Inductively coupled plasma-atomic emission spectroscopy (ICP-AES).....	42
3.1.8 Atomic absorption spectroscopy (AAS)	43
3.1.9 Gas chromatography analysis (GC)	43
3.1.10 PARR reactor.....	44
3.2 Chemicals.....	44
3.3 Synthesis of ETS-10 catalysts.....	45
3.4 Alkali ion-exchange modification of ETS-10.....	47
3.5 Standard solution and calibration solution.....	47
3.5.1 Methyl palmitate standard solution.....	47

	Page
3.5.2 Methyl oleate standard solution.....	48
3.5.3 Methyl linoleate standard solution.....	48
3.5.4 Standard calibration solution.....	49
3.6 Esterification of free fatty acids procedure.....	50
3.7 Silylation procedure [ASTM D 6584 and BS EN 14103:2003].....	52
3.8 Parameters affecting esterification reaction.....	52
3.8.1 Effect of catalyst modification method.....	52
3.8.2 Effect of catalyst amount.....	53
3.8.3 Effect of methanol to free fatty acid mol ratio.....	53
3.8.4 Effect of reaction time.....	53
3.8.5 Effect of reaction temperature.....	53
3.8.6 Activity of reuse catalyst.....	53
3.8.7 Activity of Rb-reloaded catalyst.....	53
 CHAPTER IV RESULTS AND DISCUSSIONS.....	 54
4.1 Physical and chemical properties of catalysts.....	54
4.1.1 Powder X-ray diffraction (XRD)	54
4.1.2 Scanning electron microscopy (SEM)	56
4.1.3 N ₂ - adsorption/desorption.....	59
4.1.4 Diffuse-reflectance-ultraviolet spectroscopy (DR-UV)	60
4.1.5 Elemental ratios in ETS-10 catalysts.....	62
4.1.6 Scanning electron microscopy-energy dispersive X-ray (SEM-EDX).....	63
4.2 Standard calibration curve.....	64
4.2.1 Methyl oleate calibration curve.....	64
4.2.2 Methyl palmitate calibration curve.....	65
4.2.3 Methyl linoleate calibration curve.....	66
4.3 Catalytic activity of ETS-10 and alkali-exchanged ETS-10 in esterification reaction of free fatty acid.....	67
4.3.1 Esterification of oleic acid.....	67
4.3.1.1 Catalytic activity of ETS-10 and alkali-exchanged ETS-10.....	67
4.3.1.2 Effect of methanol to oleic mole ratio.....	69

	Page
4.3.1.3 Effect of reaction temperature.....	70
4.3.1.4 Effect of reaction time.....	72
4.3.1.5 Effect of catalyst amount.....	74
4.3.1.6 Effect of stirring speed.....	75
4.3.1.7 Activities of reused and regenerated Rb-ETS-10 catalysts.....	77
4.3.2 Esterification of linoleic acid.....	79
4.3.3 Esterification of palmitic acid.....	79
4.3.3.1 Catalytic activity of ETS-10 and alkali-exchanged ETS-10.....	80
4.3.3.2 Effect of methanol to palmitic acid mole ratio.....	82
4.3.3.3 Effect of reaction temperature.....	84
4.3.3.4 Effect of reaction time.....	85
4.3.3.5 Effect of catalyst amount.....	86
4.3.3.6 Effect of stirring speed.....	88
4.3.3.7 Activities of reused and regenerated Rb-ETS-10 catalysts.....	89
4.4 Proposed esterification mechanism.....	91
4.4.1 Eesterification mechanism for ETS-10.....	91
CHAPTER V CONCLUSION AND SUGGESTION.....	93
REFERENCES.....	95
APPENDICES.....	102
VITAE.....	112

สถาบันวิทยบริการ
จุฬาลงกรณ์มหาวิทยาลัย

LIST OF TABLES

Table		Page
2.1	IUPAC classification of porous materials.....	15
2.2	Saturated fatty acids	23
2.3	Unsaturated fatty acids.....	25
2.4	Typical free fatty acid composition in palm oil.....	27
2.5	Information from powder x-ray diffraction pattern.....	36
2.6	Features of adsorption isotherms.....	38
3.1	Preparation of standard methyl palmitate calibration solution.....	49
3.2	Preparation of standard methyl oleate calibration solution.....	50
3.3	Preparation of standard methyl linoleate calibration solution.....	50
4.1	Some physical properties of calcined ETS-10 and alkali ion-exchanged ETS-10 catalysts.....	60
4.2	Elemental analysis of ETS-10 at various mole of TiO ₂	63
4.3	Elemental contents in fresh and after reaction alkali-exchanged ETS-10 catalysts.....	64
4.4	The catalytic activity of ETS-10 and alkali-exchanged ETS-10 catalysts in esterification reaction of oleic acid.....	68
4.5	The catalytic activity of K-ETS-10 and Rb-ETS-10 catalysts in esterification reaction of oleic acid.....	69
4.6	The catalytic activity of Rb-ETS-10 in the esterification of oleic acid at various ratios of methanol to acid.....	70
4.7	The catalytic activity of Rb-ETS-10 in the esterification of oleic acid at various reaction temperatures.....	71
4.8	The catalytic activity of Rb-ETS-10 in the esterification of oleic acid for different reaction time.....	72
4.9	The catalytic activity of Rb-ETS-10 in the esterification of oleic acid for different reaction time.....	73
4.10	The catalytic activity of Rb-ETS-10 at various catalyst amounts in the esterification of oleic acid.....	74

Table	Page
4.11 The catalytic activity of Rb-ETS-10 at various stirring speeds in the esterification of oleic acid.....	76
4.12 The catalytic activity of reuse and regenerated Rb-ETS-10 catalysts in the esterification of oleic acid.....	77
4.13 The catalytic activity of Rb-ETS-10 in the esterification of linoleic acid.....	79
4.14 Solubility test of palmitic acid in different solvent.....	80
4.15 The catalytic activity of ETS-10 and alkali-exchanged ETS-10 catalysts in esterification reaction of palmitic acid.....	81
4.16 The catalytic activity of K-ETS-10 and Rb-ETS-10 catalysts in esterification reaction of palmitic acid.....	82
4.17 The catalytic activity of Rb-ETS-10 in the esterification of palmitic acid at various ratios of methanol to acid without and with THF co-solvent.....	83
4.18 The catalytic activity of Rb-ETS-10 in the esterification of palmitic acid at various reaction temperatures.....	84
4.19 The catalytic activity of Rb-ETS-10 in the esterification of palmitic acid for different reaction time.....	86
4.20 The catalytic activity of Rb-ETS-10 at various catalyst amounts in the esterification of palmitic acid.....	87
4.21 The catalytic activity of Rb-ETS-10 at various stirring speeds in the esterification of palmitic acid.....	88
4.22 The catalytic activity of reuse and regenerated Rb-ETS-10 catalysts in the esterification of palmitic acid.....	90
A-1 Sodium contents in fresh and after reaction Na-ETS-10 catalyst.....	105
A-2 Potassium contents in fresh and after reaction K-ETS-10 catalyst.....	105
A-3 Rubidium contents in fresh, after reaction and regenerated Rb-ETS-10 catalyst.....	105
A-4 Cesium contents in fresh and after reaction Cs-ETS-10 catalyst.....	105
A-5 EU Specification for automotive diesel.....	109
A-6 Chemical and physical properties of diesel and biodiesel.....	110
A-7 Properties of biodiesel from different oils.....	111

LIST OF FIGURES

Figure	Page
1.1	Thailand diesel oil price [Shell in Thailand].....1
2.1	The potential energy profile of the reaction with and without catalyst.....13
2.2	Structures of some titanosilicate compounds.....17
2.3	Structure of ETS-10. The yellow polyhedra are TiO_6 octahedra running in the <i>a</i> and <i>b</i> directions. The blue polyhedra are SiO_4 tetrahedra forming 12-ring pores. Double pores arise from stacking faults in the inherently disordered material.....19
2.4	Titanosilicate ETS-10 projections: (a) down [110] direction for polymorph B and (b) down [100] direction for polymorph A, Dark TiO_6 octahedral, light grey SiO_4 tetrahedral.....19
2.5	Main clusters in ETS-10, (a) five-membered ring of SiO_4 tetrahedral; (b) two types of dimer of TiO_6 octahedral.....20
2.6	Comparison of the <i>trans</i> isomer and the <i>cis</i> -isomer of oleic acid.....25
2.7	Typical transesterification diagram of triglyceride.....31
2.8	Mechanism of acid catalyzed transesterification reaction.....32
2.9	Mechanism of base catalyzed transesterification reaction.....32
2.10	Typical esterification diagram of free fatty acid.....33
2.11	Mechanism of acid catalyzed esterification of fatty acid.....34
2.12	Mechanism of base catalyzed esterification of fatty acid.....34
2.13	Diffraction of X-rays by a crystal.....37
2.14	The IUPAC classification of adsorption isotherm.....38
2.15	Diffuse reflectance beams in the medium system.....40
3.1	Apparatus for ETS-10 synthesis.....46
3.2	Apparatus for esterification reaction.....51
4.1	XRD patterns of as-synthesized and calcined ETS-10 (\circ represents ETS-10 phase and \bullet represents quartz impurity phase and \blacklozenge represents anatase phase and $*$ for unidentified crystalline phases).....55
4.2	A proposed mechanism of polymerization of silicate species catalyzed by F^- ion.....55

Figure	Page
4.3 XRD patterns of calcined alkali-exchanged ETS-10 (○ represents ETS-10 phase and ◆ represents anatase phase).....	56
4.4 SEM images of ETS-10 synthesized from gel composition 5SiO ₂ : xTiO ₂ : 3NaOH: KF: 75H ₂ O, where x = 1.0 (a), x = 0.75 (b) and x = 0.5 (c).....	57
4.5 SEM images of calcined Na-ETS-10 (a), K-ETS-10 (b), Rb-ETS-10 (c) and Cs-ETS-10 (d).....	58
4.6 DR-UV spectra of calcined ETS-10 synthesized from gel composition 5SiO ₂ : xTiO ₂ : 3NaOH: KF: 75H ₂ O, where x = 1.0 (a), x = 0.75 (b) and x = 0.5 (c).....	61
4.7 DR-UV spectra of calcined Na-ETS-10 (a), K-ETS-10 (b), Rb-ETS-10 (c) and Cs-ETS-10 (d).....	62
4.8 Calibration curve of methyl oleate.....	65
4.9 Calibration curve of methyl palmitate.....	66
4.10 Calibration curve of methyl linoleate.....	67
4.11 The plot of methyl oleate yield using Rb-ETS-10 versus MeOH to oleic acid mole ratio.....	70
4.12 The plot of methyl oleate yield using Rb-ETS-10 versus reaction temperature.....	71
4.13 The plot of methyl oleate yield over Rb-ETS-10 versus reaction time.....	73
4.14 The plot of methyl oleate yield versus catalyst amount of Rb-ETS-10..	75
4.15 The plot of methyl oleate yield versus stirring speed	76
4.16 The plot of methyl oleate yield versus reused and regenerated Rb-ETS-10 catalysts.....	78
4.17 The plot of methyl palmitate yield using Rb-ETS-10 versus MeOH to palmitic acid mole ratio.....	83
4.18 The plot of methyl palmitate yield using Rb-ETS-10 versus reaction temperature.....	85
4.19 The plot of methyl palmitate yield over Rb-ETS-10 versus reaction time.....	86

Figure	Page
4.20 The plot of methyl palmitate yield versus catalyst amount of Rb-ETS-10.....	87
4.21 The plot of methyl palmitate yield using Rb-ETS-10 versus stirring speed.....	89
4.22 The plot of methyl palmitate yield versus catalyst.....	90
4.23 Proposed esterification mechanism for ETS-10.....	91
A-1 N ₂ adsorption-desorption isotherm and pore size distribution of ETS-10 catalyst.....	103
A-2 GC chromatogram of methyl oleate product from esterification reaction.....	106
A-3 GC chromatogram of methyl palmitate product from esterification reaction.....	107
A-4 GC chromatogram of methyl linoleate product from esterification reaction.....	108

LIST OF SCHEMES

Scheme		Page
2.1	Typical reaction	13
3.1	The temperature program for the calcination of ETS-10 catalyst	41
3.2	The temperature program used for GC analysis of fatty acid methyl ester compounds.....	44
3.3	The temperature program for esterification reaction.....	44
3.4	Diagram of ETS-10 synthesis.....	46
3.5	Diagram of esterification reaction of free fatty acids with methanol.....	51
3.6	Diagram of silylation of free fatty acid.....	52



สถาบันวิทยบริการ
จุฬาลงกรณ์มหาวิทยาลัย

LIST OF ABBREVIATIONS

Btu	British thermal unit
K	Kelvin
°C	Degree Celsius
µm	Micrometer
nm	Nanometer
rpm	Rounds per minute
ppm	Part per million
M	Molar
Å	Angstrom unit
CCD	Couple charge detector
eV	Electron volt
R.T.	Room temperature
CCT	Charge transfer
XRD	X-ray diffraction
XPS	X-ray photoelectron spectroscopy
DR-UV	Diffuse reflectance-ultraviolet spectroscopy
CO ₂ -TPD	Carbon dioxide-temperature programmed desorption
NMR	Nuclear magnetic resonance
GC	Gas chromatography
SEM	Scanning electron microscopy
SEM-EDX	Scanning electron microscopy-energy dispersive X-ray fluorescence
ETS-10	Engelhard titanosilicate-10
h	Hour or hours
min	Minute or minutes
wt%	Percent by weight
mole%	Percent by mole
FFAs	Free fatty acids

CHAPTER I

INTRODUCTION

1.1 Background

Majority of the world's energy needs are supplied through petrochemical sources, coal and natural gases. Diesel fuel is the one fraction from crude oil refinery process containing $C_{14} - C_{25}$ that have an essential function in the industrial economy, transportation and agricultural goods. The diesel fuel demand has been increasing as well as the economic growth. The world diesel consumption is about 100 billion liters per year. Currently, about 2.2 million barrels of diesel fuel is consumed everyday in the U.S. road transportation market. Thailand imports more than 100 million liters of foreign oil each year of which 46% is diesel which is the most consumption. Nowadays, the price of diesel fuel in Thailand reached a new high of almost 30 baht per litre as oil traders raised fuel prices in all categories of petroleum and its byproducts by 0.40 baht per litre on the continued rise in global fuel prices. The diesel price in Thailand from 2002-2008 was shown in Figure 1.1.

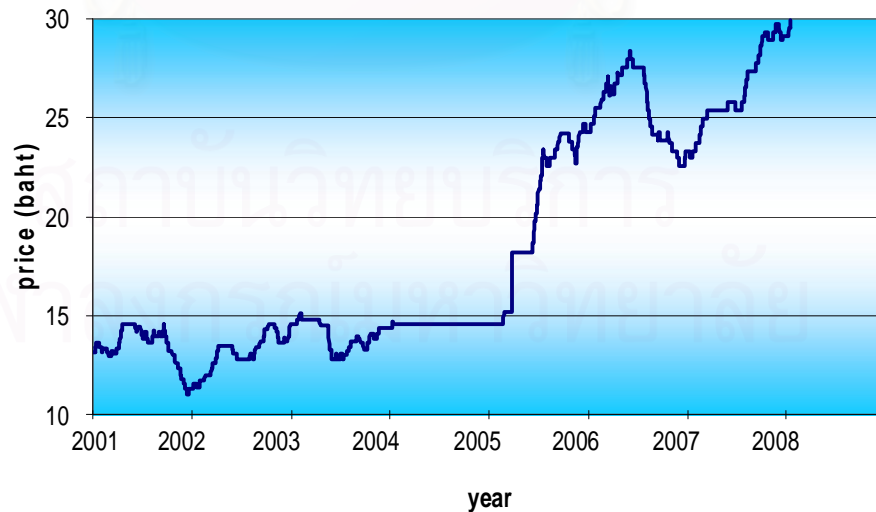


Figure 1.1 Thailand diesel oil price [Shell in Thailand].

As energy demands increase and fossil fuel reserves are limited, research is increasingly directed towards alternative renewable fuels that are environmentally more acceptable. As the calorific value of vegetable oils is comparable to that of diesel, they could be used as fuels in compression ignition engines. However, their direct use in injection diesel engines is problematic mainly due to some of their physical properties, especially their high viscosity. The viscosity of vegetable oils is about ten times higher than that of diesel, with consequent poor fuel atomization, incomplete combustion, carbon deposition on the injectors and valve seats, and fuel build-up in the lubricant oils. This can, therefore, cause serious engine deterioration, hence, it is absolutely necessary to subject the vegetable oils to treatments that diminish the viscosity. The commonly employed methods for reducing the viscosity of vegetable oils are blending with diesel, emulsification, pyrolysis, cracking and transesterification. Among these, the transesterification of vegetable oils to methyl esters appears to be the best method. These methyl esters, better known as biodiesel, are characterized by excellent properties as diesel engine fuels and thus can be used in compression-ignition (diesel) engines with little or no modifications. Biodiesel not only has proper viscosity, boiling point, and high cetane number, but also is simple to use, biodegradable, nontoxic, and essentially free of sulfur and aromatics [1-3].

The definitions of biodiesel is a mixture of vegetable oil and fossil diesel, while others take into account only mixtures of alkyl esters of vegetable oils or animal fats and diesel. The definition adopted by the Brazilian Biodiesel Programme is a fuel obtained from mixtures, in different proportions, of fossil diesel and alkyl esters of vegetable oils or animal fats. Technically speaking, biodiesel is the alkyl ester of fatty acids, made by the transesterification of oils or fats, from plants or animals and esterification of free fatty acid with short chain alcohols such as methanol and ethanol. Glycerine is, consequently, a by-product from biodiesel production [4].

Mostly, biodiesel is prepared from oil feedstocks like soybean oil, rapeseed oil, sunflower oil, palm oil, and animal fat which are comprised of complicate mixtures of triglycerides, TGs (the esters of glycerol with three chains of aliphatic or olefinic FFAs of variable carbons length) and other minor components, such as free fatty acids (FFAs), gums, waxes, etc. Biodiesel is usually made through a chemical processes

called transesterification and esterification reaction, whereby triglycerides and free fatty acid react with low molecular weight alcohols, typically methanol or ethanol in the presence of catalyst to produce a complex mixture of fatty acid alkyl esters (biodiesel). Catalysts used for the esterification of free fatty acids are classified as homogeneous catalyst, enzyme [5-6] or heterogeneous catalyst, but conventional processing mostly involves an alkali catalyzed process. Because base catalyzed process is less corrosive than the homogeneous acid catalyzed one and proceeds at higher rate. The alkali catalysts including sodium hydroxide, sodium methoxide, potassium hydroxide and potassium methoxide, etc. are effective [7]. However, the alkali catalyst is unsatisfied for low cost high free fatty acid feedstocks due to soap formation. Pretreatment processes using strong acid catalysts have been shown to provide good conversion yields and high quality final products. These techniques have even been extended to allow biodiesel production from feedstocks like soapstock that are often considered to be waste. Even though, homogeneous catalyzed biodiesel production processes are relatively fast and show high conversions with minimal side reactions, they are still not very cost competitive with petrodiesel ones because the catalyst cannot be recovered and must be neutralized at the end of the reaction. Moreover, the processes are very sensitive to the presence of water and FFAs (Free Fatty Acids).

ETS-10 is one of heterogeneous basic catalysts which are interesting in esterification reaction of free fatty acids to produce biodiesel because of their structure associated two minus charges per octahedral Ti site, leading to basic catalyst applications and containing suitable pore size 0.83 Å (12-membered ring) for changing free fatty acids to their methyl esters.

1.2 Literature reviews on the ETS-10 catalyst

1.2.1 Synthesis routes of ETS-10 catalyst

In the recent year the interest in new zeolite has increased. Some of these materials possess improved catalytic properties in comparison with the classical aluminosilicates. Subsequently, the study of ETS-10 titanium and silicon-based molecular sieve was deepened. Many studies have been carried out to synthesize

highly pure ETS-10 materials. In the synthesis routes of ETS-10, many parameters were concerned.

In the synthesis routes of ETS-10, many parameters were concerned such as titanium source, quantity of TiO_2 in the initial gel, the influence of initial pH on the two phases, fluoride ions, content of water, Na^+ and K^+ ions in the synthesis gel, $\text{SiO}_2/\text{TiO}_2$ molar ratios, synthesis time and temperature on the crystallization of ETS-10. Vuono, D *et al.* reported the determination of crystallization fields for both ETS-4 and ETS-10 from gels of the composition $x\text{Na}_2\text{O} : 0.6\text{KF} : y\text{TiO}_2 : 1.28x\text{HCl} : 1.49\text{SiO}_2 : 39.5\text{H}_2\text{O}$ with $0.5 \leq x \leq 2.5$ and $0.1 \leq y \leq 0.4$. It is shown that the crystallization field of ETS-10 is quite small. The optimal initial pH is 11.7. The formation of ETS-4 is much easier, and its crystallization field is much broader. The optimal M^+/Ti ($\text{M} = \text{Na}$ or K) ratio is equal to 3 for ETS-4 and 2 for ETS-10. It is emphasized that the cheap TiCl_4 reactant can lead to highly crystalline ETS-4 and ETS-10 samples [8].

In 1989, Kuznicki, S. M. [9] studied the synthesis of ETS-10 by using TiCl_3 as the titanium source and in presence of ETS-10 seed. The varied temperature of crystallization was about 100°C to 175°C for a period of time 12 hours to 15 days and the pH of reaction mixture within range of 9.9 to 10.3.

In 1994, Valtchev, V. *et al.* [10] studied the synthesis of ETS-10 catalyst from titanosilicate gels in the presence of an organic template tetramethylammoniumchloride (TMACl). The aim of the research was to investigate the influence of tetramethylammonium (TMA) on crystallization kinetic of ETS-10. The hydrothermal synthesis was carried out using gels of the following molar composition $40\text{R} : 52\text{Na}_2\text{O} : 42\text{K}_2\text{O} : 20\text{TiO}_2 : 100\text{SiO}_2 : 7030\text{H}_2\text{O}$ where R was TMACl at temperatures of 160, 180, and 200°C . The presence of TMA diminished the nucleation time and accelerated the crystal growth. Moreover, the incorporation of TMA in the channel system of titanium silicate changed the crystal morphology of ETS-10.

However, the involvement of organic template in catalysts is environmentally undesirable and removal of occluded templates by calcinations may

potentially damage the framework of ETS-10. Then in 1996, Sivasanker, S. *et al.* [11] reported the synthesis of ETS-10 over very short reaction time (<16 h) using TiCl_4 as the titanium source in the absence of organic template. The hydrothermal synthesis was carried out with a gel of following molar composition $3.70\text{Na}_2\text{O}: 0.95\text{K}_2\text{O}: \text{TiO}_2: 5.71\text{SiO}_2: 171\text{H}_2\text{O}$ and the crystallization were carried out at 473 K with stirrer speed of 300 rpm for 14-16 h. In this synthesis, highly crystalline nearly uniform cuboids of < 1 μm were obtained without any detectable impurity of ETS-4.

In 1998, Anderson, M. W. *et al.* [12] investigated the hydrothermal synthesis conditions to afford pure and high crystalline ETS-10 from TiCl_3 and TiO_2 (anatase). The influence effect of fluoride ions, temperature, pH of parent gel, sodium and potassium cations, seed and crystallization time have been studied. The optimum temperature and time were 230°C , 15 h (TiCl_3) and 24 h (anatase), respectively. The crystal size of ETS-10 was ranging from 0.5 μm (anatase route) to 25 μm (TiCl_3 route). The first step in TiCl_3 synthesis was the formation of a silica-titania gel which then transforms into ETS-10 and the rate-limiting step of TiO_2 route was the slow dissolution of anatase followed by condensation with silicate species. Seeding with good quality ETS-10 was important when the precursor was TiCl_3 , but this was not when anatase was used.

In 2001, Paillaud, J. L. *et al.* [13] were interested in synthesis of ETS-10 using titanium (IV) fluoride and P25 (a mixture of anatase and rutile) as the titanium source. Pure ETS-10 was obtained with TiF_4 by heating at 200°C for 168 h both with and without organic additive, whereas pure ETS-10 was obtained with P25 at 200°C for 42 h. The influence of fluoride ion, crystallization time, and organic additive were also studied. Small, loosely aggregated ETS-10 crystals up to 1 μm were obtained with P25. The amorphous TiO_2 contaminate was confirmed by diffuse reflectance UV/VIS. In the presence of organic additive TMACl, the products were large aggregate of 1 μm particle size, whereas 4 μm particle size was obtained in organic free products.

In 2004, Zhao, X. S. *et al.* [14] identified the conditions in ETS-10 synthesis. To complete the aim, the effect of titanium sources, fluoride ions, pH of

synthesis gel, contents of water, Na⁺ and K⁺ ions, SiO₂/TiO₂ molar ratios, synthesis time and temperature on the crystallization were systematically examined. It was observed that nano-sized Degussa titanium dioxide (P25) was the best titanium source which promotes highly pure ETS-10 from an optimized synthesis system of 3.4Na₂O: 1.5K₂O: TiO₂: 4.5-5.5SiO₂: 150-180H₂O at pH 10.4 without the presence of organic template. The presence of potassium ions favored the formation of pure ETS-10, due to the structure directing role of potassium ions, but the presence of fluoride ions in synthesis gel resulted in the formation of quartz impurity due to the catalytic role of fluoride ions in polymerization of silicate species. It was also reported that high quality ETS-10 was obtained in a very narrow pH range (10.4-10.5) and the molar ratio of SiO₂/TiO₂ must be maintained in a range 4.5-5.5. The crystallization kinetics of ETS-10 in the optimized synthesis system was 180, 200, 230 and 250°C.

1.2.2 Modification and application of ETS-10 catalysts

In 2000, Anderson, M. W. *et al.* [15] studied the catalytic performance of microporous titanasilicate ETS-10-type catalysts for the aldol condensation of acetone compared with zeolite X-type materials. The catalysts used were ETS-10, ETAS-10 (substitution with Al), Cs-exchanged ETS-10, Cs₂O-impregnated Cs-ETS-10, Na-X, and ion-exchanged K-X, Cs-X and Cs₂O/Cs-X. The selectivity for final products related to the acid-base character of solid catalyst. The Na-X promoted acid-catalyzed condensation reactions, leading to isobutene as a main product. Conversely, both ETS-10 and chemically treated ETS-10-type materials favored base-catalyzed condensation of acetone, resulting in high selectivity for mesityl oxides as the main product.

In 2003, Waghmode, S. B. *et al.* [16] used palladium-loaded ETS-10 molecular sieve as a catalyst in Heck reaction. The catalyst exhibited high activity and selectivity towards the carbon-carbon coupling of aryl halides with olefins, even at low concentrations of Pd (0.009 to 1.4 mole% with respect to the substrate). In the case of the coupling of ethyl acrylate with iodobenzene, 96% conversion of iodobenzene with greater than 98% selectivity were obtained within 1 h over a 0.2 wt% Pd-loaded catalyst. The reaction was investigated with different alkyl halides, olefins and bases.

In 2004, Dorskocil, E. J. *et al.* [17] studied the basic characteristics of various alkali and alkali-earth-exchanged ETS-10 zeolites for the reaction of propylene oxide and carbon dioxide to produce propylene carbonate in the absence of a solvent. The ion-exchanged ETS-10 catalysts were prepared by using 0.5 M aqueous solution of KOH, CsCl, BaCl₂, MgCl₂ and CaCl₂ at 60°C (30 ml/g) for about 5 h. Adsorption microcalorimetry of adsorbed carbon dioxide was utilized to identify the basic sites of ion-exchanged catalysts. The alkali-exchanged samples were significantly more active than the alkaline earth-exchanged catalysts due to their higher strength CO₂ adsorption sites. Surface basicity associated with the partial charge of the framework oxygen played an important role in the catalyst effectiveness for the reaction. Cs-ETS-10 catalyst exhibited the highest yield for the production of propylene carbonate, presumably due to the higher basicity compared to the other catalysts.

In 2004, Tatsumi, T. *et al.* [18] examined the epoxidation ability of ETS-10-derived materials obtained by the post-synthetic treatment with HCl, NH₄Cl and citric acid of various concentrations at room temperature for 4 h at liquid to solid ratio of 100 cm³ to 1 g followed by calcinations. The partially detitanated ETS-10 materials thus prepared proved to be active in the epoxidation of cyclohexene with H₂O₂ as an oxidant due to the formation of tetra coordinated Ti species through the treatment. The highest conversion of cyclohexene and H₂O₂ efficiency was achieved on the catalyst that was treated with 3.7 mol/dm³ NH₄Cl solution followed by the calcination at 723 K.

After that Tatsumi, T. *et al.* [19] synthesized Al and Ga-incorporated ETS-10, designated as ETAIS-10 and ETGaS-10, respectively. The introduction of Al and Ga into ETS-10 enhanced activity, due to increase of the ion-exchange sites, which act as Brønsted base sites. The ion exchange of Na, K, Rb and Cs in ETS-10 caused an increase in the activity for Knoevenagel reaction of the less reactive and less bulky substrates.

In 2008, Anson, A. *et al.* [20] synthesized silver exchanged titanosilicate molecular sieve ETS-10 for adsorption argon, oxygen and nitrogen. Ag-ETS-10 obtained by ion-exchanged method with silver nitrate at 80°C for a period of 1 h and the exchange procedure was repeated twice. The silver exchanged ETS-10 was dried at 80°C. Elemental analysis indicated essentially quantitative silver exchanged with Ag constituting slightly more than 30% of the finished material.

1.3 Literature reviews on tranesterification and esterification reaction of vegetable oils and free fatty acids

1.3.1 Catalytic-free in tranesterification and esterification reactions

There is growing interest in biodiesel (fatty acid methyl ester) because of the similarity in its properties when compared to those of diesel fuel [21]. However, production cost of biodiesel is not economically competitive with petroleum-based fuel according to relatively high cost of the lipid feedstocks. Therefore, alternatives feedstocks are being evaluated as possible substitutes of the refine oil, among other: crude vegetable oil, soapstocks and acid oils. In acid oils, the amount of free fatty acid (FFA) varies from 3% to 40% [3].

In 2004, Kusdiana, D. *et al.* [22] studied thermal catalyst-free transesterification of triglycerides and esterification of free fatty acids in rapeseed oil with supercritical methanol. The results showed that transesterification of triglycerides was slower in reaction rates than esterification of free fatty acids. Furthermore, saturated fatty acids such as palmitic and stearic acids had slightly lower reactivity than of the unsaturated fatty acids; oleic, linoleic and linolenic. The 100% highest yield of methyl esters obtained after 15 min at 300°C. A catalytic-free biodiesel production route with supercritical methanol was studied by Ayhan Demirbas [23]. Supercritical methanol has a high potential for both transesterification of triglyceride and methyl esterification of free fatty acids to methyl ester for diesel substitution. In the supercritical method, yield increased to 95% in 10 min and the viscosity values of vegetable oil methyl ester were between 3.59 and 4.63 mm²/s. However, the presence of water and free fatty acid affected positively the formation of

methyl ester in supercritical method which was opposite to the alkali and acid catalysts.

1.3.2 Transesterification and esterification over homogeneous catalysts

Santacesaria, E. *et al.* [24] studied the acetate salts of the following metals: Ca, Ba, Mg, Cd, Mn, Fe, Zn, Co and Ni as catalysts in transesterification of methanol and soybean oil with acidity of 0.2 % w/w. Moreover, the stearates of all above metals have also been investigated. The activity of the best catalyst $\text{Pb}(\text{Ac})_2$ was lowered by the water formation during esterification of FFA, it was possible to obtain high fatty acid methyl ester (FAME) yields (96%) and a low final FFA concentration (< 1%), in a relatively short reaction time (200 min). The stearates had better performance than acetates because their higher solubility in the oil phase where the reaction occurs.

Chongkhong, S. *et al.* [25] used two-step process for biodiesel production from palm fatty acid distillate (PFAD) having high free fatty acids (FFA). The first step of the process was to reduce free fatty acid content by esterification with methanol and sulfuric acid catalyst. The optimum condition for esterification was methanol to PFAD mole ratio 8:1 with 1.83 wt% of sulfuric acid at 70°C for 60 min. The amount of FFA was reduced from 93% wt% to less than 2 wt% at the end of esterification process. The FAME was purified by neutralization with 3 M sodium hydroxide in water solution at 80°C for 15 min followed by transesterification process (the second step) with 0.39 M sodium hydroxide in methanol solution at 65°C for 15 min. The final FAME product yield obtained was 98%.

1.3.3 Transesterification and esterification over heterogeneous catalysis

Lee, K. Y. *et al.* [26] used the $\text{Na}/\text{NaOH}/\gamma\text{-Al}_2\text{O}_3$ heterogeneous base catalyst for the production of biodiesel. The catalyst was prepared by treatment of $\gamma\text{-Al}_2\text{O}_3$ with sodium hydroxide and sodium at 320°C under nitrogen. The formation of the basic sites was studied with XRD, XPS and CO_2 -TPD analysis. The transesterification reaction was carried out with the MeOH/oil ratio of 9:1, 60°C under stirring speed 300 rpm for 2 h. A catalyst containing 20 wt% of Na and 20 wt% of NaOH showed the highest activity. A utilization of a co-solvent (*n*-hexane) and oil

with a loading amount of 1:5 mol ratio was found to promote the yield in the transesterification of vegetable oils (VO_s) to biodiesel. The Na/NaOH/ γ -Al₂O₃ heterogeneous base catalyst showed almost the same activity under optimized condition compared to the conventional homogeneous NaOH.

Yarmo, M. A. *et al.* [27] introduced silica-supported zirconium sulfate (ZS) as the solid acid catalyst in esterification reaction of oleic acid. The activity of silica-supported ZS exhibited a higher activity than Amberlyst-15 and conventional acid resins at reaction temperature 120°C for 4 h over 5 wt% of catalyst based on oleic free fatty acid which gave 94% conversion. After that, Ni, J. *et al.* [28] studied the esterification of free fatty acid (palmitic acid) with methanol over silica-supported Nafion® resin (SAC-13) and sulfated zirconia using batch and fixed bed-reactors. The sulfated zirconia material cannot be regenerated fully because of sulfate group leaching. The fact that the adsorbed oil decomposes to form carbonaceous deposition. The used catalyst must to activate by dehydration.

Marchetti, J. M. *et al.* [29] used basic resins (Dowex monosphere 550A and Dowex upcore Mono A-625) to perform the esterification reaction into biodiesel from frying oils with a certain high amount of free fatty acids. The effect of the most relevant variables of the process such as reaction temperature 30-55°C, ethanol to oil mole ratio 4:1-6:1, amount of catalyst 2-7% and amount of free fatty acids (oleic acid) 2-27 fed with the oil have been analyzed. The final conversion achieved was around 80%.

Suppes, G. *et al.* [30] were studied transesterification of soybean oil with methanol were performed with NaX zeolite, ETS-10 and metal catalysts. The NaX and ETS-10 were exchanged with potassium and cesium whereas NaX also contained sodium oxide and sodium azide. The reactions were carried out at 60°C, 120°C and 150°C for 24 h and mol ratio of oil to alcohol was 1:6. The result showed that the increased conversions were attributed to the higher basicity of ETS-10 zeolites and large pore structures that improved intra-particle diffusion. Conversion to methyl esters in excess of 90% was achieved at temperatures of 150°C and 120°C

with residence time of 24 h. Pretreating the ETS-10 catalyst at 500°C for 4 h increased the activity of ETS-10 catalyst. Methyl ester yield was increased with rising temperature.

From literatures that were mentioned above, the heterogeneous base catalyst was suitable for esterification reaction both in catalytic activity and separation process. Thus in this research, the basic heterogeneous catalyst ETS-10 and metal exchanged ETS-10 were chosen as catalyst in esterification reaction. The reaction was started with free fatty acids (palmitic acid, oleic acid and linoleic acid) and methanol to produce free fatty acid methyl ester (biodiesel). Moreover, Na, K, Rb and Cs-exchanged ETS-10 were prepared in order to increase the basic strength of catalysts that have the potential to increase the free fatty acid methyl ester yield. The catalytic activities of reused and regenerated ion-exchanged ETS-10 were also investigated.

1.4 Objectives

- 1.4.1 To synthesize and characterize ETS-10 catalysts with gel composition $5\text{SiO}_2:x\text{TiO}_2:3\text{NaOH}:\text{KF}:75\text{H}_2\text{O}$, where $x = 0.5-1.0$
- 1.4.2 To modify the basic strength of ETS-10 by ion-exchange method with NaOH, KOH, RbOH and CsOH.H₂O
- 1.4.3 To study the catalytic activity of ETS-10, Na-ETS-10, K-ETS-10, Rb-ETS-10 and Cs-ETS-10 in esterification reaction of palmitic, oleic and linoleic free fatty acids (FFA)
- 1.4.4 To investigate the optimum conditions in esterification reaction of FFA
- 1.4.5 To study the catalytic activity of reused and regenerated catalyst

CHAPTER II

THEORY

2.1 Catalysis

Catalysis is a way of accelerating the rate of a chemical reaction by means of contacting the reactants with a substance called a catalyst, which itself is not consumed by the overall reaction. More generally, one may at times call anything that accelerates a process, "catalyst". A catalyst provides an alternative route to products, the catalytic route being subject to lower activation energy (E_a) than in the uncatalyzed reaction. A lowered activation energy increases the reaction rate. Catalysts generally change in the course of a reaction but are regenerated. The energy profile with and without catalyst were shown in Figure 2.1.

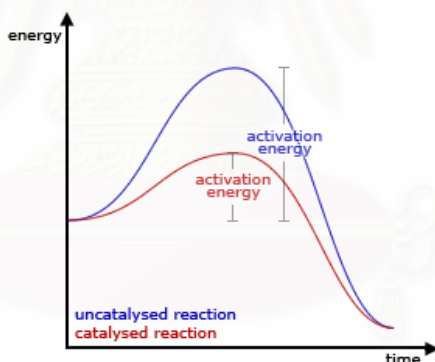
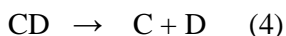
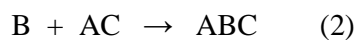
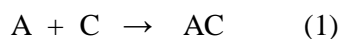


Figure 2.1 The potential energy profile of the reaction with and without catalyst.

Catalysts generally react with one or more reactants to form an intermediate that subsequently give the final reaction product, in the process regenerating the catalyst. The following is a typical reaction scheme 2.1, where C represents the catalyst, A and B are reactants, and D is the product of the reaction of A and B:



Scheme 2.1 Typical reaction.

Although the catalyst (C) is consumed by reaction (1), it is subsequently produced by reaction 4, so for the overall reaction:



Industrial catalysts comprise wide variety of materials that was manufactured by a variety of methods. Many catalysts or porous structure were studied. The commercially useful catalyst particle size is determined by the process in which to be used, fixed beds and fluidized beds. In fluidized beds reactors, usually present in the catalyst powder supplied. The particles present generally range from about 20-300 μm in diameter. For fixed beds particles generally range from about 0.0625-0.5 inches in diameter. In general, 60% of commercially produced chemical products involve catalyst at some stage in the process of their manufacture [31].

2.2 Types of catalysts

Catalysts can be divided into two main types, heterogeneous and homogeneous catalysts. Biocatalyst is often seen as a separate group. In nature enzymes are catalyst in metabolic pathway whereas in biocatalysts enzymes are used as catalyst in organic chemistry. Heterogeneous catalyst is present in different phases from the reactants. Whereas, homogeneous catalyst is in the same phase.

2.2.1 Homogeneous catalysts

Homogeneous catalysts are in the same phase as the reactants. The catalyst is a molecule which facilitates the reaction. The catalyst initiates reaction with one or more reactants to form intermediate and in some cases one or more products. Subsequent steps lead to the formation of remaining products and to the regeneration of the catalyst. Typically, everything will be presence as gas or contained in a single liquid phase. In addition, the catalysis of organic reactions by metal complexes in solution has grown rapidly in both scientific and industrial importance.

2.2.2 Heterogeneous catalysts

Heterogeneous catalyst is presented in different phases from the reactants e.g. a solid catalyst in a liquid reaction mixture. A simple model

heterogeneous catalysis involves the catalyst providing a surface on which the reactants temporarily become adsorbed. Bonds in the reactants become weakened sufficiently for new bonds to be created. The bonds between the products and the catalyst are weaker, so the products are released. The mechanism of heterogeneous catalysis comprises five steps between compounds adsorbed on the surface of solid catalyst [32].

- (1) Diffusion of the reacting substances over the catalyst particle.
- (2) Adsorption of the reacting substances on the catalyst.
- (3) Interaction of the reacting substances on the surface of catalyst.
- (4) Desorption of the reaction products from the catalyst particle.
- (5) Diffusion of the reaction products into the surrounding medium.

Furthermore, catalyst particles have internal pores that are accessible to the reactant molecules, so that diffusion proceeds in two steps, external and internal surface.

2.3 Porous materials

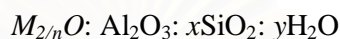
Porous materials have found wide applications in many technological fields such as adsorption and environmental technology including catalysis because of their high surface area, large pore volume, and uniformity in pore size. The design and processing of novel porous materials, driven by the rapidly growing demands of emerging applications such as separation, purification, immobilization of biological molecules, drug delivery and gas storage, etc. Porous materials can be classified based on the IUPAC pore diameter into three groups that was shown in Table 2.1.

Table 2.1 IUPAC classification of porous materials [33]

Porous material	Pore diameter (nm)
Microporous	up to 2
Mesoporous	2-50
Macroporous	50 to up

2.4 Zeolite molecular sieves

Zeolites are a well-defined class of crystalline naturally aluminosilicate minerals. They have three dimensional structures arising from a framework of $[\text{SiO}_4]^{4-}$ and $[\text{AlO}_4]^{5-}$ coordination polyhedral linked by all their corners and have minimum channel diameters in the range of 3-10 Å depend upon the type of zeolite and the nature of the cations present. Zeolite has the general formula as



Which M represents a metal cation generally from group I and II of valence n . x and y was varied with the type of zeolite. They have quite large cages joined by smaller opening then, they have a very high internal surface area in the form of pores of fixed geometry [34]. The zeolite frameworks generally are very open and contain channels and cavities in which are located cations and water molecules. The cations often have a high degree of mobility giving rise to facile ion exchange and the water molecules are readily lost and regained; this accounts for the well-known desiccant properties of zeolites [35].

2.4.1 Uses of zeolite

2.4.1.1 Commercial and domestic

Zeolites are widely used as ion-exchange beds in domestic and commercial water purification, softening, and other applications. In chemistry, zeolites are used to separate molecules (only molecules of certain sizes and shapes can pass through), as traps for molecules so they can be analyzed.

2.4.1.2 Petrochemical industry

Synthetic zeolites are widely used as catalysts in the petrochemical industry, for instance in fluid catalytic cracking and hydro-cracking. Zeolites confine molecules in small spaces, which causes changes in their structure and reactivity. The hydrogen forms of zeolites (prepared by ion-exchange) are powerful solid-state acids, and can facilitate a host of acid-catalyzed reactions, such as isomerisation, alkylation, and cracking. Catalytic cracking uses a furnace and reactor. First crude oil distillation

fractions are heated in the furnace and passed to the reactor. In the reactor the crude meets with a catalyst such as zeolite. It goes through this step three times, each time getting cooler. Finally it reaches a step known as separator. The separator collects recycled hydrogen. Then it goes through fractionators and becomes the final item [36].

2.5 Titanosilicate materials

Microporous titanosilicate is one of zeolite-type materials. They are considered as possible new catalysts or molecular sieves and ion exchangers. They have been interested since the discovery of important catalytic properties of ZSM-5 structure titanium silicalite-1 (TS-1) in oxidation reactions in 1983. Titanosilicate compound was represented by the following compositional formula $x\text{TiO}_2(1-x)\text{SiO}_2$, where x is form 0.0001-0.2. In this group, octahedral and tetrahedral atoms are exclusively corner-linked. The UND-1 is a titanosilicate compound that built up from SiO_4 six-membered ring and isolated TiO_6 octahedral. The ion-exchange behavior of AM-2 ($\text{K}_2\text{TiSi}_3\text{O}_9 \cdot \text{H}_2\text{O}$) was also studied and showed that selectivity for extra-framework cations [37]. Other examples of titanosilicate compounds were TSP used as photocatalyst and EMS-3 that has high exchange capacity due to the divalent anionic charge on the Ti nuclei [38]. The structures of UND-1, AM-2 and TSP are shown in Figure 2.2.

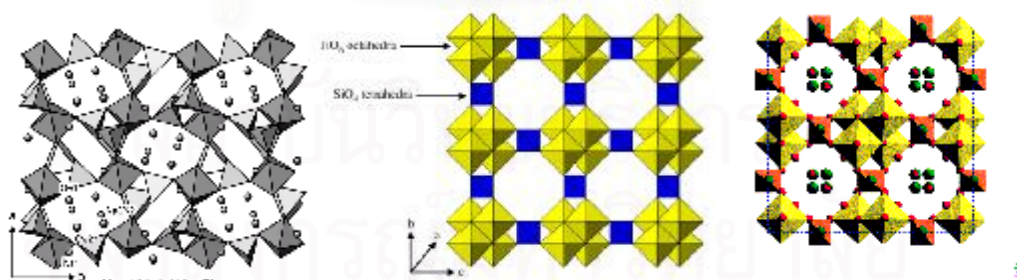


Figure 2.2 Structures of some titanosilicate compounds.

2.6 ETS-10 (Engelhard titanasilicate -10)

ETS-10 (Engelhard titanasilicate structure 10) is a microporous titanasilicate discovered by Engelhard in 1989 [9]. Unlike traditional aluminosilicates, aluminosphosphates, and titanosilicates in which Al, P, and Ti atoms are four-coordinated, ETS-10 comprises corner-sharing SiO_4 tetrahedra and TiO_6 octahedra linked through oxygen atoms, forming a three-dimensional 12-membered ring network with a pore-opening size of about 0.8 nm. The presence of each tetravalent Ti atom in an octahedron generates two negative charges, which are balanced by non-framework and exchangeable cations Na^+ and K^+ . Such a unique framework property has been demonstrated to display unusual adsorption properties towards heavy metal ions in aqueous solution [14]. The size and shape of ETS-10 crystals can be controlled by adjusting the synthesis conditions, including pH, temperature, and initial gel compositions [18].

2.6.1 Structures of ETS-10

This layout of structural units generates 12- and 7-membered ring channels which possess a free entrance of about 0.8×0.5 and 0.55×0.15 nm, respectively. Each TiO_6 octahedron carries two negative charges, and the electrical neutrality of the framework is preserved by extra-framework charge-balancing cations, which are exchangeable; in the as-synthesized material, which has the nominal chemical formula $(\text{Na},\text{K})_2\text{-TiSi}_5\text{O}_{13}$, two extra-framework alkali metal cations are incorporated for every titanium atom present in the framework [39]. The structure of ETS-10 was shown in Figure 2.3. The TiO_6 octahedral share *trans* vertices to form TiO_5 infinite chains. These chains are each connected two folded chains of SiO_4 tetrahedral to form $[\text{TiSi}_4\text{O}_{13}]$ columns. The column are packed into layers parallel to the (001) plane with the columns in neighboring layers perpendicular to each other. The connection between Ti and Si atom to form framework structure was shown in Figure 2.4 [40]. The framework topology and novel chemical composition of ETS-10 endow this microporous material with potential interest in heterogeneous catalysis.

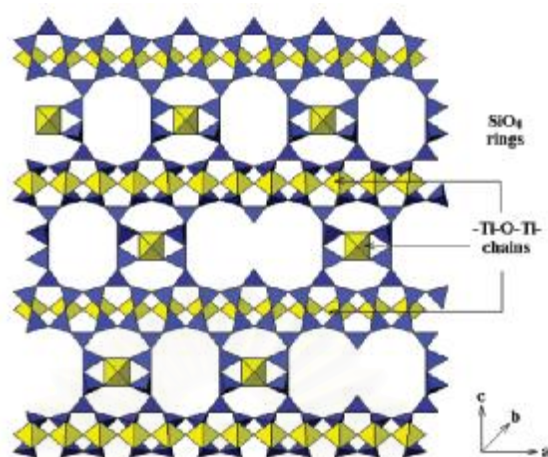


Figure 2.3 Structure of ETS-10. The yellow polyhedra are TiO_6 octahedra running in the a and b directions. The blue polyhedra are SiO_4 tetrahedra forming 12-ring pores. Double pores arise from stacking faults in the inherently disordered material.

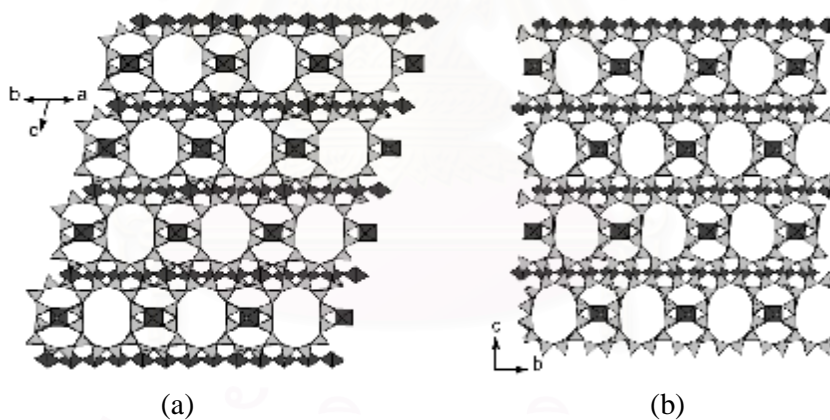


Figure 2.4 Titanosilicate ETS-10 projections: (a) down $[110]$ direction for polymorph B and (b) down $[100]$ direction for polymorph A, Dark TiO_6 octahedral, light grey SiO_4 tetrahedral.

The structure of ETS-10 is built of strips of five-membered silicon-oxygen rings and two orthogonal sets of titanium-oxygen chains, which differ from each other in their surrounding. The three representative clusters describing ETS-10 were shown in Figure 2.5 [41].

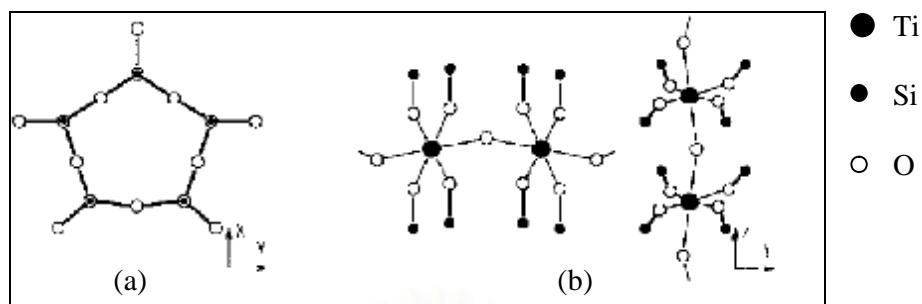


Figure 2.5 Main clusters in ETS-10, (a) five-membered ring of SiO₄ tetrahedral; (b) two types of dimer of TiO₆ octahedral.

From NMR investigation, Na⁺ ions reside in the both 12- and 7-member ring channels in NaETS-10. They are very mobile and weakly bond to framework as counter ions and can be exchanged reversibly without damaging the framework structure. In addition, only extra framework positions which corresponded to general sites in the space group. Two chemical environments of extra-framework sodium cations were measured by solid-state NMR [42].

2.6.2 Properties and application of ETS-10

The ETS-10 structure contains two minus charge per Ti atom. It has the possibility as ion-exchanger and basic catalyst. ETS-10 was used in a number of chemical processes, which mainly exploit the strong basic character of the alkali form for catalyzing such processes as hexane reforming [43], Aldol-type condensation [44] and alcohol dehydrogenation [16]. However, an acid form of ETS-10 obtained by thermolysis of an ammonium-exchanged sample (HETS-10) was shown to be active in the acid-catalyzed isomerization of but-1-ene [45].

In addition to its unique adsorption or ion exchange property, one of the most striking features of ETS-10 is that the TiO₆ octahedral form linear chains confined atomic -O-Ti-O-Ti-O- wires display peculiar optical and electronic properties [46-48]. The well defined mono-atomic -O-Ti-O- chains with band gap energy of 4.03 eV of ETS-10 makes it a promising candidate for photocatalytic applications. Substitution for titanium atom with other elements such as Ag, Co, and Cu can lead to significantly higher photocatalytic activity. The photo-degradation is

expected to occur similar to that on TiO_2 . Because of large pore containing structure, ETS-10 has projected as one of the best candidate to replace conventional zeolite to removal of heavy metals in waste water [49].

Two principal methods to create and enhance basicity in zeolite have been proposed and investigated. First one is modification of intrinsic basicity, i.e. the Lewis basicity of the framework oxygen, by either using different framework cation, or exchange of cation that balance the charge of framework. Another method is using of the zeolite as a support for basic species, i.e. the occlusion of metal (alkali) clusters, or small metal hydroxide and/or oxide particles.

2.6.3 Catalytic activity of ETS-10, Na-ETS-10, K-ETS-10, Rb-ETS-10 and Cs-ETS-10 catalysts

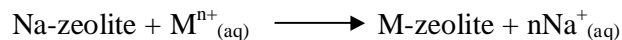
In this work, the palmitic acid, oleic acid and linoleic acid free fatty acids were chosen to starting material for the esterification reaction. Because of in Thailand, palm oil tree is cultivated higher than another oil tree such as jatropha tree. Palm oil is a source already scaled up for biodiesel production and has a large quantity of oleic, palmitic and linoleic free fatty acid. The esterification will be used to handle free fatty acid commonly found in crude palm oil, used cooking oil, crude jatropha oil. The biodiesel process can be done with esterification instead of deacidification during pretreatment.

2.7 Modification of catalysts

2.7.1 Ion-exchange

Ion exchange is an exchange of ions between two electrolytes or between an electrolyte solution and a complex. Typical ion exchangers are zeolites, ion exchange resins and clay. Ion exchangers are either cation exchangers that exchange positively charged ions (cations) or anion exchangers that exchange negatively charged ions (anions). There are also amphoteric exchangers that are able to exchange both cations and anions simultaneously. However, the simultaneous exchange of cations and anions can be more efficiently performed in mixed beds that contain a mixture of anion and cation exchange resins, or passing the treated solution

through several different ion exchange materials. Metal ion and cationic complexes can occupy framework cationic sites of zeolite as shown in equation 2.1.



Ion exchangers can be unselective or have binding preferences for certain ions or classes of ions, depending on their chemical structure. This can be dependent on the size of the ions, their charge, or their structure. Ion exchange is a reversible process and the ion exchanger can be regenerated or loaded with desirable ions by washing with an excess of these ions [50-51].

2.7.2 Impregnation

Many catalyst types are produced by impregnation. It consists in repeated dipping of porous support pellets into a solution containing a desired catalytic agent. The agent must be applied uniformly in a predetermined quantity to a preset depth of penetration. This is especially true of catalysts based on noble metals. Various techniques like pressurizing, vacuum treatment, acoustic activation are used to facilitate the impregnation process. They, however, are expensive and allow only limited control of absorption and penetration depth.

Supported metal catalysts may be prepared by three distinct methods (i) deposition, (ii) co-precipitation and (iii) impregnation. All of these, the last mentioned is the most important. It consists of soaking the carrier with a solution of a suitable metal salt, followed by evaporation to dryness. The supported salt is then either reduced or, in certain case, calcined in air to convert the salt to the oxide which is then reduced to the metal. The main functions of carrier are to provide a structural framework for the catalytic component and increase the surface area per unit weight of metal. Other desirable effects may include such factors as increased stability due to small crystallites of metal being sufficiently separated to prevent sintering and a greater resistance to poisoning. The choice of carrier depends to a large extent upon the purpose for which the catalyst is required [52].

2.8 Free fatty acids (FFAs)

The oil palm gives its name to the 16 carbon saturated fatty acid palmitic acid found in palm oil; monounsaturated oleic acid is also a constituent of palm oil while palm kernel oil contains mainly lauric acid . Palm oil is the largest natural source of tocotrienol, part of the Vitamin E family. Palm oil and palm kernel oil are one of the few vegetable oils relatively high in saturated fat [53].

Fatty acids are aliphatic monocarboxylic acids derived from or contained in esterified form in an animal or vegetable fat, oil or wax. Natural fatty acids commonly have a chain of 4 to 28 carbons (usually unbranched and even numbered), which may be saturated or unsaturated. By extension, the term is sometimes used to embrace all acyclic aliphatic carboxylic acids.

2.8.1 Types of fatty acid

2.8.1.1 Saturated fatty acids

Saturated fatty acids do not contain any double bonds or other functional groups along the chain. The term saturated refers to hydrogen, in that all carbons (apart from the carboxylic acid group) contain as many hydrogens as possible. Each carbon within the chain contains 2 hydrogen atoms. Saturated fatty acids form straight chains and, as a result, can be packed together very tightly, allowing living organisms to store chemical energy very densely. The fatty tissues of animals contain large amounts of long-chain saturated fatty acids. The saturated fatty acids are shown in Table 2.2.

Table 2.2 Saturated fatty acids

Common name	IUPAC name	Chemical structure	C no. : db
Lauric	Dodecanoic acid	$\text{CH}_3(\text{CH}_2)_{10}\text{COOH}$	C12:0
Myristic	Tetradecanoic acid	$\text{CH}_3(\text{CH}_2)_{12}\text{COOH}$	C14:0
Palmitic	Hexadecanoic acid	$\text{CH}_3(\text{CH}_2)_{14}\text{COOH}$	C16:0
Stearic	Octadecanoic acid	$\text{CH}_3(\text{CH}_2)_{16}\text{COOH}$	C18:0

C: carbon, DB: double bond

2.8.1.2 Unsaturated fatty acids

Unsaturated fatty acids are of similar form, except that one or more alkenyl functional groups exist along the chain, with each alkene substituting a single-bonded part of the chain with a double-bonded portion. The two next carbon atoms in the chain that are bound to either side of the double bond can occur in a *cis* or *trans* configurations, its were shown in Figure 2.6.

(a) *cis* Isomer

A *cis* configuration means that adjacent carbon atoms are on the same side of the double bond. The rigidity of the double bond freezes its conformation and, in the case of the *cis* isomer, causes the chain to bend and restricts the conformational freedom of the fatty acid. The more double bonds the chain has in the *cis* configuration, the less flexibility it has. When a chain has many *cis* bonds, it becomes quite curved in its most accessible conformations. For example, oleic acid, with one double bond, has a kink in it, whereas linoleic acid, with two double bonds, has a more pronounced bend. Alpha-linolenic acid, with three double bonds, favors a hooked shape. The effect of this is that, in restricted environments, such as when fatty acids are part of a phospholipid in a lipid bilayer, or triglycerides in lipid droplets, *cis* bonds limit the ability of fatty acids to be closely packed, and therefore could affect the melting temperature of the fat.

(b) *trans* Isomer

A *trans* configuration, by contrast, means that the next two carbon atoms are bound to opposite sides of the double bond. As a result, they do not cause the chain to bend much, and their shape is similar to straight saturated fatty acids.

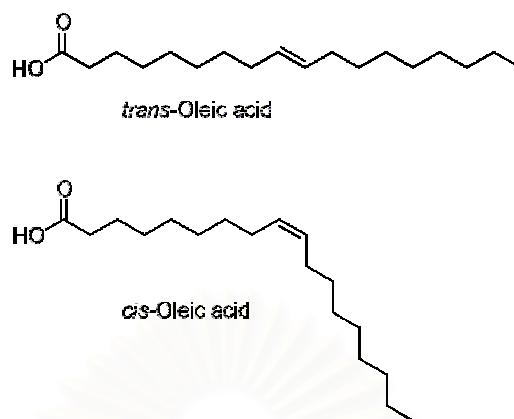


Figure 2.6 Comparison of the *trans* isomer and the *cis*-isomer of oleic acid.

In most naturally-occurring unsaturated fatty acids, most fatty acids in the *trans* configuration (trans fats) are not found in nature and are the result of human processing. Examples of unsaturated fatty acids were presented in Table 2.3 [54].

Table 2.3 Unsaturated fatty acids

Common name	Chemical structure	C no. : db
Myristoleic acid	$\text{CH}_3(\text{CH}_2)_3\text{CH}=\text{CH}(\text{CH}_2)_7\text{COOH}$	C14:1
Palmitoleic acid	$\text{CH}_3(\text{CH}_2)_5\text{CH}=\text{CH}(\text{CH}_2)_7\text{COOH}$	C16:1
Oleic acid	$\text{CH}_3(\text{CH}_2)_7\text{CH}=\text{CH}(\text{CH}_2)_7\text{COOH}$	C18:1
Linoleic acid	$\text{CH}_3(\text{CH}_2)_4\text{CH}=\text{CHCH}_2\text{CH}=\text{CH}(\text{CH}_2)_7\text{COOH}$	C18:2

2.8.2 Palmitic acid

Palmitic acid is one of the most common saturated fatty acids found in animals and plants. It has the formula $\text{C}_{16}\text{H}_{32}\text{O}_2$ and is a major component of the oil from palm trees (palm oil and palm kernel oil). Palmitic acid was discovered by Edmond Frémy in 1840, in saponified palm oil and is the first fatty acid produced during lipogenesis (fatty acid synthesis) and from which longer fatty acids can be produced. Palmitate negatively feeds back on acetyl-CoA carboxylase (ACC) which is responsible for converting acetyl-ACP to malonyl-ACP on the growing acyl chain, thus preventing further palmitate generation.

2.8.3 Oleic acid

Oleic acid is a monounsaturated omega-9 fatty acid found in various animal and vegetable sources. It has the formula $C_{18}H_{34}O_2$. The saturated form of this acid is stearic acid. Oleic acid makes up 55-80% of olive oil, 40-50% of palm oil and 15-20% of grape seed oil.

2.8.4 Linoleic acid

Linoleic acid is an unsaturated omega-6 fatty acid. It is a colorless liquid. In physiological literature, it is called 18:2(n-6). Chemically, linoleic acid is a carboxylic acid with an 18-carbon chain and two *cis* double bonds; the first double bond is located at the sixth carbon from the omega end. It is found in the lipids of cell membranes. It is abundant in many vegetable oils, especially safflower and sunflower oils.

2.8.5 Fatty acids composition of palm oil

The fatty acids of palm oil could be of the same type or different. The property of a triglyceride will depend on the different fatty acids that combine to form the triglyceride. The fatty acids themselves are different depending on their chain length and degree of saturation. The short chain fatty acids are of lower melting point and are more soluble in water. Whereas, the longer chain fatty acids have higher melting points. The melting point is also dependent on degree of non-saturation. Unsaturated acids will have a lower melting point compared to saturated fatty acids of similar chain length. The two most predominant fatty acids in palm oil are C18:1 (unsaturated) oleic acid and C16:0 (saturated) palmitic acid. Typical fatty acid composition of palm oil is given in Table 2.4.

Table 2.4 Typical free fatty acid composition in palm oil

Fatty acid	C no. : db	% wt
Oleic acid	C18 : 1	45.22
Palmitic acid	C16 : 0	37.94
Linoleic acid	C18 : 2	10.89
Stearic acid	C18 : 0	3.84
Myristic acid	C14 : 0	1.19
Lauric acid	C12 : 0	0.67
Linolenic acid	C18 : 3	0.25

C: carbon, DB: double bond

2.9 Diesel Fuel

Diesel or diesel fuel is a specific fractional distillate of petroleum fuel oil or a washed form of vegetable oil that is used as fuel in a diesel engine. The term typically refers to fuel that has been processed from petroleum, but increasingly, alternatives such as biodiesel or biomass to liquid (BTL) or gas to liquid (GTL) diesel that are not derived from petroleum are being developed and adopted. For clarity, petroleum-derived diesel is increasingly called petrodiesel.

2.9.1 Petroleum diesel

Petroleum diesel is produced from petroleum and is a hydrocarbon mixture, obtained in the fractional distillation of crude oil between 200°C and 350°C at atmospheric pressure. The density of petroleum diesel is about 850 g/L. The cost of diesel traditionally rises during colder months as demand for heating oil, which is refined in much the same way, rises. Due to its higher level of pollutants, diesel must undergo additional filtration which contributes to a sometimes higher cost. While petrol diesel-powered cars of equivalent displacement nearly always have substantially better fuel economy than equivalent gasoline engines, they do not produce significantly less greenhouse gas pollution. Their greater economy is due to the higher energy per-litre content of diesel fuel, a reduction maintenance costs due to fewer parts and longer engine life, and also because of the intrinsic efficiency of the diesel engine.

2.9.1.1 Chemical composition

Petroleum-derived diesel is composed of about 75% saturated hydrocarbons (primarily paraffins including *n*-, *iso*-, and cycloparaffins), and 25% aromatic hydrocarbons (including naphthalenes and alkylbenzenes). The average chemical formula for common diesel fuel is $C_{10}H_{20}$ to $C_{15}H_{28}$.

2.9.2 Synthetic diesel

Wood, hemp, straw, corn, garbage, food scraps, and sewage-sludge may be dried and gasified to synthesis gas. After purification the Fischer-Tropsch process is used to produce synthetic diesel. This means that synthetic diesel oil may be one route to biomass based diesel oil. Such processes are often called Biomass-To-Liquids or BTL. Synthetic diesel may also be produced out of natural gas in the Gas-to-liquid (GTL) process or out of coal in the Coal-to-liquid (CTL) process. Such synthetic diesel has 30% less particulate emissions than conventional diesel.

2.9.3 Biodiesel

Biodiesel can be obtained from vegetable oil or animal fats using esterification and transesterification. Biodiesel is a non-fossil fuel alternative to petrodiesel. It can also be mixed with petrodiesel in any amount in modern engines, though when first using it, the solvent properties of the fuel tend to dissolve accumulated deposits and can clog fuel filters. Biodiesel has a higher gel point than petrodiesel, but is comparable to diesel. This can be overcome by using a biodiesel/petrodiesel blend or by installing a fuel heater, but this is only necessary during the colder months. A diesel-biodiesel mix results in lower emissions than either can achieve alone except for NO_x emissions. A small percentage of biodiesel can be used as an additive in low-sulfur formulations of diesel to increase the lubricity lost when the sulfur is removed. In the event of fuel spills, biodiesel is easily washed away with ordinary water and is nontoxic compared to other fuels.

Biodiesel can be produced using kits. Certain kits allow for processing of used vegetable oil that can be run through any conventional diesel motor with modifications. The modification needed is the replacement of fuel lines from the intake and motor and all affected rubber fittings in injection and feeding pumps. This

is because biodiesel is an effective solvent and will replace softeners within unsuitable rubber with itself over time. Synthetic gaskets for fittings and hoses prevent this. Chemically, most biodiesel consists of alkyl (usually methyl) esters instead of the alkanes and aromatic hydrocarbons of petroleum derived diesel. However, biodiesel has combustion properties very similar to petrodiesel, including combustion energy and cetane ratings. Paraffin biodiesel also exists. Due to the purity of the source, it has a higher quality than petrodiesel [55].

2.9.4 Properties of diesel fuels

The first property is Cetane Number (CN). It is a measurement of ignition quality or ignition delay, and is related to the time required for a liquid fuel to ignite after injection into a compression ignition engine. Two standards, cetane (n-hexadecane) and 1-methylnaphthalene (1-MN) are assigned CN values of 100 and 0, respectively. Heating value is defined as the amount of heat released per unit mass of fuel from its complete combustion. This property is also referred to as calorific value or energy content. Typical heating values for diesel fuels are in the range of 134,000 Btu /gal to 148,000 Btu/gal.

Density is the mass per unit volume of diesel fuel at a given temperature. It has an importance in diesel engine performance, since fuel injection operates on a volume metering system. In the case of viscosity, it is a measure of the internal fluid friction, which tends to oppose any dynamic change in the fluid motion. It is an important property of diesel fuel because of its relevance to the performance of the fuel injection equipment, particularly at low temperatures when the increase in the fluidity of fuel.

Low temperature characteristics of diesel fuel including cloud point that is the temperature at which wax is first precipitated. Usually it is in the range between 10 and -20°C. Whereas pour point is the temperature at which the amount of wax precipitated out of the solution is sufficient to gel the fuel that is generally 5-11°C below cloud point. Another important property is sulfur content. It is expressed as weight percentage of sulfur in the fuel. Upon combustion, sulfur is converted to

SO_x (SO₂ and SO₃) which poison the catalytic converter and also contributes to acid rain. The maximum value depends on each country.

2.10 The production of biodiesel

2.10.1 Direct use and blending

All research focusing on the use of vegetable oils to feed diesel engine showed coking and trumpet formation on the injectors to such an extent that fuel atomization does not occur properly or is even prevented. There have been many problems associated with using vegetable oils directly in diesel engines, such as: decrease in power output and thermal efficiency of the engine; thickening or gelling of the lubricating oil as a result of contamination by vegetable oils. Other disadvantages to the use of vegetable oils and especially animal fats are the high viscosity (about 11–17 times higher than diesel fuel) and lower volatility that result in carbon deposits in engines due to incomplete combustion.

In 1980, Bartholomew addressed the concept of using food for fuel. It was not practical to substitute 100% vegetable oil for diesel fuel. But a blend of 20% vegetable oil and 80% diesel fuel was successful. Mixture of degummed soybean oil and No. 2 diesel fuel in the ratio of 1:2 and 1:1 were tested for engine performance, the results indicated that 1:2 blend should be suitable as a fuel for agricultural. Two problems associated with the use of vegetable oil as fuels were oil deterioration and incomplete combustion [3].

2.10.2 Thermal cracking (pyrolysis)

To solve the problem of high viscosity of vegetable oils, the pyrolysis was chosen to produce the biodiesel. The pyrolysis of fats has been investigated for more than 100 years, especially in areas without deposits of petroleum. Copra oil and palm oil stearin were cracked over SiO₂/Al₂O₃ at 450°C to produce biodiesel fuels. The chemical compositions of diesel fractions were similar to fossil fuels. Pyrolyzed soybean oil has 79.0% of carbon and 11.9% of hydrogen. Its cetane number (43) is higher than the oil cetane number (37.9) and its viscosity (10.2 cSt at 38°C) is lower than the vegetable oil viscosity (32.6 cSt at 38°C). Nevertheless, this value is higher

than that required for diesel (7.5 cSt). Pyrolysed oils have acceptable levels of sulphur, water and particulate matter. Otherwise, they have unacceptable levels of ashes and carbon deposits and high pour point [4].

2.10.3 Transesterification (alcoholysis)

Transesterification is widely used to reduce vegetable oil viscosity. Most industrial processes employ alkaline catalysis and methanol. In almost all countries methanol is more available than ethanol. Transesterification or alcoholysis is the displacement of alcohol from ester by another in a process similar to hydrolysis, except that alcohol is used instead of water. A catalyst is usually used to improve the reaction rate and yield. Because the reaction is reversible, excess alcohol is used in shifting the equilibrium to the product side. The reaction can be catalyzed by alkali, acid or enzyme such as NaOH, KOH, H₂SO₄ and lipase, respectively. Pure biodiesel fuel (100% esters of fatty acids) is called B100. When blended with diesel fuel the designation indicates the amount of B100 in the blend, *e.g.* B20 is 20% B100 and 80% diesel, and B5 used in Europe is contains 5% B100 in diesel [4]. The transesterification reaction diagram of triglycerides is presented in the Figure 2.7.

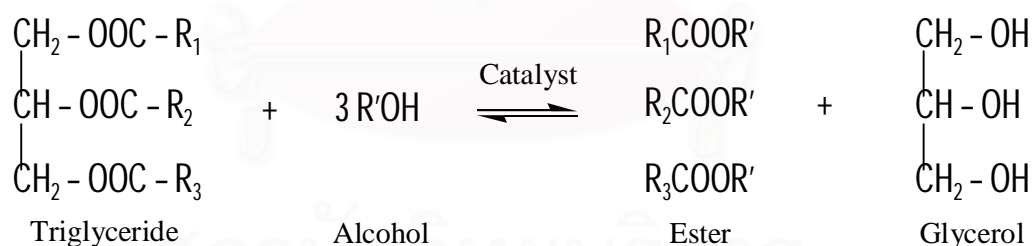


Figure 2.7 Typical transesterification diagram of triglyceride.

2.10.3.1 Transesterification kinetics and mechanism

Transesterification of triglycerides (TGs) with alcohol proceeds via three consecutive and reversible reactions where the FFA ligands combine with alcohol to produce a fatty acid alkyl ester, diglyceride and monoglyceride intermediates, and finally glycerol by-product. The stoichiometric reaction requires 1 moles of TG and 3 mole of methanol to produce 3 mole of linear ester and 1 mole of glycerol. In presence of excess alcohol, the forward reaction is pseudo-first order and

2.10.4 Esterification

Esterification is the chemical process for making esters, which are compounds of the chemical structure R-COOR', where R and R' are either alkyl or aryl groups. The most common method for preparing esters is to heat a carboxylic acid or free fatty acid with an alcohol, while removing the water that is formed. Esterification is among the simplest and most often performed organic transformations. The esterification reaction diagram of free fatty acid is shown in the Figure 2.10. The mechanism of acid and alkali catalyzed esterifications are presented in Figure 2.11 and 2.12, respectively.

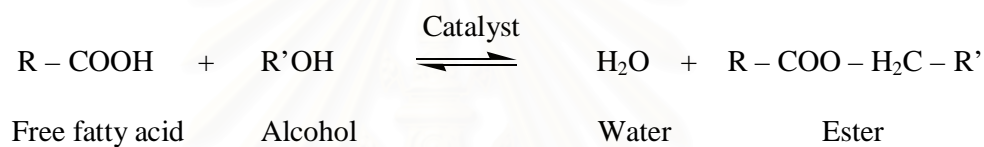


Figure 2.10 Typical esterification diagram of free fatty acid.

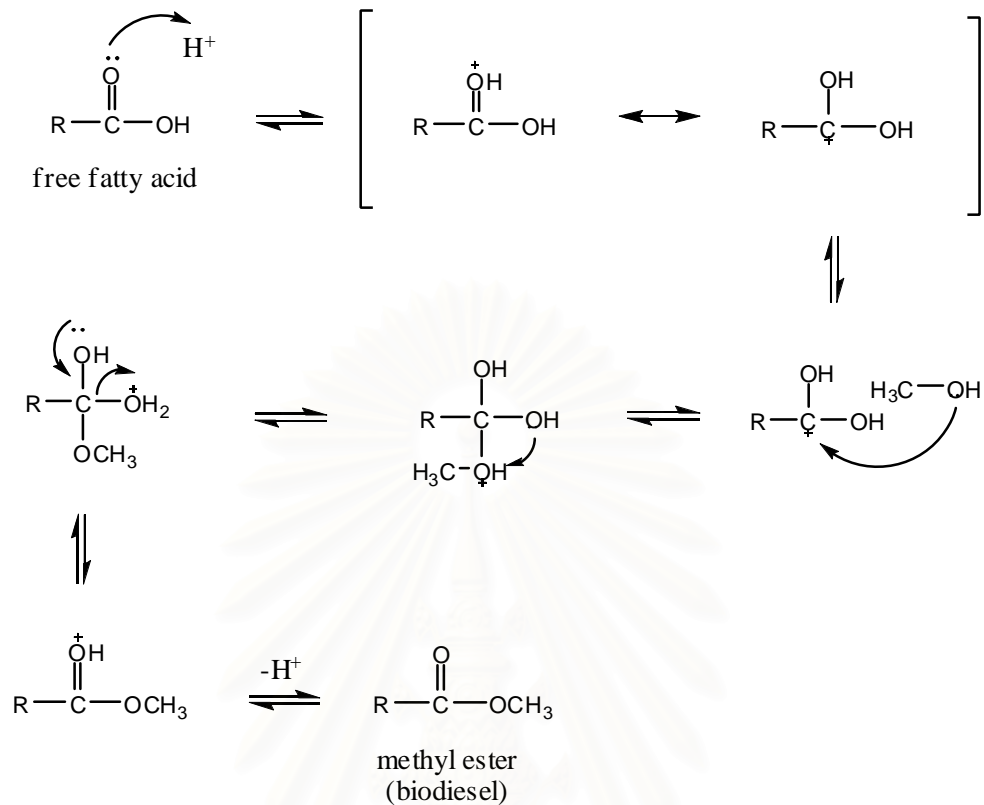


Figure 2.11 Mechanism of acid catalyzed esterification of fatty acid.

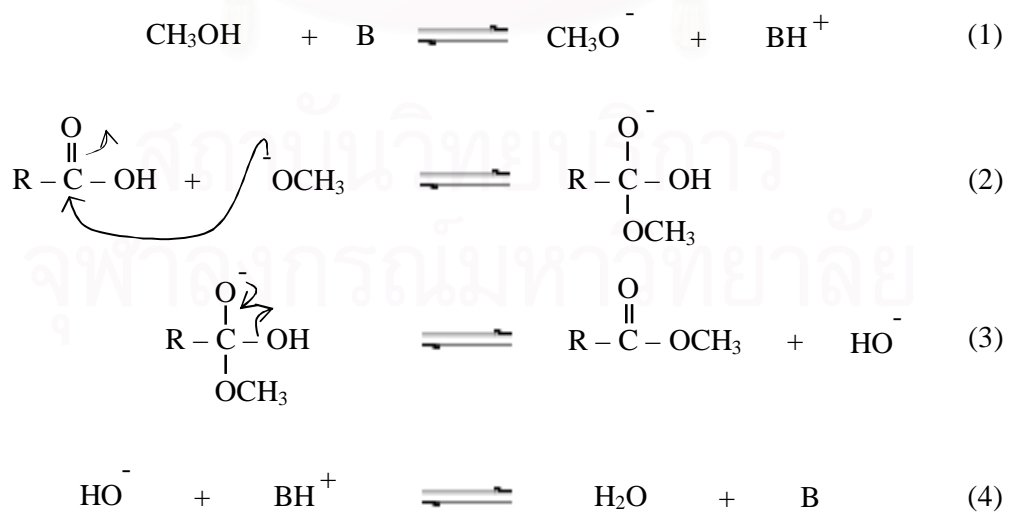


Figure 2.12 Mechanism of base catalyzed esterification of fatty acid.

2.10.4.1 Esterification parameters

The most relevant variables that influence the esterification reactions are the following: [57]

(a) Moisture and free fatty acid

All materials should be substantially anhydrous. If the acid value was greater than 1, more NaOH was required to neutralize the free fatty acids. Water also caused soap formation, which consumed the catalyst and reduced catalyst efficiently.

(b) Molar ratio of alcohol to free fatty acid

One of most important variables affecting the yield of ester is the molar ratio of alcohol to FFA. The molar ratio is associated with the type of catalyst used. Higher molar ratios result in greater ester conversion in a shorter time.

(c) Catalyst type and concentration

Catalysts in esterification reaction are classified as alkali, acid, or enzyme. Acid-catalyzed reaction is more efficient and less side reaction than alkali-catalyzed. It is suitable if the glycerides contain high free fatty acid content and more water. Acid catalysts include sulfuric acid (H_2SO_4), hydrochloric acid (HCl) and phosphoric acid (H_3PO_4)

Lipase is enzymes that can be used as catalyst for transesterification and esterification reactions. It has many advantages such as possibility to regeneration and reuse and high thermal stability, but it also has some disadvantages include lose some activity, support enzymes is not uniform and more expensive.

(d) Reaction time

The conversion rate and fatty acid methyl ester yield are increase with increase reaction time.

(e) Reaction temperature

Esterification can occur at different temperature, depending on the oil used and catalyst types. Temperature clearly influenced the reaction rate and yield of esters.

2.11 Characterization of materials

2.11.1 Powder X-ray diffraction (XRD)

Many different experimental techniques have been utilized to characterize the microporous materials. Often several techniques are used in combination, in order to provide unambiguous structural information. XRD technique provides direct information of the pore architecture of the materials.

Different features of a powder diffraction pattern can be exploited in the characterization of a material (Table 2.5). Powder diffraction data is most commonly used as fingerprint in the identification of a material, but the other information that can be gleaned from a diffraction pattern should be concerned. The diffraction experiment should be adapted to optimize that feature which provides the information desired.

The main components of XRD instrument are an X-ray source, a specimen holder and a detector, and almost all are capable of recording a respectable powder diffraction pattern [58].

Table 2.5 Information from powder x-ray diffraction pattern

Feature	Information
Peak positions (2θ values)	Unit cell dimensions
Non-indexable lines	Presence of a crystalline impurity
Systematically absent reflections	Symmetry
Background	Presence (or absence) of amorphous material
Width of peaks	Crystallite (domain) size, stress/strain and stacking faults
Peak intensities	Crystal structure

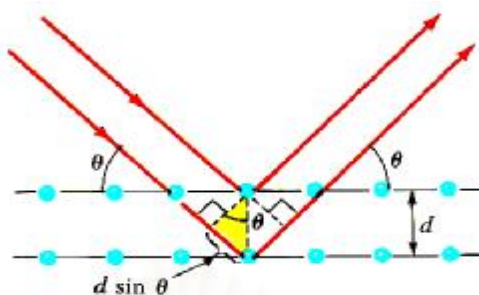


Figure 2.13 Diffraction of X-rays by a crystal.

Figure 2.13 shows a monochromatic beam of X-ray incident on the surface of crystal at angle θ . The scattered intensity can be measured as a function of scattering angle 2θ .

$$n\lambda = 2d \sin\theta$$

From the Bragg equation (above), d is the distance between equivalent atomic planes, θ is the angle between the incident beam and these planes, n is an integer and λ is the wavelength of X-ray source. Then from XRD results, it is able to determine the interplanar spacing of the sample.

2.11.2 N₂ adsorption-desorption technique

A great deal of very useful information is derived from measurement of the physical adsorption of gases on porous solids. The monolayer capacity of non-porous solid, measured by chemisorption, or by physisorption well above the boiling point of the adsorbing gas, can be easily translated into a surface area. The most common adsorbate is probably N₂ at 77 K. Adsorption amount depends on gas pressure, adsorption temperature, and properties of adsorptive gas and adsorbent solid. In nitrogen adsorption isotherm measurement, temperature is constant and gas is limited, thus the isotherm changes according to the property of solid. The surface area of a solid includes both the external surface and the internal surface of the pores. Several forms of isotherm besides the langmuir type have been shown in Figure 2.14. According to the IUPAC definition, microporous materials exhibit a Type I

adsorption-desorption isotherm. Nonporous or macroporous exhibit types II, III, and VI and mesoporous exhibits types IV and V.

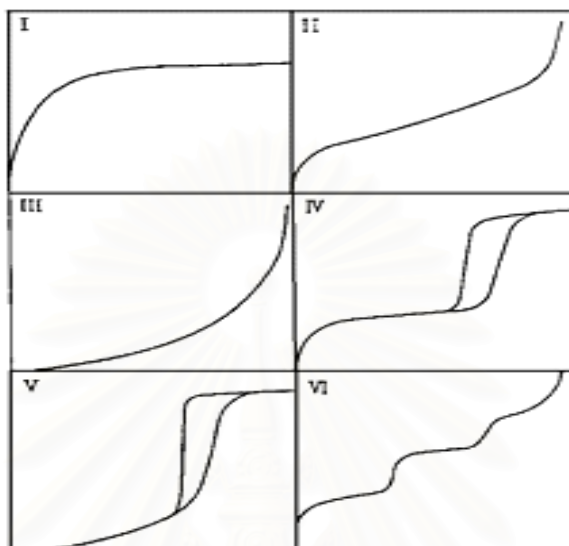


Figure 2.14 The IUPAC classification of adsorption isotherm.

Adsorption isotherms are described as shown in Table 2.6 based on the strength of the interaction between the sample surface and gas adsorbate [33].

Table 2.6 Features of adsorption isotherms

Type	Features	
	Interaction between sample surface and gas adsorbate	Porosity
I	Relatively strong	Micropores
II	Relatively strong	Nonporous
III	Weak	Nonporous
IV	Relatively strong	Mesopore
V	Weak	Micropores or Mesopore
VI	Relatively strong Sample surface has an even distribution of energy	Nonporous

The t-plot method was invented by Lippens and de Boer. Standard isotherm shows the relationship between relative pressure and thickness of adsorption layer. Specific surface area, a_s (m^2/g) can be calculated from the equation 2.3 with the slope of t-plot [59].

$$a_s = \frac{s \times 0.354 \times L \times \sigma}{22414} = 1.541 \times s$$

Where L is Avogadro constant and σ is cross sectional area of adsorptive. There are 3 different types of t-plot isotherm. If t-plot is a linear curve the original point, and thus the adsorbent is considered to be non-porous material. If t-plot has 2 slopes, the one is a sharp slope passing the original point and the other is more gradual slope, it means that the adsorbent has homogenized sized micropores. And the last isotherm that draws a sharp strength line but become smoother curve from some point, it is considered to have mesopores.

MP method measures distribution from the curvature of t-plot. v_p is an integrated value of pore volume (v_1), which can be obtained from below equation.

$$v_1 = (a_1 - a_2) \times (t_1 + t_2) / 2 \times 10^{-3}$$

Although d_{peak} is the peak position it is not suitable for MP method analysis when d_{peak} is below 0.71 nm, due to the same reason for the fact that average pore diameter is not accurate unless 2 or more adsorption layers are formed in pores.

2.11.3 Diffuse reflectance-ultraviolet spectroscopy (DR-UV)

UV-Vis analysis is commonly associated with liquid. However, the state of the art DR-UV cell allows solid to be analyzed. Generally, DR-UV was used to study various metal-containing species, coupled with different epoxides in an attempt to obtain information on the effects of temperature and time on their reaction. Theories of diffuse reflectance are compared and applied to experimental results. Expressions are obtained for the Kubelka-Munk constants and the remission function in terms of fundamental optical parameters. The depth of penetration of light into a

sample is calculated using the modified particle model theory. It is concluded that most powdered samples of only 1-mm thickness can be regarded as infinitely thick for diffuse reflectance purposes. The Kubelka-Munk equation is expressed as follows:

$$f(R) = \frac{(1-R)^2}{2R} = \frac{k}{s}$$

Where R is the absolute reflectance of the sampled layer, k is the molar absorption coefficient and s is the scattering coefficient.

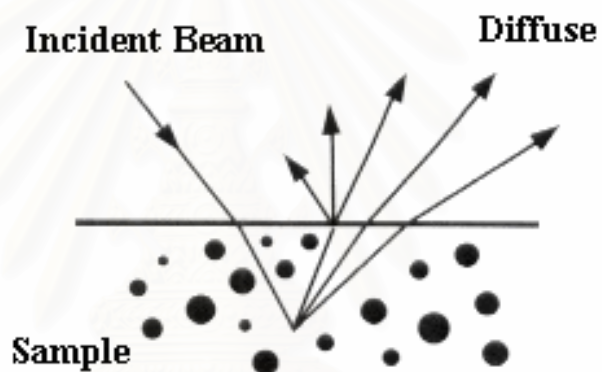


Figure 2.15 Diffuse reflectance beams in the medium system.

CHAPTER III

EXPERIMENTAL

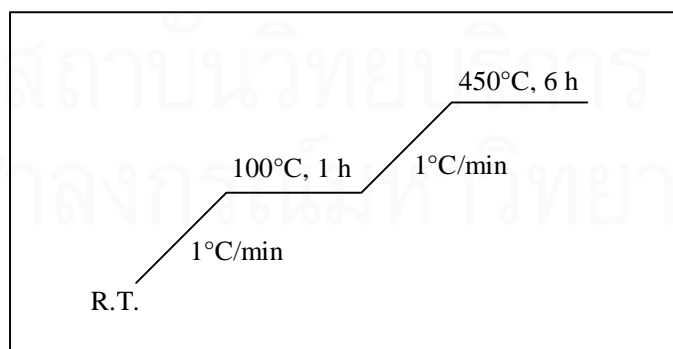
3.1 Instruments, apparatus and analytical techniques

3.1.1 Centrifuge

The separation and collection of the ETS-10 solid after hydrothermal crystallization and metal ion-exchanged ETS-10 were processed by a Sanyo Centaur 2 centrifuge at speed of 6,000 rpm. In addition, this equipment was used in recovering the catalyst after esterification reaction.

3.1.2 Oven and furnace

ETS-10 catalysts were hydrothermally synthesized in a Memmert UM-500 oven at 200°C for 45 h. Moreover, the ETS-10 and metal ion-exchanged ETS-10 catalysts were dried at 100°C, overnight in the oven. The calcination was performed on a Carbolite RHF 1600 muffle furnace in air. Calcination of ETS-10 catalyst was conducted in order to remove moisture and some impurities from the catalyst. The temperature program used for the calcination of ETS-10 catalyst is shown in Scheme 3.1.



Scheme 3.1 The temperature program for the calcination of ETS-10 catalyst.

3.1.3 Powder X-ray diffraction (XRD)

The XRD pattern and d-spacing of ETS-10 and metal ion-exchanged ETS-10 catalysts were determined by a Rigaku, Dmax 2200/Ultima⁺ diffractometer equipped with a monochromator and Cu K α radiation. The tube voltage and current were set at 40 kV and 30 mA, respectively. The diffraction pattern was recorded in the 2-theta ranged from 1 to 45 degree with scan speed of 3 degree/min and scan step of 0.02 degree. The scattering slit, divergent slit and receiving slit were fixed at 0.5 degree, 0.5 degree and 0.15 mm, respectively.

3.1.4 Scanning electron microscopy (SEM)

The morphology and size of ETS-10 and metal ion exchanged ETS-10 particles were identified by a JSM-5410 LV scanning electron microscope (SEM). In SEM analysis, the samples were coated with gold.

3.1.5 Nitrogen adsorption-desorption technique

Microporous surface area and porosity properties of ETS-10 and metal ion-exchanged ETS-10 catalysts were determined by a BEL Japan BELSORP-mini 28SP adsorptometer in t-plot and MP (microporous) mode, respectively. The ETS-10 and metal ion-exchanged ETS-10 samples were degassed at 400°C for 2 h and nitrogen gas was used as an adsorbate at 77 K in measurement step.

3.1.6 Diffuse-reflectance UV-Visible technique (DR-UV)

Titanium coordination in ETS-10 catalyst was measured by a Shimadzu UV-2550 UV-Visible spectrophotometer in the reflectance mode equipped with an integrating sphere of 60° and BaSO₄ as reference. The measurement was in the range of 200 to 400 nm, the sampling interval and slit width were 0.1 nm and 2.0 nm, respectively.

3.1.7 Inductively coupled plasma-atomic emission spectroscopy (ICP-AES)

Titanium contents in the catalysts were analyzed using the Perkin Elmer Plasma-1000 inductively coupled plasma-atomic emission spectrometer (ICP-AES). The sample prepared for ICP-AES and AAS analysis was as in general

procedure of HF digestion of insoluble samples as follows: In a 100-cm³ Teflon beaker 0.0400 g of a calcined catalyst was soaking with 10 cm³ of conc. HCl and subsequently 10 cm³ of 48% hydrofluoric acid (Merck) was added dropwise to get rid off silica in the form of volatile SiF₄. The sample was heated but not boiled until dryness on a hot plate and the fluoride treatment was repeated twice more. An amount of 10 cm³ of a mixture of 6 M HCl : 6 M HNO₃ at a ratio of 1:3 was added slowly and warmed until dryness again. An amount of 10 cm³ deionized water was added to and warmed about 5 min to complete dissolution. The solution was transferred to a 50-cm³ polypropylene volumetric flask and made to the volume with 1,000 ppm of cesium chloride aqueous solution. The flask was capped and shaken thoroughly. The solution was transferred into a plastic bottle with a treaded cap lined under with a polyethylene seal.

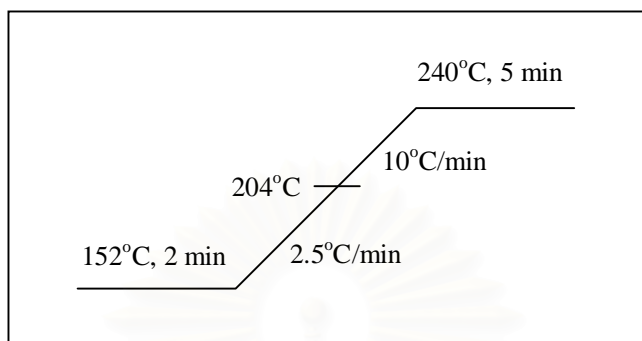
3.1.8 Atomic absorption spectroscopy (AAS)

Varian, 280FS atomic absorption spectroscopy was used in determination of the sodium and potassium contents in the catalysts. The method of preparing sample for AAS analysis was as same as ICP-AES technique described above.

3.1.9 Gas chromatography analysis (GC)

The free fatty acid methyl ester yield can be analyzed by gas chromatography which was carried out on a VARIAN CP-3800 chromatography equipped with split ratio 1:50, flame ionization detector (FID, N₂ as a carrier gas and a 30 m in length of CP-sil-8 column equivalent to HP-5 with a 0.25-mm outer diameter and a 0.25 μm film thickness. The capillary column has maximum temperature limit of 300°C. Eicosane 1.2 x 10⁻¹ M was used as an internal standard for analysis. Samples were prepared for GC analysis by silylation method (Fat and oil derivatives-Fatty Acid Methyl Ester (FAME) – Determination of free and total glycerol and mono-, di-, triglyceride contents (BS EN 14105:2003)) and 1 μL of sample was injected into the column. The GC temperature program for product analysis was 152°C hold for 2 min, programmed at 2.5°C/min up to 204°C,

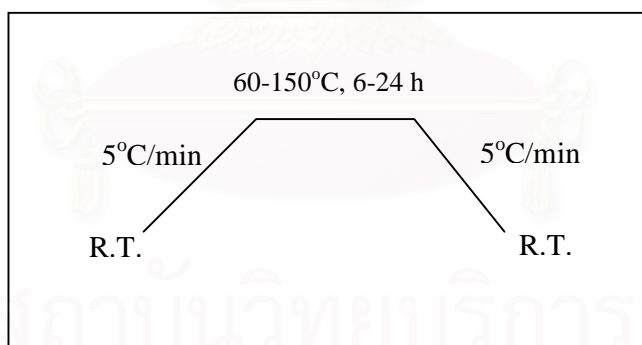
programmed at 10°C/min up to 240°C, final temperature hold for 5 min, it was shown in Scheme 3.2.



Scheme 3.2 The temperature program used for GC analysis of fatty acid methyl ester compounds.

3.1.10 PARR reactor

The esterification reaction of free fatty acids (palmitic acid, oleic acid and linoleic acid) was performed in 100 ml PARR reactor. The temperature program for the reaction was shown in Scheme 3.3.



Scheme 3.3 The temperature program for esterification reaction.

3.2 Chemicals

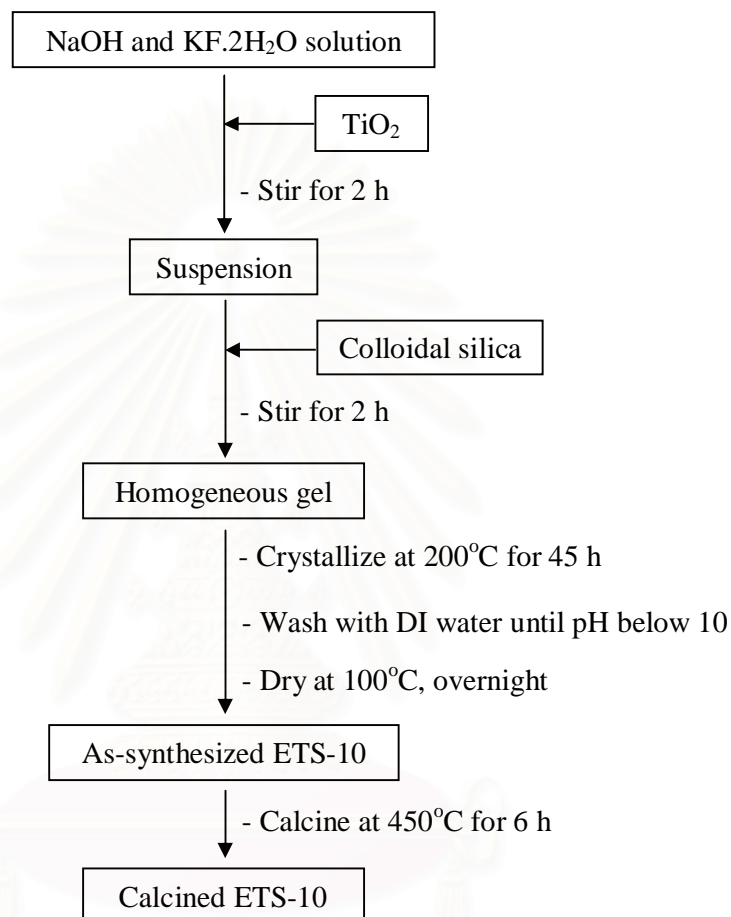
1. Titanium (II) dioxide, TiO_2 (Riedel-deHaën, 99-100.5%)
2. Colloidal silica, SiO_2 (Aldrich, 40%)
3. Sodium hydroxide, NaOH (Merck, 99%)
4. Potassium fluoride dihydrate, $\text{KF} \cdot 2\text{H}_2\text{O}$ (Sigma-Aldrich, 98%)
5. Palmitic acid, $\text{C}_{16}\text{H}_{32}\text{O}_2$ (Fluka, $\geq 97\%$)

6. Oleic acid, C₁₈H₃₄O₂ (Aldrich, 90%)
7. Linoleic acid, C₁₈H₃₂O₂ (Fluka, ≥99%)
8. Methanol, CH₃OH (Merck, 99.9%)
9. Tetrahydrofuran (THF), C₄H₈O (Baker, reagent grade)
10. Eicosane, C₂₀H₄₂ (Fluka, ≥97%)
11. N-methyl-N-trimethylsilyltrifluoroacetamide (MSTFA), (Fluka, ≥97%)
12. Methyl palmitate, C₁₇H₃₄O₂ (Fluka, ≥97.%)
13. Methyl oleate standard, C₁₉H₃₆O₂ (Aldrich, 99%)
14. Methyl linoleate standard, C₁₉H₃₄O₂ (Fluka, ≥98.5%)
15. Acetone, C₃H₆O (Merck, 99.5%)
16. *n*-Hexane, C₆H₁₄ (Lab-Scan, reagent grade)
17. Dichloromethane, CH₂Cl₂ (Lab-Scan, reagent grade)
18. Diethyl ether, (C₂H₅)₂O (Lab-Scan, HPLC grade)
19. Hydrofluoric acid, HF (Merck, 48%)
20. Hydrochloric acid, HCl (CARLO ERBA, 37%)
21. Nitric acid, HNO₃ (Lab Scan, 65%)
22. Cesium chloride, CsCl (Nacalai Tesque, 99%)
23. Potassium hydroxide, KOH (BDH, ≥85%)
24. Rubidium hydroxide, RbOH (Aldrich, 99%)
25. Cesium hydroxide monohydrate, CsOH.H₂O (Fluka, ≥95%)

3.3 Synthesis of ETS-10 catalysts

ETS-10 was hydrothermally synthesized following the chemical composition of the mother gel was adjusted to 5SiO₂: xTiO₂: 3NaOH: KF: 75H₂O, where x = 0.5-1.0 according to Tatsumi, T. *et al.* [18]. The synthesis was prepared in a 500 cm³ 4-necked round bottom flask. In a typical synthesis procedure, titanium dioxide was dispersed in an aqueous solution of sodium hydroxide and potassium fluoride dihydrate. The milky suspension was stirred about 2 h and then the Ludox® HS-40 colloidal silica was added dropwise into the above suspension. After vigorous stirring for 2 h, the resulting white opaque silica–titania hydrogel was transferred to a PTFE-lined PARR autoclave and hydrothermally crystallized at 200°C for 45 h. After the hydrothermal crystallization, the ETS-10 solid was centrifuged and well washed with

deionized water until the pH of the top clear layer became below 10. The product was dried at 100°C overnight and finally calcined to remove the moisture and some volatile impurities at 450°C for 6 h. The ETS-10 synthesis procedure was illustrated in Scheme 3.4.



Scheme 3.4 Diagram of ETS-10 synthesis.



Figure 3.1 Apparatus for ETS-10 synthesis.

3.4 Alkali ion-exchange modification of ETS-10

The sodium, potassium, rubidium and cesium-exchanged ETS-10 catalysts were prepared by treatment of 1 g of as-synthesized ETS-10 using 30 mL of 0.5 M aqueous solutions of sodium hydroxide, potassium hydroxide, rubidium hydroxide and cesium hydroxide monohydrate, respectively, at 60°C under reflux for 3 h. The resulting solid was collected by centrifugation and dried overnight at 100°C, followed by calcination at 450°C for 6 h. Sodium, potassium, rubidium and cesium-exchanged ETS-10 catalysts were referred to as Na-ETS-10, K-ETS-10, Rb-ETS-10 and Cs-ETS-10.

3.5 Standard solution and calibration solution

3.5.1 Methyl palmitate standard solution

3.5.1.1 Stock standard solution 1.0×10^{-1} M

The stock standard solution prepared by weigh approximately 0.2705 g of methyl palmitate into a 10 mL volumetric flask and make up to the mark with THF.

3.5.1.2 Working standard solution 5.0×10^{-2} M

Using a pipette transferred 5 mL of stock solution into a 10 mL volumetric flask and make up to the mark with THF.

3.5.1.3 Working standard solution 1.0×10^{-2} M

Using a pipette transferred 2 mL of working solution 5.0×10^{-2} M into a 10 mL volumetric flask and make up to the mark with THF.

3.5.1.4 Working standard solution 5.0×10^{-3} M

Using a pipette transferred 5 mL of working solution 1.0×10^{-2} M into a 10 mL volumetric flask and make up to the mark with THF.

3.5.1.5 Working standard solution 1.0×10^{-3} M

Using a pipette transferred 2 mL of working solution 5.0×10^{-3} M into a 10 mL volumetric flask and make up to the mark with THF.

3.5.2 Methyl oleate standard solution

3.5.2.1 Stock standard solution 1.0×10^{-1} M

The stock standard solution prepared by weigh approximately 0.2965 g of methyl oleate into a 10 mL volumetric flask and make up to the mark with THF.

3.5.2.2 Working standard solution 5.0×10^{-2} M

Using a pipette transferred 5 mL of stock solution into a 10 mL volumetric flask and make up to the mark with THF.

3.5.2.3 Working standard solution 1.0×10^{-2} M

Using a pipette transferred 2 mL of working solution 5.0×10^{-2} M into a 10 mL volumetric flask and make up to the mark with THF.

3.5.2.4 Working standard solution 5.0×10^{-3} M

Using a pipette transferred 5 mL of working solution 1.0×10^{-2} M into a 10 mL volumetric flask and make up to the mark with THF.

3.5.2.5 Working standard solution 1.0×10^{-3} M

Using a pipette transferred 2 mL of working solution 5.0×10^{-3} M into a 10 mL volumetric flask and make up to the mark with THF.

3.5.3 Methyl linoleate standard solution

3.5.3.1 Stock standard solution 5.0×10^{-2} M

The stock standard solution was prepared by weigh approximately 0.1472 g of methyl linoleate into a 10 mL volumetric flask and make up to the mark with THF.

3.5.3.2 Working standard solution 1.0×10^{-2} M

Using a pipette transferred 2 mL of stock solution into a 10 mL volumetric flask and make up to the mark with THF.

3.5.3.3 Working standard solution 5.0×10^{-3} M

Using a pipette transferred 5 mL of working solution 1.0×10^{-2} M into a 10 mL volumetric flask and make up to the mark with THF.

3.5.3.4 Working standard solution 1.0×10^{-3} M

Using a pipette transferred 2 mL of working solution 5.0×10^{-3} M into a 10 mL volumetric flask and make up to the mark with THF.

3.5.3.5 Working standard solution 5.0×10^{-4} M

Using a pipette transferred 5 mL of working solution 1.0×10^{-3} M into a 10 mL volumetric flask and make up to the mark with THF.

3.5.4 Standard calibration solution

Five calibration solutions were prepared into a series of vials. The weigh 2.5 g of stock and working methyl palmitate, methyl oleate and methyl linoleate solutions were transferred into the five vials and added 0.5 g of internal standard eicosane stock solution 1.2×10^{-1} M to the five standard solutions. After that, the five standard solutions of each methyl esters were analyzed by GC technique under the condition described above (3.1.9). Preparation of calibration solutions listed in Table 3.1, 3.2 and 3.3.

Table 3.1 Preparation of standard methyl palmitate calibration solution

Methyl palmitate calibration solution	1	2	3	4	5
1.0×10^{-1} M (g)	2.50	-	-	-	-
5.0×10^{-2} M (g)	-	2.50	-	-	-
1.0×10^{-2} M (g)	-	-	2.50	-	-
5.0×10^{-3} M (g)	-	-	-	2.50	-
1.0×10^{-3} M (g)	-	-	-	-	2.50
Internal standard solution 1.2×10^{-1} M (g)	0.50	0.50	0.50	0.50	0.50

Table 3.2 Preparation of standard methyl oleate calibration solution

Methyl oleate calibration solution	1	2	3	4	5
1.0×10^{-1} M (g)	2.50	-	-	-	-
5.0×10^{-2} M (g)	-	2.50	-	-	-
1.0×10^{-2} M (g)	-	-	2.50	-	-
5.0×10^{-3} M (g)	-	-	-	2.50	-
1.0×10^{-3} M (g)	-	-	-	-	2.50
Internal standard solution 1.2×10^{-1} M (g)	0.50	0.50	0.50	0.50	0.50

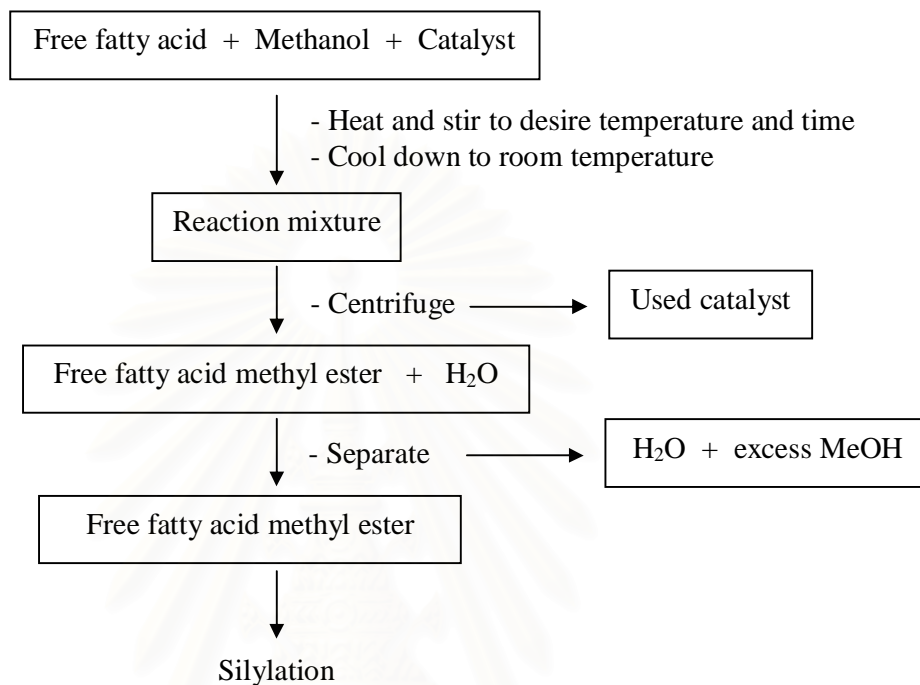
Table 3.3 Preparation of standard methyl linoleate calibration solution

Methyl linoleate calibration solution	1	2	3	4	5
5.0×10^{-2} M (g)	2.50	-	-	-	-
1.0×10^{-2} M (g)	-	2.50	-	-	-
5.0×10^{-3} M (g)	-	-	2.50	-	-
1.0×10^{-3} M (g)	-	-	-	2.50	-
5.0×10^{-4} M (g)	-	-	-	-	2.50
Internal standard solution 1.2×10^{-1} M (g)	0.50	0.50	0.50	0.50	0.50

3.6 Esterification of free fatty acids procedure

The esterification reaction was performed in a PARR 4843 reactor using palmitic acid, oleic acid and linoleic acid (Free fatty acids, FFA) and methanol as starting materials. The reaction was conducted in the presence of 9 mole of methanol to 1 mole of free fatty acid over 10 wt.% of ETS-10 or alkali exchanged ETS-10 catalysts. The reaction mixture was continuously stirred to reach reaction temperature and reaction time. After reaction, the sample chamber was cooled down to room temperature and the used catalyst was separated from the liquid phase by centrifugation. The reaction mixture was separated free fatty acid methyl ester phase (bottom phase) from mixed water and methanol phase (top phase) by separate funnel. After that, the free fatty acid methyl ester was silylated with N-methyl-N-trimethylsilyltrifluoroacetamide (MSTFA). The used catalyst was washed with

acetone, dried and calcined for reuse and regeneration. The esterification of free fatty acid procedure was illustrated in Scheme 3.5.



Scheme 3.5 Diagram of esterification reaction of free fatty acids with methanol.

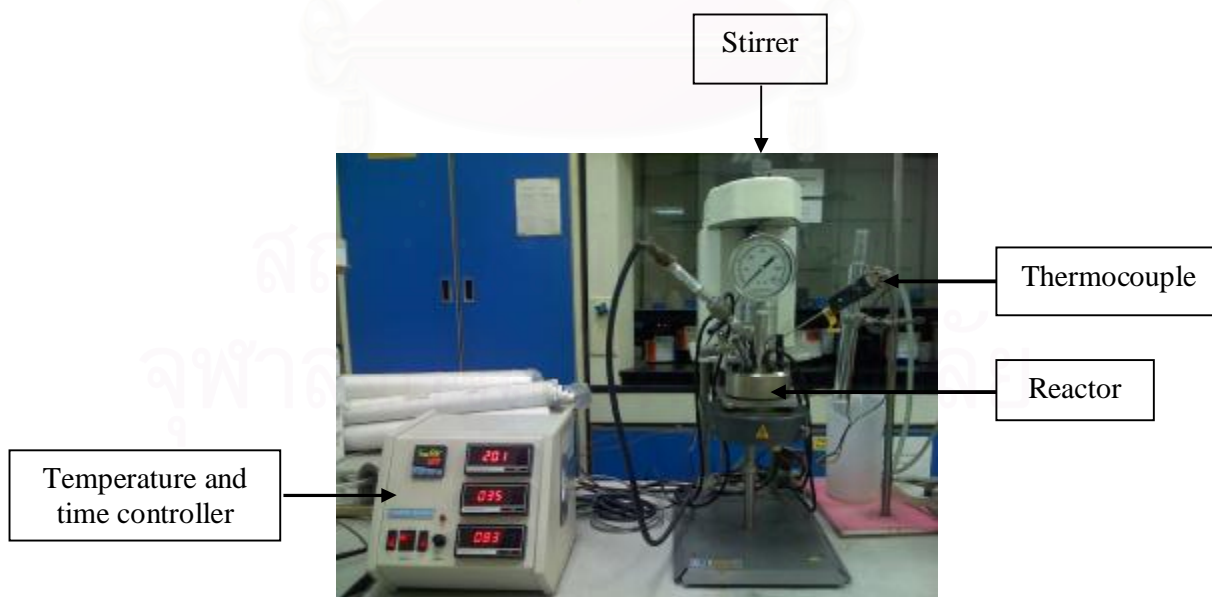
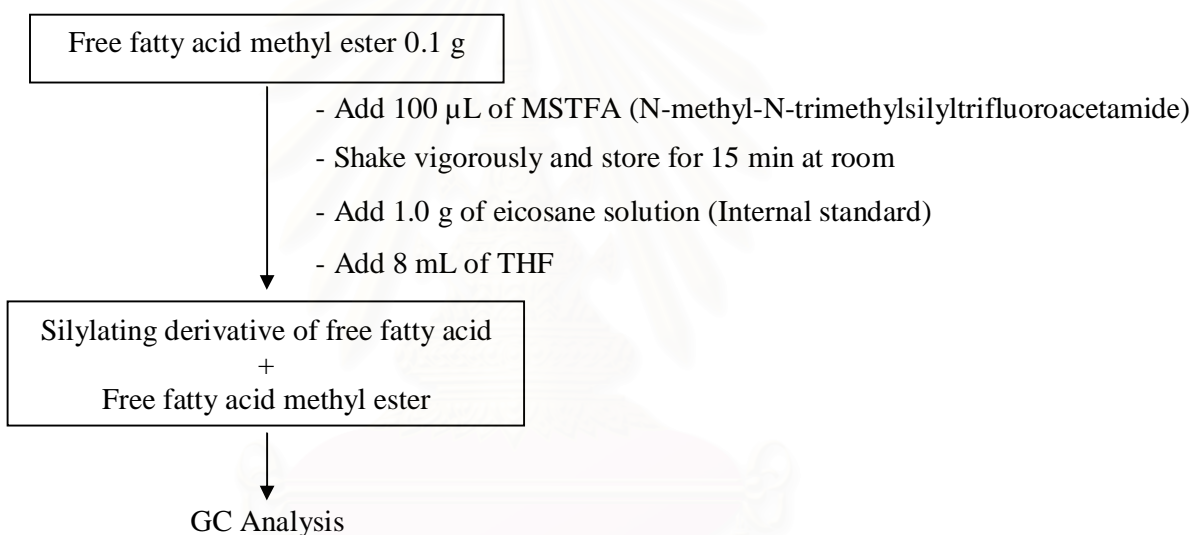


Figure 3.2 Apparatus for esterification reaction.

3.7 Silylation procedure [ASTM D 6584 and BS EN 14103:2003]

One hundred milligrams of free fatty acid methyl ester was silylated with 100 μL of MSTFA then, shaken vigorously and stored at room temperature for 15 minutes. Inclusion of MSTFA appeared to help reduce clumping due to agitation and freezing of the free fatty acid methyl ester (biodiesel). After that, one gram of internal standard stock solution (1.2×10^{-1} M eicosane in THF) and 8 mL of THF were added before gas chromatography analysis. Each GC run contained 1 μL of solution. A modified temperature profile was defined as section 3.1.9. The silylation procedure was illustrated in Scheme 3.6.



Scheme 3.6 Diagram of silylation of free fatty acid.

3.8 Parameters affecting esterification reaction

3.8.1 Effect of catalyst modification method

Esterification reaction of free fatty acids was performed according to the general procedure mentioned above. The effect of catalyst type was studied using the ETS-10, N-ETS-10, K-ETS-10, Rb-ETS-10 and Cs-ETS-10 catalysts. The calcined catalysts (450°C for 6 h) were introduced to the reaction mixture at MeOH to free fatty acid (FFA) mole ratio of 9:1. The reaction was performed at 120°C for 24 h, stirring speed 200 rpm and amount of catalyst 10 wt%.

3.8.2 Effect of catalyst amount

The effect of catalyst loading was also studied in esterification reaction. The catalyst amounts to reaction mixture were varied to 2.5-15 wt% at methanol to FFA mole ratio of 9:1 at 110-120°C for 18-24 h and stirring speed 200 rpm.

3.8.3 Effect of methanol to free fatty acid mol ratio

The esterification reaction was performed at various methanol to FFA mole ratios according to the general procedure described above. The effect of methanol to FFA mole ratios were investigated at the value of 6:1-30:1 at 100-120°C for 18 h, stirring speed 200 rpm and amount of catalyst 10 wt%.

3.8.4 Effect of reaction time

The reaction time was studied for 6-24 h at 100-120°C. The methanol to FFA mole ratio 9:1, amount of catalyst 10 wt% and stirring speed 200 rpm.

3.8.5 Effect of reaction temperature

To investigate the effect of temperature and time in esterification reaction, the reaction was also performed at various temperatures as the general procedure above. The reaction temperature was varied to 60-150°C and methanol to FFA mole ratio 9:1 and the reaction time was kept for 24 h.

3.8.6 Activity of reused catalyst

The used Rb-ETS-10 catalyst was tested for their activity again without any treatment except washing with acetone and calcination at 450°C for 6 h.

3.8.7 Activity of Rb-reloaded catalyst

After reaction, the catalyst was washed with acetone to remove some impurities. Then it was dried overnight at 100°C and calcined at 450°C for 6 h. The used catalyst was reloaded with Rb source by ion-exchanged method prior to use. The catalytic activity of Rb-reloaded catalyst was also studied in esterification reaction at FFA to methanol mole ratio of 9:1, at 110-120°C, and for 18-24 h. Moreover, the retained structure of catalyst was confirmed by XRD technique.

CHAPTER IV

RESULTS & DISCUSSIONS

4.1 Physical and chemical properties of catalysts

4.1.1 Powder X-ray diffraction (XRD)

(a) ETS-10 catalyst

The influence of $\text{SiO}_2/\text{TiO}_2$ mole ratio of the initial gels on the formation of ETS-10 was examined in system $5\text{SiO}_2: x\text{TiO}_2: 3\text{NaOH}: \text{KF}: 75\text{H}_2\text{O}$, where x was varied between 0.5-1.0. Figure 4.1 shows the XRD patterns of the final solid products both as-synthesized and calcined. It can be seen that the ratio of $\text{SiO}_2/\text{TiO}_2$ has a significant influence on the quality of ETS-10. All samples proved to be mainly ETS-10 structure at 24.7° of 2-theta, together with co-crystallized anatase at 25.3° of 2-theta and small amount of quartz at 21° and 26.8° of 2-theta [14]. At 0.75 mole of TiO_2 , the XRD pattern indicated rising in the crystallinity of ETS-10 phase and decreasing of quartz impurity phase. Highly pure ETS-10 can only be obtained at 0.75 mole of TiO_2 . At 0.5 mole of TiO_2 , quartz impurity phase increases from XRD results. The formation of the quartz phase increased with a decreasing amount of TiO_2 due to increasing of Si/Ti mole ratio in gel. The excess silica reacts with alkali base in gel [50] and self-condensation and polymerization under the experimental condition to produce a quartz impurity, the mechanism of polymerization of silicate is shown in Figure 4.2 [14]. However, the sample is prepared by using 0.75 mole of TiO_2 giving the highest pure ETS-10 phase then this sample will be used in alkali ion-exchange process.

(b) Alkali ion-exchange modification of ETS-10 catalyst

After the ETS-10 synthesis, basic strength of catalyst was modified by ion-exchanged method with sodium hydroxide, potassium hydroxide, rubidium hydroxide and cesium hydroxide monohydrate solution to receive alkali ion-

exchanged ETS-10 catalyst denoted as Na-ETS-10, K-ETS-10, Rb-ETS-10 and Cs-ETS-10, respectively.

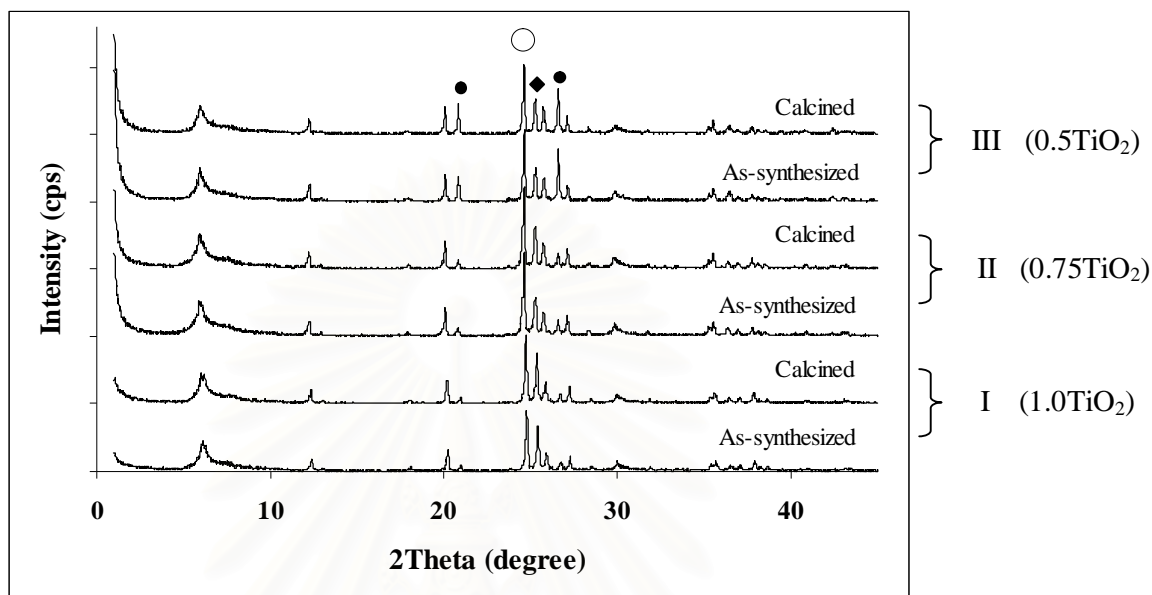


Figure 4.1 XRD patterns of as-synthesized and calcined ETS-10 (○ represents ETS-10 phase and ● represents quartz impurity phase and ◆ represents anatase phase and * present unidentified crystalline phase).

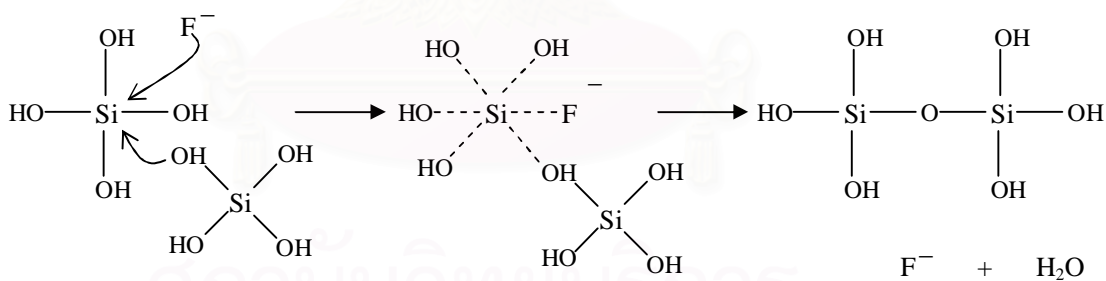


Figure 4.2 A proposed mechanism of polymerization of silicate species catalyzed by F⁻ ion.

XRD patterns of calcined alkali-exchanged ETS-10 catalysts from parent ETS-10 using 0.75 mole of TiO₂ are shown in Figure 4.3. Na-ETS-10, K-ETS-10, Rb-ETS-10 and Cs-ETS-10 maintain characteristic peaks of the ETS-10 structure without other impurity phases from ETS-10 parent sample. However, the intensity of ETS-10 peaks decrease by increasing alkaline metal radius. The main reason is

probably the scattering effect of alkali metal cations to X-ray. Rb-ETS-10 and Cs-ETS-10 samples contain a larger number of randomly distribution electrons [19].

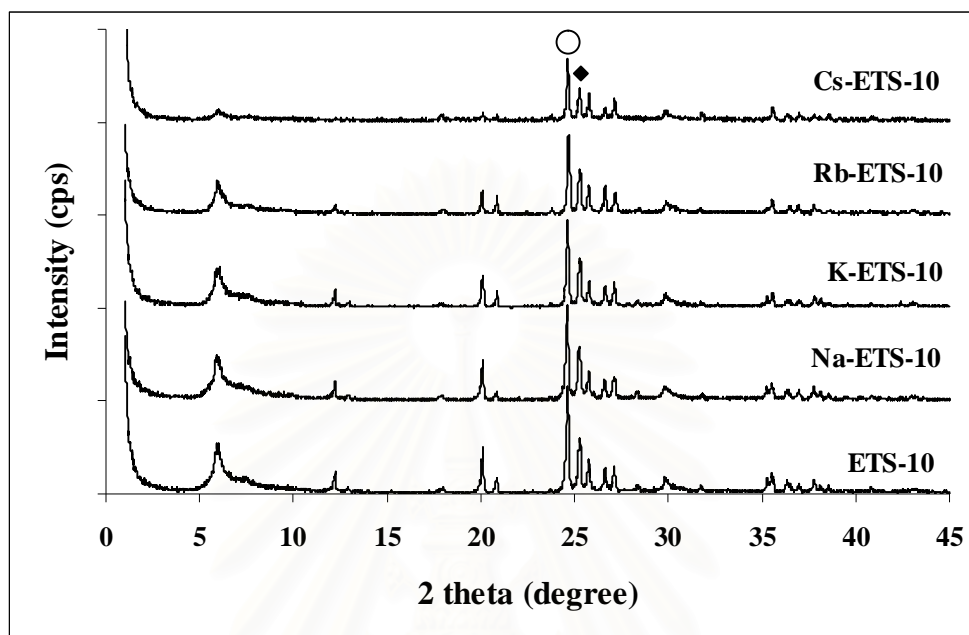


Figure 4.3 XRD patterns of calcined alkali-exchanged ETS-10 (○ represents ETS-10 phase and ◆ represents anatase phase).

4.1.2 Scanning electron microscopy (SEM)

(a) ETS-10 catalyst

The SEM images of calcined ETS-10 samples synthesized with different amount of TiO_2 from gel composition $5\text{SiO}_2 : x\text{TiO}_2 : 3\text{NaOH} : \text{KF} : 75\text{H}_2\text{O}$, where $x = 0.5-1.0$ are shown in Figure 4.4. It indicates that ETS-10 (1.0TiO_2) has the morphology as quasi-cubic shape and the particles tend to agglomerate. The particle size of ETS-10 synthesized from 1.0TiO_2 was in the range of 300-500 nm. The both ETS-10 samples prepared from 0.75 and 0.5TiO_2 display mixed a quasi-cubic form and bipyramid morphology and they tend to agglomerate with a particle sizes of about 300-500 nm. The agglomeration leads to elongated crystal assemblies as shown for the pure ETS-10 sample.

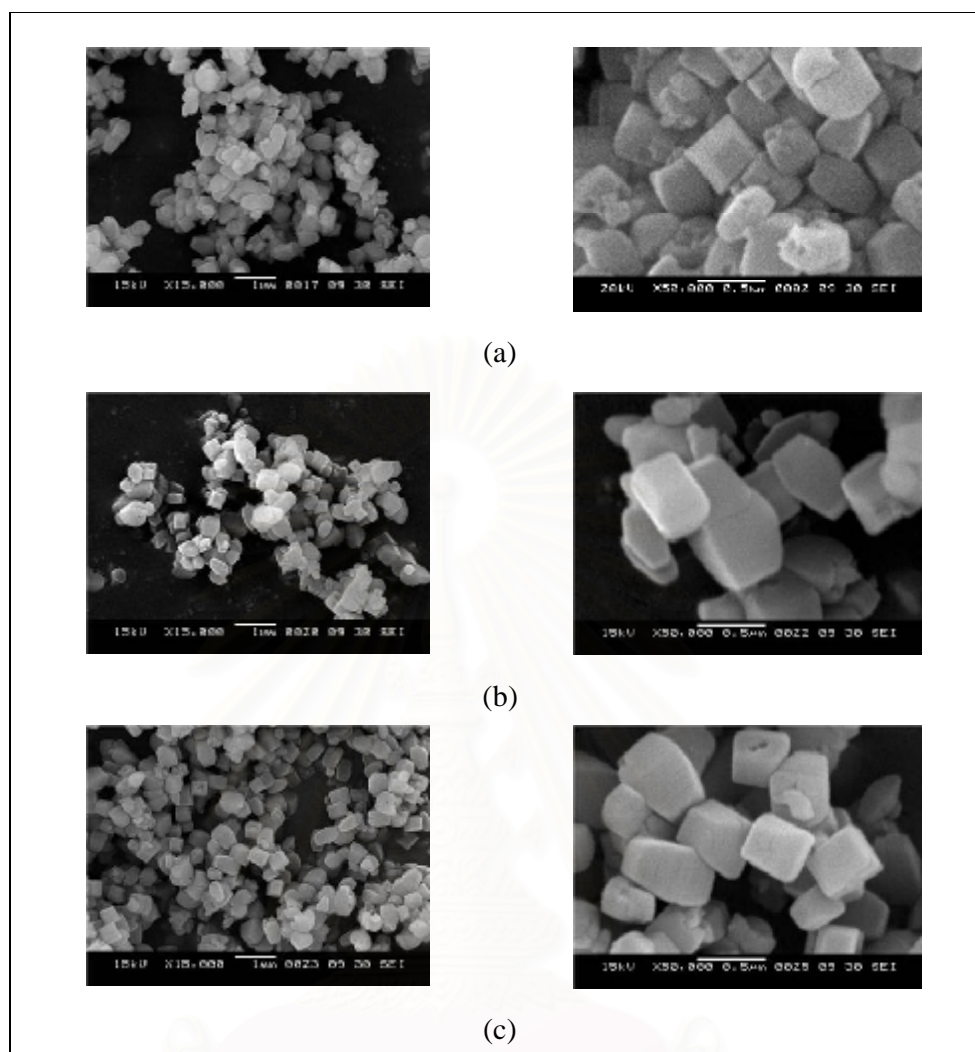


Figure 4.4 SEM images of ETS-10 synthesized from gel composition $5\text{SiO}_2: x\text{TiO}_2: 3\text{NaOH}: \text{KF}: 75\text{H}_2\text{O}$, where $x = 1.0$ (a), $x = 0.75$ (b) and $x = 0.5$ (c).

(b) Alkali ion-exchange modification of ETS-10 catalyst

The structure modification is confirmed by scanning electron microscopy technique. SEM images of calcined alkali ion-exchanged ETS-10 catalysts from parent ETS-10 using 0.75 mole of TiO_2 are shown in Figure 4.5. The Na-ETS-10, K-ETS-10, Rb-ETS-10 and Cs-ETS-10 samples display a similar morphology as parent ETS-10 with particle sizes ranging from 300-500 nm, indicating that the incorporation of the ion atoms into the framework of ETS-10 hardly affected the particle morphology. In addition, it was clear that no other new phases occurred after exchange ETS-10 with sodium, potassium, rubidium and cesium ions.

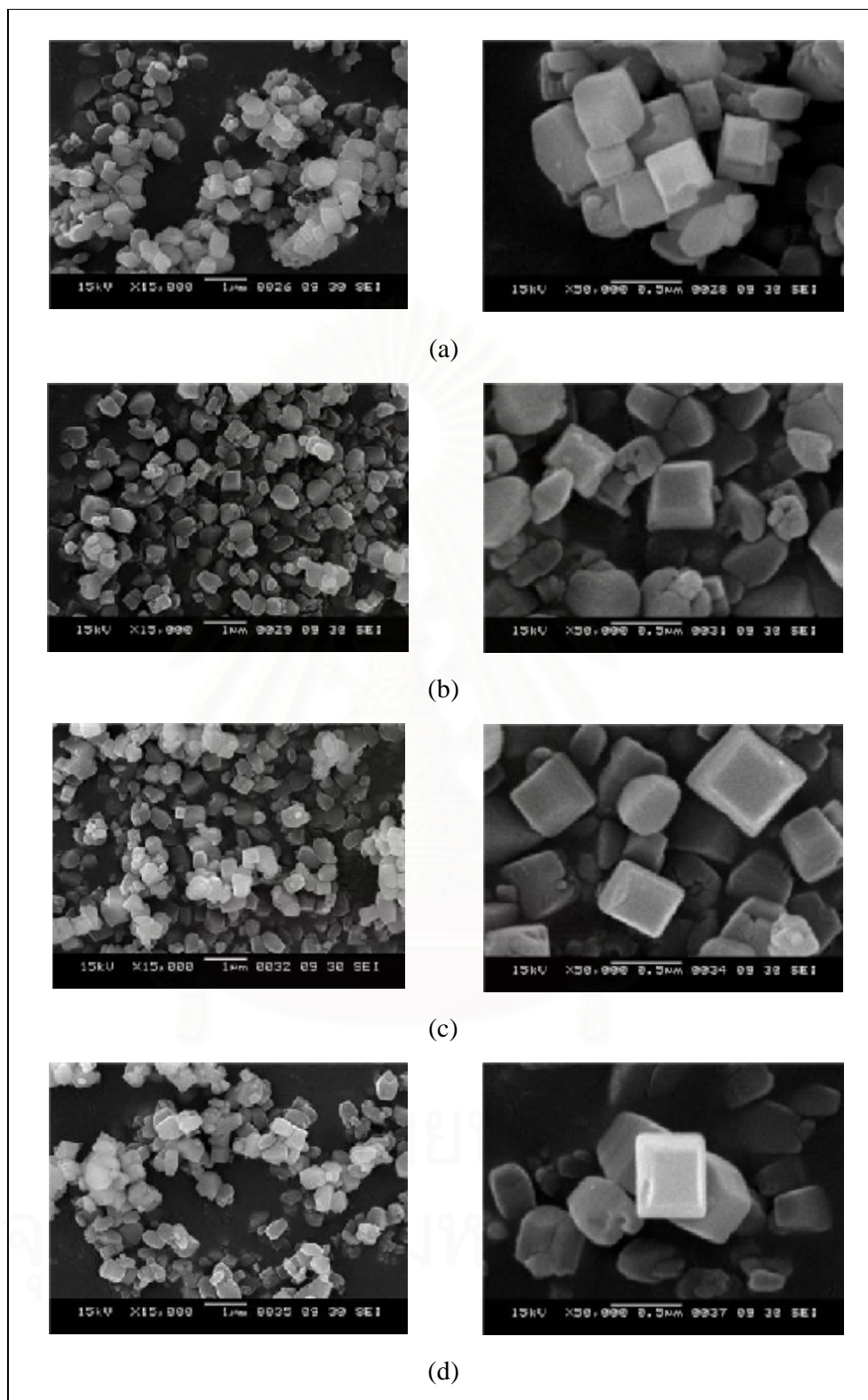


Figure 4.5 SEM images of calcined Na-ETS-10 (a), K-ETS-10 (b), Rb-ETS-10 (c) and Cs-ETS-10 (d).

4.1.3 N₂- adsorption/desorption

ETS-10 prepared from gel composition $5\text{SiO}_2: x\text{TiO}_2: 3\text{NaOH}: \text{KF}: 75\text{H}_2\text{O}$, where $x = 0.5-1.0$ and alkali ion-exchanged ETS-10 (0.75TiO_2) sample exhibits a N₂ adsorption isotherm of type I, characteristic of micropores as shown in Figure A-1 (appendices). Some physical properties derived from the adsorption isotherms of ETS-10 and alkali-exchanged ETS-10 samples are compiled in Table 4.1. BET specific surface areas of ETS-10 prepared from various moles of TiO₂ for x equal to 0.75 was higher than that, x are 1.0 and 0.5, respectively and also similar trend for their external surface areas. All of them have the same average pore diameter of 0.6 nm. Na-ETS-10, K-ETS-10, Rb-ETS-10 and Cs-ETS10 samples exhibit lower BET specific surface area compared with parent ETS-10 (0.75TiO_2) because the alkali metal species transfer into ETS-10 pore structure. The BET specific surface area significantly decreases about 31%, 36%, 39% and 52% after increasing cation size from Na⁺, K⁺, Rb⁺ and Cs⁺, respectively. However, the alkali ion-exchanged samples maintain average pore diameter values in the range of typical porous materials. All samples exhibit low external surface area as an usual behavior of microporous zeolites.

Table 4.1 Some physical properties of calcined ETS-10 and alkali ion-exchanged ETS-10 catalysts

Sample	BET specific surface area, a_s ($m^2 g^{-1}$)	External surface area, a_{ext} ($m^2 g^{-1}$)	Micropore volume, V_p ($m^3 g^{-1}$)	Average pore diameter, d_p (nm)
Gel composition ; 5SiO ₂ : 1.0TiO ₂ : 3NaOH : KF : 75H ₂ O				
ETS-10	422.7	7.7	0.13	0.6
Gel composition ; 5SiO ₂ : 0.75TiO ₂ : 3NaOH : KF : 75H ₂ O				
ETS-10	571.1	10.9	0.17	0.6
Na-ETS-10	391.7	4.7	0.12	0.6
K-ETS-10	365.3	5.7	0.11	0.6
Rb-ETS-10	346.6	6.6	0.10	0.6
Cs-ETS-10	273.1	12.6	0.08	0.6
Gel composition ; 5SiO ₂ : 0.5TiO ₂ : 3NaOH : KF : 75H ₂ O				
ETS-10	400.9	8.1	0.12	0.6

4.1.4 Diffuse-reflectance-ultraviolet spectroscopy (DR-UV)

(a) ETS-10 catalyst

Form of titanium in ETS-10 can be divided into three types. The first one at 245 nm is tetrahedral form ($O=TiO_4^{-4}$) at extra-framework position. The second is octahedral form (TiO_6^{-8}) at 280 nm and the last one is anatase (TiO_2) at 330 nm. The absorption spectra of parent and modified ETS-10 samples are shown in Figures 4.6 and 4.7. In Figure 4.6, three UV absorption bands at 245, 280 and 330 nm attributed to the O2p to Ti3d charge transfer (CTT) were observed. The bands at 245

and 280 were assigned to the charge transfer from Si-O-Ti linking and Ti-O-Ti linking, respectively. The two absorption bands in the range of 260-330 nm were observed. They would be assigned to the charge transfer from Ti-O-Ti-linking with different Ti-O lengths according to Tasumi, T. *et al.* [18]. The band at 215 nm typically assigned to framework was not observed. This is different from other zeolite-structure titanosilicates like TS-1, which usually exhibits the band at 215 nm. The band at 330 nm is assigned to anatase and it was confirmed by XRD diffraction peak at 2-theta about 25.3.

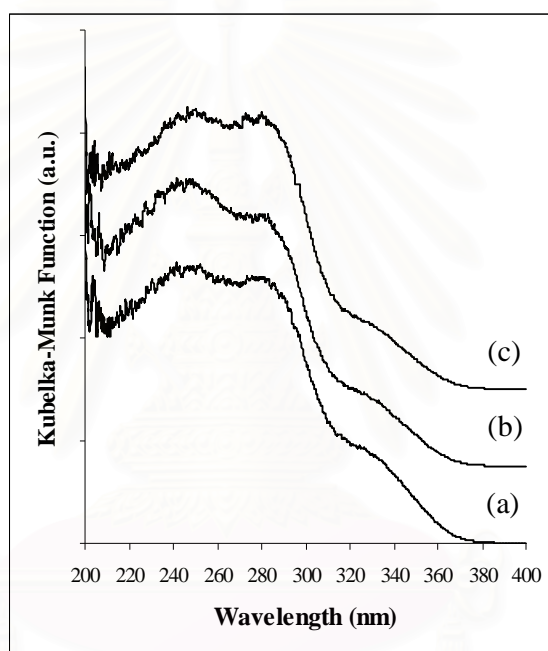


Figure 4.6 DR-UV spectra of calcined ETS-10 synthesized from gel composition $5\text{SiO}_2: x\text{TiO}_2: 3\text{NaOH}: \text{KF}: 75\text{H}_2\text{O}$, where $x = 1.0$ (a), $x = 0.75$ (b) and $x = 0.5$ (c).

(b) Alkali ion-exchange modification of ETS-10 catalyst

From DR-UV spectra in Figure 4.7, it is obvious that Na-ETS-10, K-ETS-10, Rb-ETS-10 and Cs-ETS-10 catalysts prepared from gel composition $5\text{SiO}_2: 0.75\text{TiO}_2: 3\text{NaOH}: \text{KF}: 75\text{H}_2\text{O}$ show three absorption bands located in the same wavelength range except intensity of octahedral form at 280 nm was decreased, by reason of larger atom size of alkali metal exchanged ETS-10 overshadowed on the TiO_6^{-8} octahedral. This result indicates that sodium, potassium, rubidium and cesium

species were in octahedral site and do not have any effects on the tetrahedral titanium species.

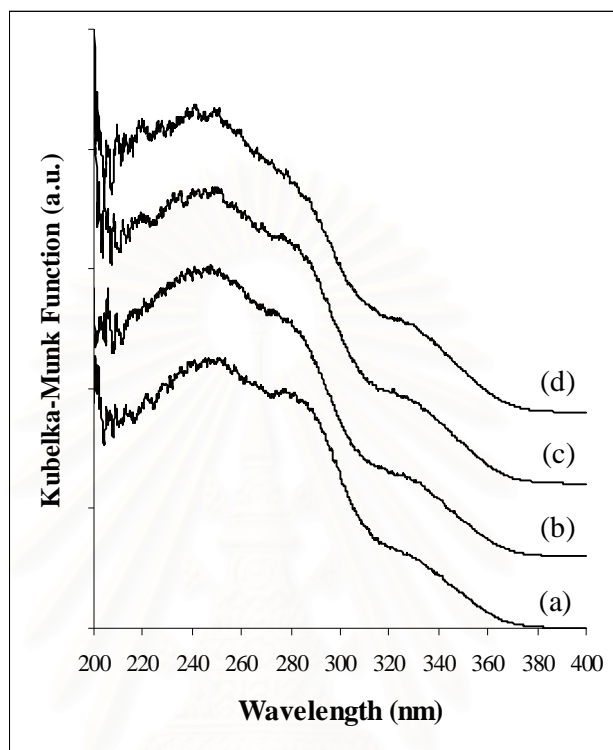


Figure 4.7 DR-UV spectra of calcined Na-ETS-10 (a), K-ETS-10 (b), Rb-ETS-10 (c) and Cs-ETS-10 (d).

4.1.5 Elemental ratios in ETS-10 catalysts

ETS-10 prepared from gel composition $5\text{SiO}_2: x\text{TiO}_2: 3\text{NaOH}: \text{KF}: 75\text{H}_2\text{O}$, where $x = 0.5-1.0$. The titanium content in ETS-10 catalyst was determined by ICP-AES, whereas amounts of sodium and potassium were obtained by AAS. The analysis data are compiled in Table 4.2. If the SiO_2 content is maintained constant at 5.0 mole, while the TiO_2 content in the gel was decreased between 1.0, 0.75 and 0.5 mole. The Si/Ti mole ratio was increased, respectively and also similar trend occurred with Na/Ti and K/Ti mole ratios. The Si/Ti mole ratios of all products were less than in starting gel.

Table 4.2 Elemental analysis of ETS-10 at various mole of TiO₂

Sample	Si/Ti ^a		Na ^b /Ti	K ^b /Ti
	in gel	in product		
ETS-10 (1.0TiO ₂)	5.00	4.35	0.64	0.23
ETS-10 (0.75TiO ₂)	6.67	5.61	0.83	0.27
ETS-10 (0.5TiO ₂)	10.0	7.72	0.88	0.28

^a from ICP-AES analysis

^b from AAS analysis

4.1.6 Scanning electron microscopy-energy dispersive X-ray (SEM-EDX)

SEM-EDX technique was used in the measurement of sodium, potassium, rubidium and cesium amount in alkali cation-exchanged ETS-10 catalysts. Alkali content in alkali-exchanged ETS-10 catalysts from parent ETS-10 using 0.75 mole of TiO₂ are shown in Table 4.3. The alkali content in freshly ion-exchange ETS-10 catalysts varied from 12.2 to 5.4 weight percentage in order of Cs⁺, Na⁺, Rb⁺ and K⁺, respectively. As expected after the first run reaction, alkali content was dramatically decreased in range 9.5 to 3.7 wt%. K-ETS-10 catalyst is the highest alkali leaching out sample from 5.39 to 3.71 wt%. While, Na-ETS-10 shows the least alkali leaching out only 1.34 wt% from 8.82 wt%.

สถาบันวิทยบริการ
จุฬาลงกรณ์มหาวิทยาลัย

Table 4.3 Elemental contents in fresh and after reaction alkali-exchanged ETS-10 catalysts

Sample	Elemental contents (%wt)				Alkali content loss after rxn. (%)
	Na	K	Rb	Cs	
Na-ETS-10	8.82				
Na-ETS-10 after rxn.	7.48				15.19
K-ETS-10		5.39			
K-ETS-10 after rxn.		3.71			31.17
Rb-ETS-10			7.87		
Rb-ETS-10 after rxn.#1			6.47		17.79
Rb-ETS-10 after rxn.#2			5.34		32.14
Regenerated Rb-ETS-10			11.35		
Cs-ETS-10				12.17	
Cs-ETS-10 after rxn.				9.47	22.19

4.2 Standard calibration curve

4.2.1 Methyl oleate calibration curve

The standard calibration curve of methyl oleate is shown in figure 4.8.

The standard curve equation is expressed as following

$$y = 1.2247x + 0.0733$$

where y is M_{MO}/M_{Int} ; M_{MO} = Mass of methyl oleate (g)
 M_{Int} = Mass of internal standard (g)
 x is A_{MO}/A_{int} ; A_{MO} = Peak area of methyl oleate
 A_{Int} = Peak area of internal standard

The correlation coefficient R^2 value for methyl oleate calibration curve is 0.9998

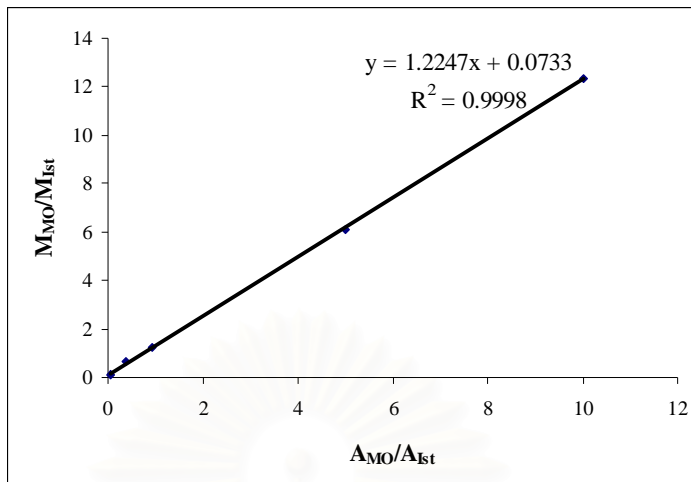


Figure 4.8 Calibration curve of methyl oleate.

4.2.2 Methyl palmitate calibration curve

The standard calibration curve of methyl palmitate is shown in figure 4.9. The standard curve equation is expressed as following

$$y = 1.4488x + 0.0181$$

where y is M_{MP}/M_{Int} ; M_{MP} = Mass of methyl palmitate (g)
 M_{Int} = Mass of internal standard (g)
 x is A_{MP}/A_{int} ; A_{MP} = Peak area of methyl palmitate
 A_{Int} = Peak area of internal standard

The correlation coefficient R^2 value for methyl palmitate calibration curve is 0.9997

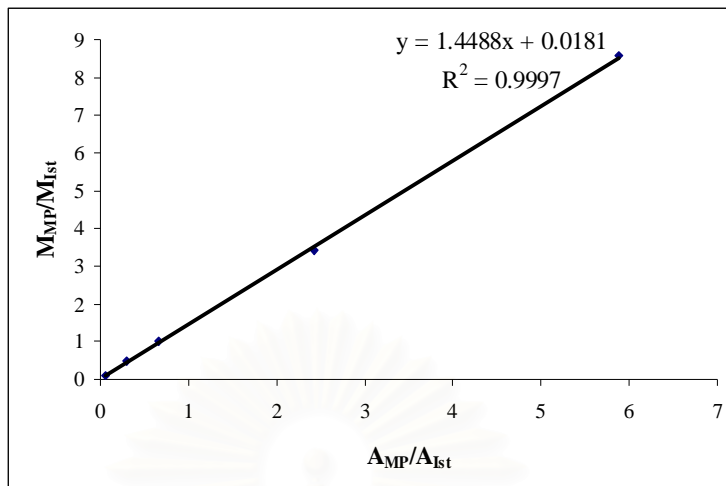


Figure 4.9 Calibration curve of methyl palmitate.

4.2.3 Methyl linoleate calibration curve

The standard calibration curve of methyl linoleate is shown in figure 4.10. The standard curve equation is expressed as following

$$y = 0.0143x + 0.0006$$

where y is M_{ML}/M_{Int} ; M_{ML} = Mass of methyl linoleate (g)
 M_{Int} = Mass of internal standard (g)
 x is A_{ML}/A_{int} ; A_{ML} = Peak area of methyl linoleate
 A_{Int} = Peak area of internal standard

The correlation coefficient R^2 value for methyl linoleate calibration curve is 0.9997

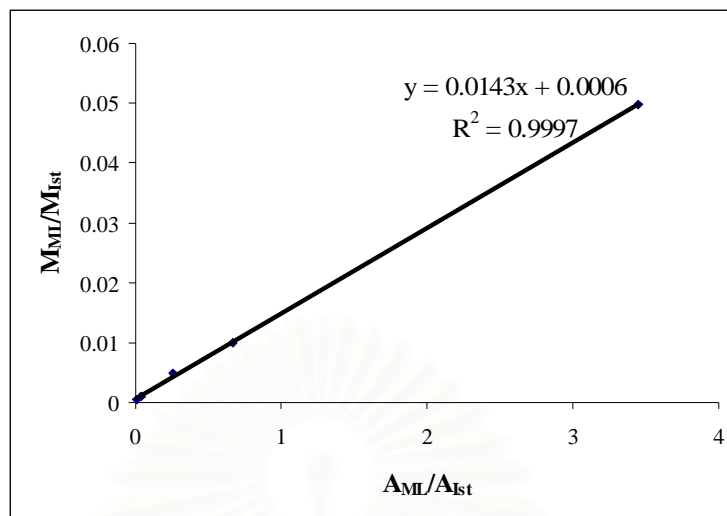


Figure 4.10 Calibration curve of methyl linoleate.

From methyl oleate, methyl palmitate and methyl linoleate calibration curves, the integrated areas were converted to mole percentage for present component in each sample. From these calibration results confirm the exactly measurement method to quantify the methyl ester products from esterification in the following experiments.

4.3 Catalytic activity of ETS-10 and alkali-exchanged ETS-10 in esterification reaction of free fatty acid

4.3.1 Esterification of oleic acid

4.3.1.1 Catalytic activity of ETS-10 and alkali-exchanged ETS-10

The ETS-10 prepared from 0.75 mole of TiO_2 in gel and alkali exchanged ETS-10 base materials are compared in their catalytic activities in esterification reaction of oleic acid at 9:1 mole ratio of methanol to oleic acid, $120^\circ C$ for 24 h and 10 wt% of catalyst and the results are shown in Table 4.4. The corresponding plot of methyl oleate yield versus type of catalyst is shown in Figure 4.11. Comparing to the blank test, ETS-10 sample is moderately active for esterification of oleic acid to methyl oleate. ETS-10 provides 26.6% yield higher than blank test, whereas, provides 20.6% lower than K-, Rb and Cs-ETS-10 catalysts. K-ETS-10, Rb-ETS-10 and Cs-ETS-10 catalysts gave an excellent yield whereas Na-

ETS-10 exhibits 92.75%. Among alkali-ion exchanged ETS-10 base catalysts, the order of reactivity in esterification reaction of oleic acid was K-ETS-10 = Rb-ETS-10 = Cs-ETS-10 > Na-ETS-10 > ETS-10. Base-modified ETS-10 catalysts provide higher methyl oleate yield compared to parent ETS-10.

Table 4.4 The catalytic activity of ETS-10 and alkali-exchanged ETS-10 catalysts in esterification reaction of oleic acid

Catalyst	Methyl oleate yield (%mole)
None	52.81
ETS-10 (0.75TiO ₂)	79.42
Na-ETS-10	92.75
K-ETS-10	100
Rb-ETS-10	100
Cs-ETS-10	100

Reaction condition: 10 %wt catalyst, 9:1 of MeOH to oleic acid mole ratio at 120°C, for 24 h and stirring speed 200 rpm.

Both K-ETS-10 and Rb-ETS-10 catalysts exhibit the highest methyl oleate yield of 100% at 120°C for 24 h. Nevertheless, it could not confirm which catalysts show better activity. Accordingly, the oleic acid esterification was done at milder condition to test activities of K-ETS-10 and Rb-ETS-10 catalysts. Table 4.5 shows catalytic activities of K-ETS-10 and Rb-ETS-10 at 110°C for 18 h. The Rb-ETS-10 catalyst still provides 100% of methyl oleate yield higher than K-ETS-10. Cs-ETS-10 catalyst was not tested in this study because its performance is not high as 100% yield in case of palmitic acid esterification (4.3.2.1). Then Rb-ETS-10 was chosen to study for further optimum condition of oleic acid esterification.

Table 4.5 The catalytic activity of K-ETS-10 and Rb-ETS-10 catalysts in esterification reaction of oleic acid

Catalyst	Methyl oleate yield (%mole)
K-ETS-10	84.27
Rb-ETS-10	100

Reaction condition: 10 wt% catalyst, 9:1 of MeOH to oleic acid mole ratio at 110°C, for 18 h and stirring speed 200 rpm.

4.3.1.2 Effect of methanol to oleic mole ratio

The esterification reaction was carried out at constant temperature, 100°C, for 18 h at stirring speed 200 rpm and 10 wt% of Rb-ETS-10 catalyst. The mole ratio of methanol to oleic acid was varied from 6:1 to 30:1. Table 4.6 shows the variation of methanol to oleic acid mole ratio for four different experiments and the corresponding plot of methyl oleate yield versus ratio of methanol to oleic acid is shown in Figure 4.12. The stoichiometric molar ratio requires one mole of methanol and a mole of oleic acid to produce one mole of methyl oleate and water, but in practice the excess amount of alcohol in esterification of free fatty acids is needed in order to shift the equilibrium to the right-hand side to produce more methyl oleate product. By increasing methanol to oleic acid mole ratio from 6:1 to 9:1, the methyl ester yield considerably increased from 47.17 to 90.24%. From the experimental results methanol to oleic acid ratio of 9:1 is the most appropriate one to give the highest yield of methyl oleate. Beyond the molar ratio of 9:1, the excessively added methanol had decreasing methyl oleate yield, due to the difficulty of methoxide nucleophile to react with carboxyl group.

Table 4.6 The catalytic activity of Rb-ETS-10 in the esterification of oleic acid at various ratios of methanol to acid

MeOH to oleic acid mole ratio	Methyl oleate yield (%mole)
6:1	47.17
9:1	90.24
15:1	61.56
30:1	42.84

Reaction condition: 10 wt% catalyst, at 100°C, for 18 h and stirring speed 200 rpm.

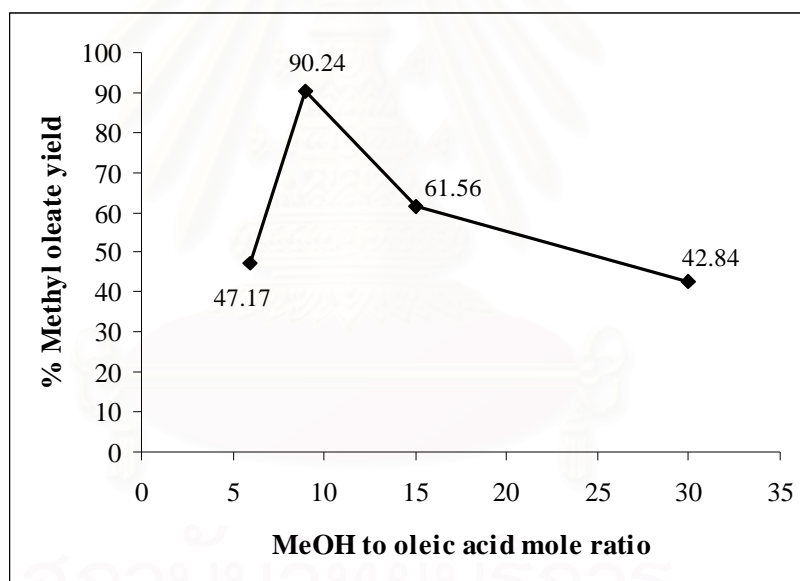


Figure 4.11 The plot of methyl oleate yield using Rb-ETS-10 versus MeOH to oleic acid mole ratio.

4.3.1.3 Effect of reaction temperature

To determine the effect of reaction temperature on methyl oleate yield, the esterification reaction was carried out under the optimum condition obtained in the previous section i.e. 9:1 methanol to oleic acid mole ratio, 10 wt% Rb-ETS-10 catalyst, for 24 h and stirring speed 200 rpm. The experiments were conducted at temperature ranging from 60-120°C. The effect of reaction temperature on the product

yield was presented in Table 4.5. The corresponding plot of methyl oleate yield versus reaction temperature is shown in Figure 4.13. In Table 4.7 it can be seen that as the temperature increase, the final product yield increases as well. At 100, 110 and 120°C, 97-100% methyl oleate yield was observed whereas below 90°C the product yield was <61%. Therefore, the optimal reaction temperature is 110°C for esterification reaction of oleic acid and gave 100% methyl oleate yield.

Table 4.7 The catalytic activity of Rb-ETS-10 in the esterification of oleic acid at various reaction temperature values

Reaction temperature (°C)	Methyl oleate yield (% mole)
60	11.73
90	61.11
100	97.21
110	100
120	100

Reaction condition: 10 wt% catalyst, 9:1 of MeOH to oleic acid mole ratio, for 24 h and stirring speed 200 rpm.

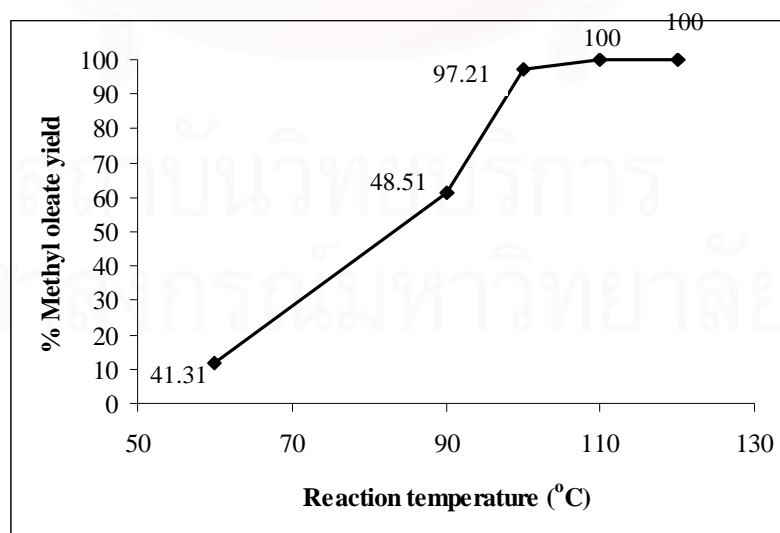


Figure 4.12 The plot of methyl oleate yield using Rb-ETS-10 versus reaction temperature.

4.3.1.4 Effect of reaction time

The catalytic activities of Rb-ETS-10 in the esterification of oleic acid at reaction temperature 100 and 110°C with different reaction time are shown in Table 4.8 and 4.9. The corresponding plot of methyl oleate yield versus reaction time is shown in Figure 4.14. The reaction time was varied in the range of 6-24 h. The rate of oleic acid esterification reaction is strongly influenced by the reaction temperature. However, given enough time, the reaction will proceed to near completion even at 100°C for 24 h, whereas at 110°C reaction temperature for 18 h gave completion of oleic acid esterification reaction over Rb-ETS-10. On the other hands, when the reaction temperature and reaction time were not enough, maximum production yield could not be reached. The results showed that esterification of oleic acid at 100°C were slower in reaction rates than esterification at 110°C for any reaction times. A maximum product yield of 100% is obtained from 18 h reaction time at reaction temperature 110°C.

Table 4.8 The catalytic activity of Rb-ETS-10 in the esterification of oleic acid for different reaction time

Reaction time (h)	Methyl oleate yield (%mole)
6	40.58
12	57.41
18	90.24
24	97.21

Reaction condition: 10 wt% catalyst, 9:1 of MeOH to oleic acid mole ratio, at 100°C and stirring speed 200 rpm.

Table 4.9 The catalytic activity of Rb-ETS-10 in the esterification of oleic acid for different reaction time

Reaction time (h)	Methyl oleate yield (%mole)
6	54.49
12	73.93
18	100
24	100

Reaction condition: 10 wt% catalyst, 9:1 of MeOH to oleic acid mole ratio, at 110°C and stirring speed 200 rpm.

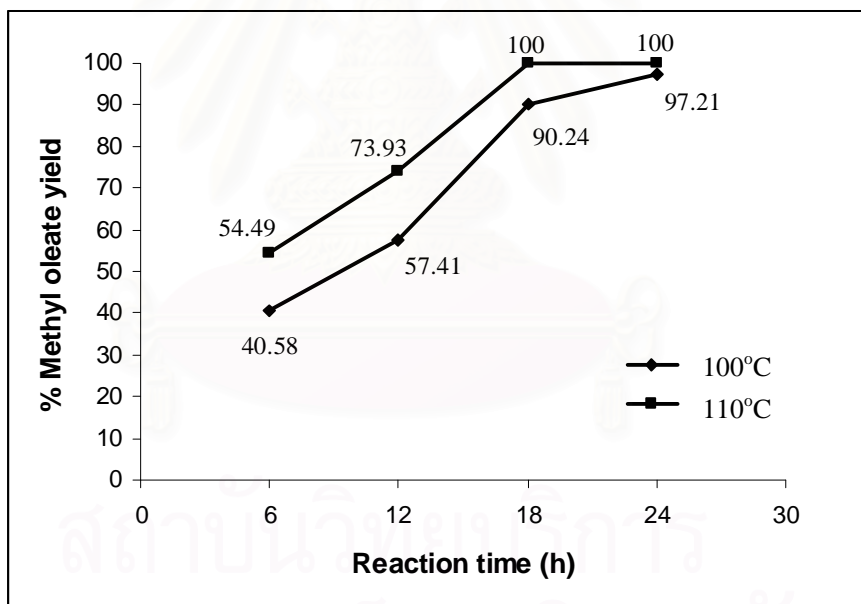


Figure 4.13 The plot of methyl oleate yield over Rb-ETS-10 versus reaction time.

4.3.1.5 Effect of catalytic amount

The optimizing catalyst amount based on limiting reactant was studied. The effect of the catalyst amount over the methyl oleate yield is presented in Table 4.10 and the corresponding plot of methyl oleate yield versus catalyst amount is shown in Figure 4.15. The catalytic activities of Rb-ETS-10 at various catalyst amounts of 2.5, 5, 10 and 15 wt% in the esterification of oleic acid can be observed the yield of methyl oleate which increased by rising the catalyst amount. This result is expected because of catalyst loading increment is proportional to availability of active sites. The drastically increased yield was obtained by increasing the catalytic amount from 2.5 to 10 wt%. When rising amount of catalyst from 10 to 15%, the methyl oleate yield was decreased because the reaction mixture became viscous, giving rise to a mixing problem [26]. On the other hands, when the catalyst amount was lower than 10 wt%, the maximum production yield could not be achieved. According to the methyl oleate yield, 10 wt% of the catalytic amount to reactant mixture was chosen for further study.

Table 4.10 The catalytic activity of Rb-ETS-10 at various catalyst amounts in the esterification of oleic acid

Catalyst amount (wt%)	Methyl oleic yield (%mole)
2.5	76.66
5.0	91.31
10.0	100
15.0	87.87

Reaction condition: 9:1 of MeOH to oleic acid mole ratio at 110°C, for 18 h and stirring speed 200 rpm.

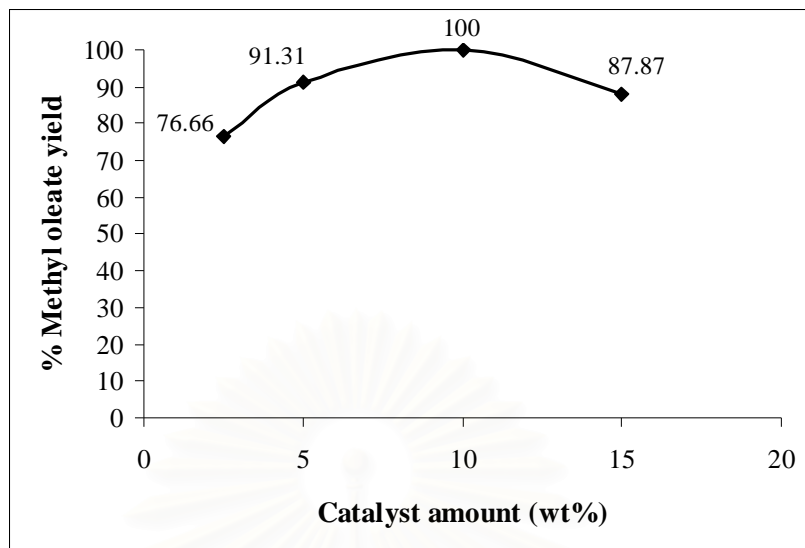


Figure 4.14 The plot of methyl oleate yield versus catalyst amount of Rb-ETS-10.

4.3.1.6 Effect of stirring speed

Stirring speeds of 50, 100, 200 and 400 rpm were varied to find out the most appropriate one. The effect of the stirring speed over the methyl oleate yield is presented in Table 4.11 and the corresponding plot of methyl oleate yield versus catalyst stirring is shown in Figure 4.16. It can be observed that the yield of methyl oleate was increased by rising the stirring speed, except for the stirring speed from 200 to 400 rpm because too vigorous stirring speed leads to problem of catalyst spread out from bottom of reactor to the reactor wall. On the other hands, when the stirring speed was not reach 200 rpm, maximum production yield could not be reached.

Table 4.11 The catalytic activity of Rb-ETS-10 at various stirring speeds in the esterification of oleic acid

Stirring speed (rpm)	Methyl oleate yield (%mole)
50	78.35
100	79.77
200	100
400	94.44

Reaction condition: 9:1 of MeOH to oleic acid mole ratio at 110°C, for 18 h and stirring speed 200 rpm.

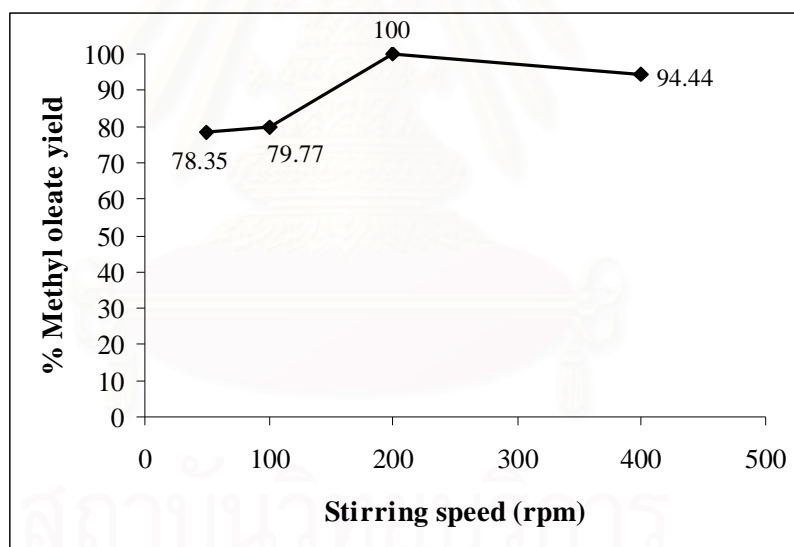


Figure 4.15 The plot of methyl oleate yield versus stirring speed.

4.3.1.7 Activities of reused and regenerated Rb-ETS-10 catalysts

Heterogeneous catalyst has a potential to be recovered, reused and regenerated. In this research, the used catalyst was reused by washing with acetone, drying and calcination prior to the retest for its activity. The catalytic activities of fresh Rb-ETS-10, reused Rb-ETS-10 and regenerated Rb-ETS-10 catalysts in the esterification of oleic acid are shown in Table 4.12 and the corresponding plot of methyl oleate yield versus 3 type of catalysts is shown in Figure 4.17. Reused Rb-ETS-10 exhibited a significant drop in activity from 100% methyl oleate yield of fresh Rb-ETS-10 to 87% yield of reused Rb-ETS-10 under the same operational conditions. The loss in activities of catalysts may be from the deactivation of active sites, whereas, the structure of ETS-10 was still similar as the fresh one, it was confirmed by XRD pattern.

However, the used catalyst was developed in order to improve its performance. After reused catalyst was calcined, it was reloaded with RbOH solution by ion-exchange method, dried and calcined till receiving regenerated Rb-ETS-10. The methyl oleate yield was improved from 87% for reused catalyst to 100% for regenerated Rb-ETS-10 catalyst, the methyl oleate yield was obtained same as the fresh one. Therefore the Rb-ETS-10 catalyst can be regenerated fully.

Table 4.12 The catalytic activity of reuse and regenerated Rb-ETS-10 catalysts in the esterification of oleic acid

Catalyst	Methyl oleate yield (%mole)
Rb-ETS-10	100
Reused Rb-ETS-10	86.82
Regenerated Rb-ETS-10	100

Reaction condition: 10 wt% catalyst, 9:1 of MeOH to oleic acid mole ratio at 110°C, for 18 h and stirring speed 200 rpm.

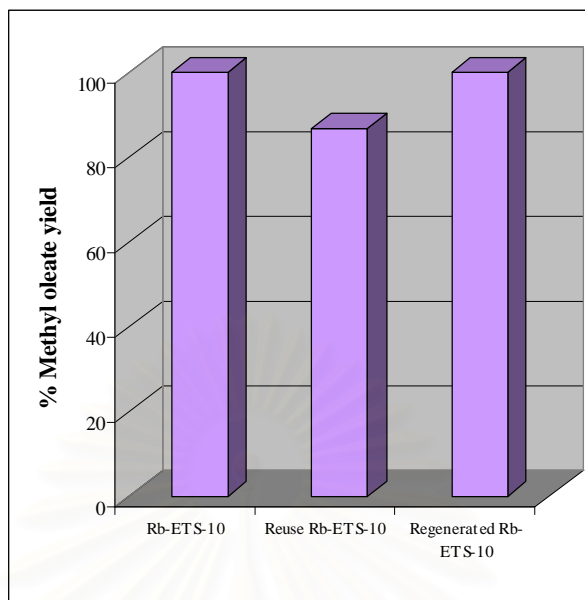


Figure 4.16 The plot of methyl oleate yield versus reused and regenerated Rb-ETS-10 catalysts.

In conclusion the optimized condition for esterification of oleic acid to methyl oleate with Rb-ETS-10 catalyst was found to be 10 wt% of catalyst to reactant mixture, 9:1 of methanol to oleic acid mole ratio, at 110°C for 18 h and stirring speed 200 rpm. The basicity of catalyst was the most significant factor to reach the high methyl oleate yield and other parameters such as catalyst amount, molar ratio, reaction temperature, reaction time and stirring speed also affect the yield of methyl oleate or biodiesel. This optimized condition was applied in further esterification reaction study of linoleic acid with Rb-ETS-10 catalyst (4.3.3).

4.3.2 Esterification of linoleic acid

Linoleic acid is 18-carbon chain carboxylic acid, similar to oleic acid but contains two *cis* double bonds while oleic acid has only one *cis* double bond. The properties of both carboxylic acids are probable nearly same. Then the same reaction condition was applied for linoleic acid esterification. Table 4.22 shows catalytic activity of Rb-ETS-10 in esterification of linoleic acid. Esterification over Rb-ETS-10 provides 33% higher methyl linoleate yield than blank test. The maximum yield of methyl linoleate was obtained at 110°C for 18 h. When the reaction temperature was decreased 10 degree, the reducing of product yield was observed 16%. As a result, the optimal reaction conditions are 110°C for 18 h, 9:1 of methanol to linoleic acid mole ratio, stirring speed 200 rpm and 10 wt% of Rb-ETS-10 catalyst.

Table 4.13 The catalytic activity of Rb-ETS-10 in the esterification of linoleic acid

Catalyst	Reaction temperature (°C)	Methyl linoleate yield (%mole)
None	110	66.82
Rb-ETS-10		100
Rb-ETS-10	100	83.80

Reaction condition: 10 wt% catalyst, 9:1 of MeOH to linoleic acid mole ratio, for 18 h, stirring and speed 200 rpm.

4.3.3 Esterification of palmitic acid

First, the effect of mixing was investigated because starting palmitic acid is a solid compound. Basically, methanol and palmitic acid was immiscible, and the reactants were separated into two phases, which retarded the reaction rate. To overcome this mixing problem, an appropriate co-solvent had to be introduced. From the result shown in Table 4.13, diethyl ether and THF were the most effective co-solvent. When diethyl ether and THF were added, the immiscible two phase system was changed to the homogeneous solution. Therefore, diethyl ether is an extremely

flammable solvent and higher vaporization value favour than THF. In this work, THF was chosen to be co-solvent for esterification of palmitic acid.

Table 4.14 Solubility test of palmitic acid in different solvent*

Solvent	Solubility
Hexane	Slightly dissolved
Heptane	Slightly dissolved
Dichloromethane	Slightly dissolved
Diethyl ether	Totally dissolved
Tetrahydrofuran (THF)	Totally dissolved
Acetone	Slightly dissolved

* Palmitic acid to solvent; 1.0 g : 2 mL

4.3.3.1 Catalytic activity of ETS-10 and alkali-exchanged ETS-10

The ETS-10 catalyst, prepared from 0.75 mole of TiO_2 in gel and different alkali-exchange ETS-10 base were used as catalyst in esterification reaction of palmitic acid. Reaction condition for catalytic test is 9:1 mole ratio of methanol to palmitic acid, 120°C for 24 h and 10 wt% of catalyst. The catalytic activity is presented in Table 4.14 and corresponding plot of methyl palmitate yield versus type of catalyst is shown in Figure 4.18. Comparing to the blank test, ETS-10 sample is moderately active for esterification of palmitic acid to methyl palmitate. ETS-10 provides 21.6% methyl palmitate yield higher than blank test, whereas, gave 31.0% lower than alkali-exchanged ETS-10. Na-ETS-10, K-ETS-10 and Rb-ETS-10 catalysts gave an excellent yield whereas Cs-ETS-10 exhibits a little bit lower yield at 97.8%. Among alkali-ion exchanged ETS-10 base catalysts, the order of reactivity in esterification reaction of palmitic acid was Na-ETS-10 = K-ETS-10 = Rb-ETS-10 > Cs-ETS-10 > ETS-10. Base-modified ETS-10 catalysts exhibit higher methyl palmitate yield compared to parent ETS-10.

Table 4.15 The catalytic activity of ETS-10 and alkali-exchanged ETS-10 catalysts in esterification reaction of palmitic acid

Catalyst	Methyl palmitate yield (%mole)
None	47.40
ETS-10 (0.75TiO ₂)	69.00
Na-ETS-10	100
K-ETS-10	100
Rb-ETS-10	100
Cs-ETS-10	97.81

Reaction condition: 10 %wt catalyst, 9:1 of MeOH to palmitic acid mole ratio at 120°C, for 24 h, stirring speed 200 rpm and 0.94 g of THF in 10 g of reactants

Considering, both K-ETS-10 and Rb-ETS-10 catalysts show the highest methyl palmitate yield of 100% at 120°C for 24 h. However, it could not tell that K-ETS-10 is better activity than Rb-ETS-10. Then, the palmitic acid esterification was done at milder condition to test activities of K-ETS-10 and Rb-ETS-10 catalysts. Table 4.15 shows catalytic activities of K-ETS-10 and Rb-ETS-10 at 120°C for 18 h. The Rb-ETS-10 catalyst provides 10.76% methyl palmitate yield higher than K-ETS-10. Na-ETS-10 catalyst was not tested in this study due to the lower performance in methyl oleate production (4.3.1.1). Rb-ETS-10 was chosen to study for further optimum condition of palmitic acid esterification.

Table 4.16 The catalytic activity of K-ETS-10 and Rb-ETS-10 catalysts in esterification reaction of palmitic acid

Catalyst	Methyl palmitate yield (%mole)
K-ETS-10	69.37
Rb-ETS-10	80.13

Reaction condition: 10 wt% catalyst, 9:1 of MeOH to palmitic acid mole ratio at 120°C, for 18 h, stirring speed 200 rpm and 0.94 g of THF in 10 g of reactants

4.3.3.2 Effect of methanol to palmitic acid mole ratio

The esterification reaction was carried out at constant temperature, 120°C, for 24 h with stirring speed 200 rpm over 10 wt% of Rb-ETS-10 catalyst. The mole ratio of methanol to palmitic acid was varied from 6:1 to 15:1 with and without THF co-solvent. The reaction result is shown in Table 4.16 and the corresponding plot of methyl palmitate yield versus methanol to palmitic acid mole ratio is plotted in Figure 4.19. The stoichiometric mole ratio requires one mole of methanol and a mole of palmitic acid to produce one mole of methyl palmitate and water, but in practice the excess amount of alcohol is needed in order to shift the equilibrium to the right-hand side to produce more methyl palmitate product. From result in Table 4.16 the esterification of palmitic acid with methanol to acid mole ratio of 9:1 and 15:1 systems, without THF co-solvent did not give a good methyl palmitate yield by mixing problem between starting materials. Basically, methanol and palmitic acid are immiscible, which retarded the reaction rate. Therefore, Tetrahydrofuran (THF) was introduced to solve this problem as co-solvent. At 9:1 of methanol to acid mole ratio and absence of THF, methyl palmitate yield (84%) was lower than using THF as co-solvent (100%). When THF was added to reaction, the methyl palmitate yield was increased from 81.73 to 100% under condition 6:1 and 9:1 of methanol to acid mole ratio. The optimum mole ratio of methanol to palmitic acid was found to be 9:1. Beyond the molar ratio of 9:1, the excessively added methanol had effect in decreasing methyl palmitate yield, due to the difficulty of methoxide nucleophile to react with carboxyl group.

Table 4.17 The catalytic activity of Rb-ETS-10 in the esterification of palmitic acid at various ratios of methanol to acid without and with THF co-solvent

MeOH to palmitic acid mole ratio	Co-solvent	Methyl palmitate yield (%mole)
9:1	None	84.03
15:1		65.00
6:1	THF	81.73
9:1		100
15:1		58.60
30:1		40.21

Reaction condition: 10 wt% catalyst, at 120°C, for 24 h, stirring speed 200 rpm and 0.94 g of THF in 10 g of reactants

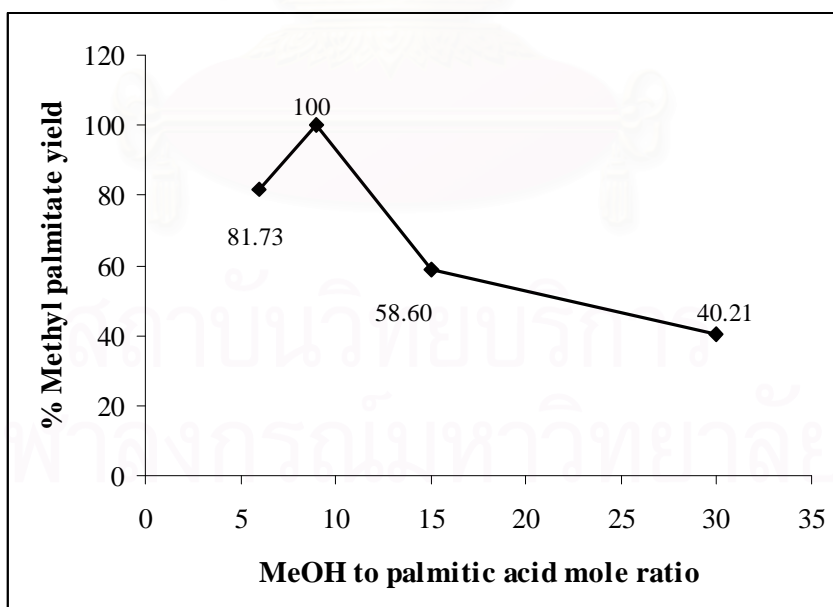


Figure 4.17 The plot of methyl palmitate yield using Rb-ETS-10 versus MeOH to palmitic acid mole ratio.

4.3.3.3 Effect of reaction temperature

The catalytic activity of Rb-ETS-10 in the esterification of palmitic acid was carried out under the same as previous standard condition. The reaction temperature was varied in the range of 90-120°C. The obtained results are shown in Table 4.17 and the corresponding plot of methyl palmitate yield versus reaction temperature is shown in Figure 4.20. The catalytic activity depends strongly on the reaction temperature. By increasing temperature from 90 to 120°C, methyl palmitate yield were increased from 41.31, 48.51, 63.9 and 100% by every 10 degree rising temperature. Whereas, the reaction temperature was not high enough, maximum production yield could not be reached. As a result, the optimal reaction temperature is 120°C for esterification reaction of palmitic acid at this reaction condition.

Table 4.18 The catalytic activity of Rb-ETS-10 in the esterification of palmitic acid at various reaction temperature values

Reaction temperature (°C)	Methyl palmitate yield (%mole)
90	41.31
100	48.51
110	63.90
120	100

Reaction condition: 10 wt% catalyst, 9:1 of MeOH to palmitic acid mole ratio, for 24 h, stirring speed 200 rpm and 0.94 g of THF in 10 g of reactants

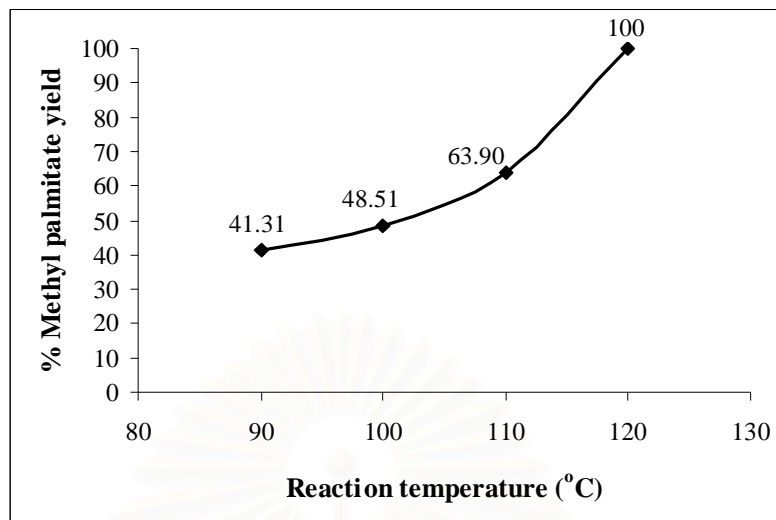


Figure 4.18 The plot of methyl palmitate yield using Rb-ETS-10 versus reaction temperature.

4.3.3.4 Effect of reaction time

The effect of reaction time on methyl palmitate yield was studied. The catalytic activities of Rb-ETS-10 in the esterification of palmitic acid at different reaction time are shown in Table 4.18. The corresponding plot of methyl palmitate yield versus reaction time is shown in Figure 4.21. The reaction time was varied in the range of 12 to 24 h. For instance, the yield of methyl palmitate is 62.37% at the first 12 h and rises to 80.13% at 18 h. When increasing the reaction time to 24 h, the methyl palmitate yield was increased to 100%. On the other hands, when the reaction time is shorter than 24 h, maximum production yield could not be reached.

Table 4.19 The catalytic activity of Rb-ETS-10 in the esterification of palmitic acid for different reaction time

Reaction time (h)	Methyl palmitate yield (% mole)
12	62.37
18	80.13
24	100

Reaction condition: 10 wt% catalyst, 9:1 of MeOH to palmitic acid mole ratio, at 120°C, stirring speed 200 rpm and 0.94 g of THF in 10 g of reactants

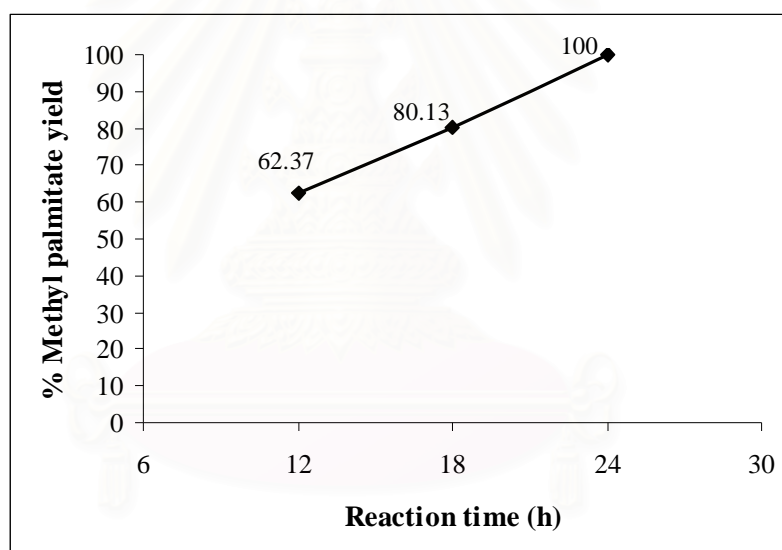


Figure 4.19 The plot of methyl palmitate yield over Rb-ETS-10 versus reaction time.

4.3.3.5 Effect of catalytic amount

Catalytic amount based on reactant mixture was varied from 2.5 to 15 wt% to find the most appropriate one. The catalytic activities of Rb-ETS-10 at various catalyst amounts in the esterification of palmitic acid are shown in Table 4.19. The corresponding plot of methyl palmitate yield versus catalyst amount is shown in Figure 4.22. It can be observed that the yield of methyl palmitate was increased by rising the catalytic amount from 2.5 to 10 wt%. This result is expected because catalyst loading increment is proportional to availability of active sites. Whereas, the

lower yield was surprisingly obtained when the catalyst amount was increased to 15 wt%. The reason may be the slurry (mixture of catalyst and reactants) became too viscous giving rise to mixing problem [26]. On the other hands, when the catalyst amount was lower than 10 wt%, the maximum production yield could not be achieved. According to the methyl palmitate yield, 10 wt% of catalytic amount to reactant mixture was chosen for further study.

Table 4.20 The catalytic activity of Rb-ETS-10 at various catalyst amounts in the esterification of palmitic acid

Catalyst amount (wt%)	Methyl palmitate yield (% mole)
2.5	90.05
5.0	94.16
10.0	100
15.0	81.05

Reaction condition: 9:1 of MeOH to palmitic acid mole ratio at 120°C, for 24 h, stirring speed 200 rpm and 0.94 g of THF in 10 g of reactants

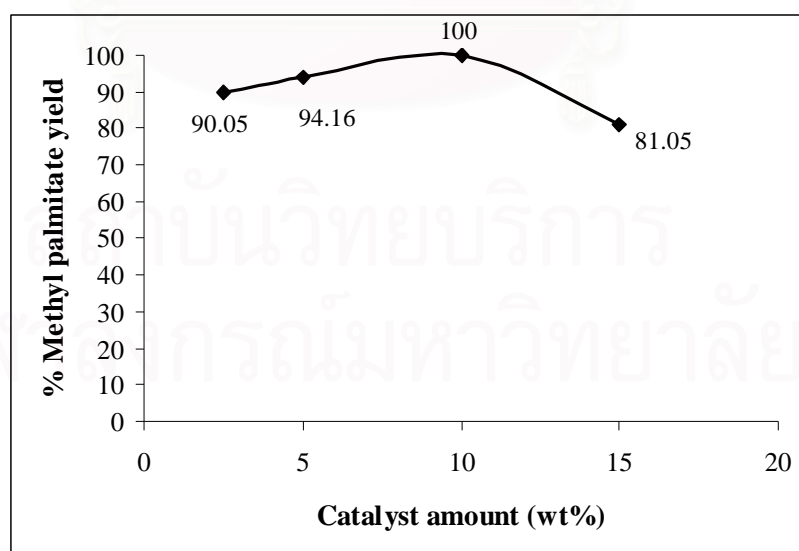


Figure 4.20 The plot of methyl palmitate yield versus catalyst amount of Rb-ETS-10.

4.3.3.6 Effect of stirring speed

The stirring speed optimizing was studied. The effect of the stirring speed over the methyl palmitate yield is presented in Table 4.20 and the corresponding plot of methyl palmitate yield versus catalyst stirring is shown in Figure 4.23. The catalytic activity of Rb-ETS-10 at various stirring speeds from 50 to 400 rpm can be observed the increasing yield of methyl palmitate by rising the stirring speed to 200 rpm. When the stirring speed was increased to 400 rpm, the product decreasing was observed, due to the vigorous stirring speed leading to mixing problem between solid catalyst and reactants. The evidence can be seen by amount of dried catalyst remained at higher reaction mixture level of reactor wall. On the other hands, when the stirring speed was not reach 200 rpm, the maximum production yield could not be received.

Table 4.21 The catalytic activity of Rb-ETS-10 at various stirring speeds in the esterification of palmitic acid

Stirring speed (rpm)	Methyl palmitate yield (%mole)
50	52.08
100	69.06
200	100
400	96.61

Reaction condition: 10 wt% catalyst, 9:1 of MeOH to palmitic acid mole ratio at 120°C, for 24 h and 0.94 g of THF

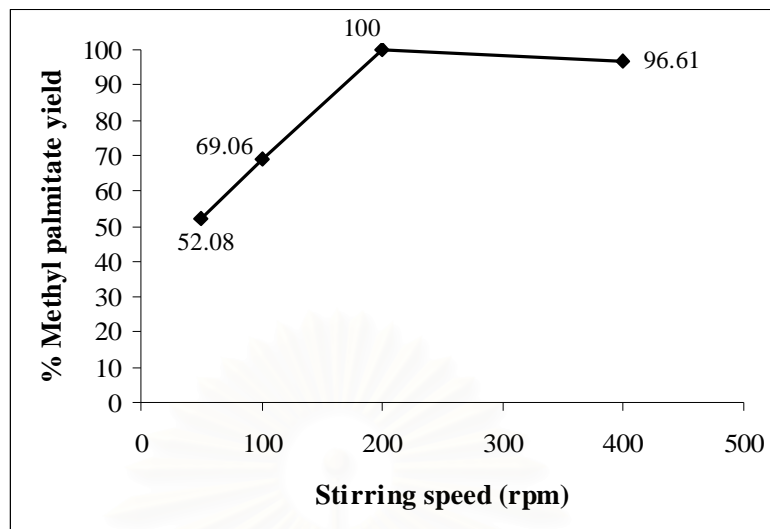


Figure 4.21 The plot of methyl palmitate yield using Rb-ETS-10 versus stirring speed

4.3.3.7 Activities of reused and regenerated Rb-ETS-10 catalysts

To examine the reusability of Rb-ETS-10, it was repeatedly served for methyl palmitate production. After the first reaction, catalyst was washed with acetone, dried and calcined then reused in a new reaction cycle. Table 4.21 shows the results obtained from fresh Rb-ETS-10, reused Rb-ETS-10 and regenerated Rb-ETS-10 catalysts and the corresponding plot of methyl palmitate yield versus 3 type of catalysts is shown in Figure 4.24. When the reused Rb-ETS-10 was utilized, the methyl palmitate yield was decreased by 22% compared with fresh one. The loss in activity of catalyst may be caused by the deactivation of active sites. In addition, the decrease in activity match well with a result from SEM-EDX, 17.79% loss of rubidium leaching out compared to fresh one.

Therefore, the used catalyst was developed in order to improve its performance. After first run, catalyst was calcined, and was reloaded with RbOH solution by ion-exchange method, dried and calcined till receiving regenerated Rb-ETS-10. The methyl palmitate yield was improved from 78% for reused catalyst to 96% for regenerated Rb-ETS-10 catalyst, nearly the fresh one.

Table 4.22 The catalytic activity of reused and regenerated Rb-ETS-10 catalysts in the esterification of palmitic acid

Catalyst	Methyl palmitate yield (% mole)
Rb-ETS-10	100
Reused Rb-ETS-10	78.04
Regenerated Rb-ETS-10	96.34

Reaction condition: 10 wt% catalyst, 9:1 of MeOH to palmitic acid mole ratio at 120°C, for 24 h, stirring speed 200 rpm and 0.94 g of THF in 10 g of reactants

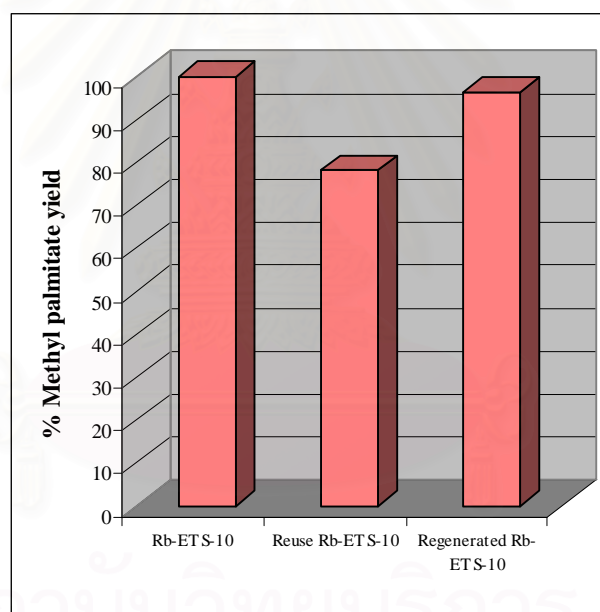


Figure 4.22 The plot of methyl palmitate yield versus catalyst.

Palmitic acid was esterified by methanol and heterogeneous base modified Rb-ETS-10 as catalyst to form methyl palmitate. The methyl palmitate yield was obtained 100% at 120°C for 24 h with 9:1 of methanol to palmitic acid mole ratio, stirring speed 200 rpm and 10 wt% of catalyst. The esterification parameters such as catalyst amount, molar ratio, reaction temperature, reaction time and stirring speed also affect the yield of methyl palmitate or biodiesel.

4.4 Proposed esterification mechanism

4.4.1 Eesterification mechanism for ETS-10

ETS-10 structure is composed of TiO_6 octahedral and SiO_4 tetrahedral link through the oxygen atom. The ETS-10 framework consisted two negative charges and the electrical balance was preserved by extra-framework cations. The mechanism was started from a framework octahedral Ti atom reacting with methanol to generate methoxide ion. Then methoxide active species further react with free fatty acid to produce methyl ester as shown in Figure 4.25. [19]

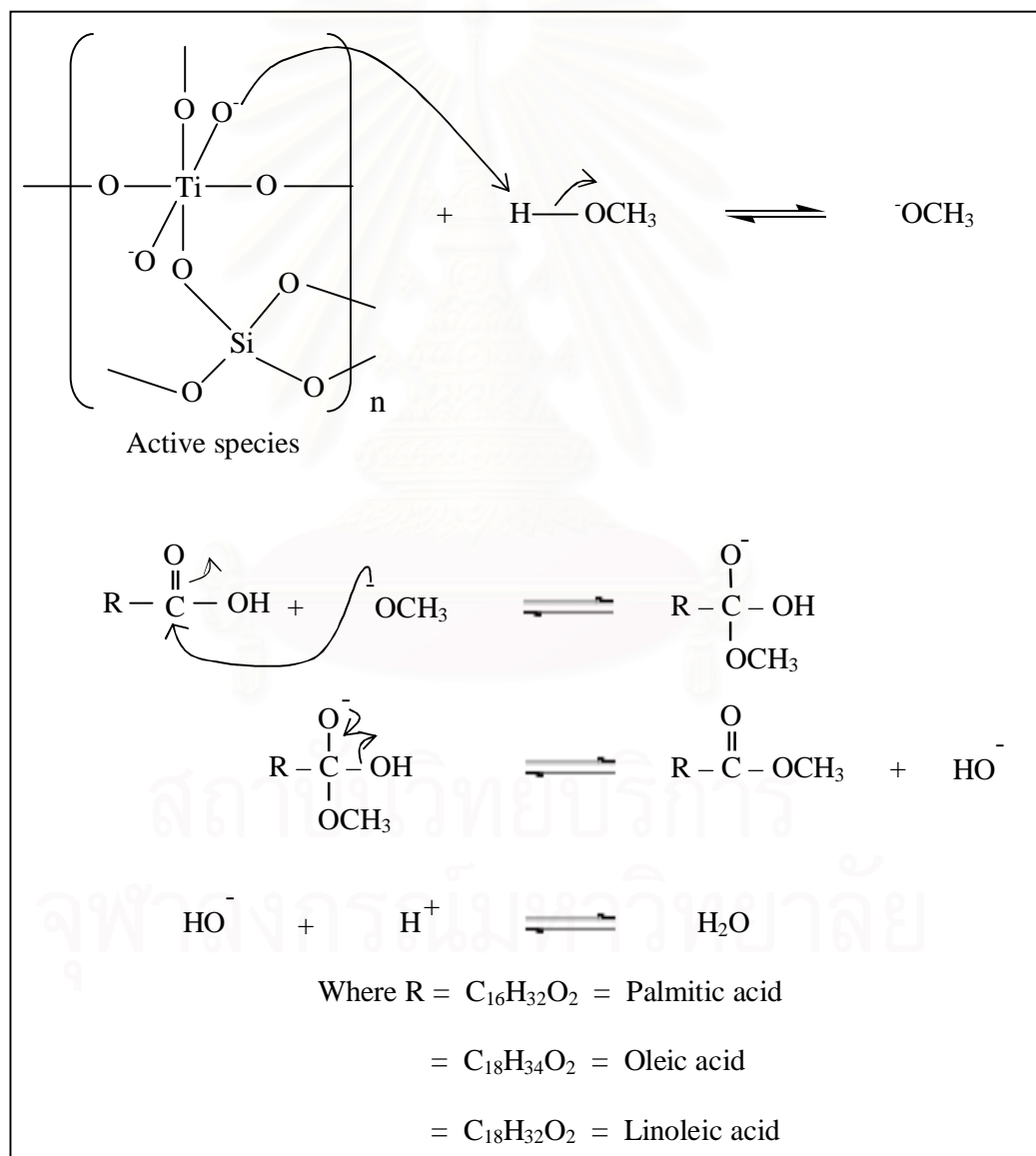


Figure 4.23 Proposed esterification mechanism for ETS-10.

The ion-exchange treatment of parent ETS-10 with various alkali metal salts caused the change of the catalytic properties of ETS-10 materials, heavier alkali metal cation exchanged ETS-10 exhibited higher basicity. The increasing of basicity in ETS-10 catalyst introduce to easier proton abstraction of methanol, which methoxide ion further reacts to free fatty acid [19].



สถาบันวิทยบริการ
จุฬาลงกรณ์มหาวิทยาลัย

CHAPTER V

CONCLUSIONS

To study the effect of basic heterogeneous catalyst on the activity of oleic, palmitic and linoleic acid esterification (biodiesel production), ETS-10 from various $\text{SiO}_2/\text{TiO}_2$ mole ratios and base modified ETS-10 catalysts were used. Moreover, the optimum condition was investigated for each free fatty acid to increase the methyl ester yield.

ETS-10 catalyst was synthesized under basic condition by modifying method according to Tatsumi, T., *et al.* [18] and Anderson, M. W., *et al.* [15] with the gel composition $5\text{SiO}_2: x\text{TiO}_2: 3\text{NaOH}: \text{KF}: 75 \text{H}_2\text{O}$, where $x = 0.5-1.0$. Moreover, basic modified ETS-10 catalyst was also prepared by ion-exchange method (Na-ETS-10, K-ETS-10, Rb-ETS-10 and Cs-ETS-10) and subsequent calcination at 450°C for 6 h.

From characterization of all materials, XRD patterns of synthesized ETS-10 samples exhibit main phase as ETS-10 structure together with small amount of co-crystallized anatase. Upon decreasing the TiO_2 loading from 1.0 to 0.75 mole, the characteristic peaks of ETS-10 increase in intensity. When TiO_2 was reduced to 0.5 mole, the increasing of quartz impurity phase was obtained. For alkali cation modified ETS-10 materials also maintain characteristic peaks of the ETS-10 structure with lower crystallinity. From SEM technique, all of catalysts were quasi-cubic shape and particle size was in the range of 300-500 nm. In addition, all of catalysts exhibit N_2 adsorption isotherm of type I, characteristic of micropore material. The ETS-10 was synthesized by using 0.75 mole of TiO_2 gave highest surface area. Surface area of alkali-exchanged ETS-10 samples reduce when compared with parent ETS-10 sample. DR-UV spectra can identify titanium form that occupied in catalyst including tetrahedral, octahedral form and anatase. Sodium, potassium, rubidium and cesium alkali content was quantitative analyzed by SEM-EDX technique and Si/Ti, Na/Ti and K/Ti mole ratio of all catalysts were determined by ICP-AES and AAS.

In esterification reaction of palmitic and oleic acid, all of catalysts were applied to study the catalytic activity. ETS-10 exhibits higher activity than blank test in all free fatty acid esterifications. Rb-ETS-10 was distinguishable in both oleic acid and palmitic acid esterification. Moreover, it can be concluded that the optimum conditions of oleic and linoleic acid esterifications were 10 wt% of Rb-ETS-10 catalyst to reactant mixture, 9:1 of methanol to oleic acid mole ratio at 110°C for 18 h with stirring speed 200 rpm. The optimum condition for palmitic acid was nearly the same as oleic acid except for 10 degree higher of reaction temperature (120°C) and 6 hours longer for reaction time (24 h). The maximum methyl ester yield reached to 100% by mole when reaction was carried out under each the optimum condition. The catalytic activity of reused Rb-ETS-10 catalyst decreased in both oleic and palmitic esterifications while regenerated Rb-ETS-10 could boost methyl palmitate yields nearly the fresh one.

The suggestion for future work

The catalyst in esterification reaction can be adapted to improve the product yield. Aluminium and gallium substituted ETS-10 samples are interesting as basic catalyst to improve the methyl ester yield, due to the increase of the ion-exchange sites. Base-modified ETS-10 by multiple ion-exchanges with higher concentration of RbOH solution is also an attractive point.

สถาบันวิทยบริการ
จุฬาลงกรณ์มหาวิทยาลัย

REFERENCES

- [1] Schuchardt, U.; Sercheli, R.; Vargas, R. M. Transesterification of vegetable oils: A review. *J. Braz. Chem. Soc.* 9(1998) : 199.
- [2] Michael, S. G.; McCormick, R. L. Combustion of fat and vegetable oil derived fuels in diesel engines. *Prog. Energy Combust. Sci.* 24(1998) : 125.
- [3] Ma, F., Hanna, M. A. Biodiesel production: A review. *Biores. Tech.* 70(1999) : 1.
- [4] Pintoa, A. C.; Guarieiroa, L. L. N.; Rezendea, M. J. C.; Ribeiroa, N. M.; Torresb, E. A.; Lopesc, W. A.; Pereirac, P. A. P.; Andrade, J. B. Biodiesel: An Overview. *J. Braz. Chem. Soc.* 16(2005) : 131.
- [5] Royon, D.; Daz, M.; Ellenrieder, G.; Locatelli. Enzymatic production of biodiesel from cotton seed oil using *t*-butanol as a solvent. *Biores. Tech.* 98(2006) : 648.
- [6] Yadav, G. D.; Lathi, P. S. Lipase catalyzed transesterification of methyl acetoacetate with *n*-butanol. *J. Mol. Cat. B* 32(2005) : 107.
- [7] Aracil, J.; Vicente, G.; Martinez, M. Integrated biodiesel production: a comparison of different homogeneous catalysts systems. *Biores. Tech.* 92(2004) : 297.
- [8] Pavel, C. C.; Vuono, D.; Catanzaro, L.; De Luca, P.; Bilba, N.; Nastro, N.; Nagy, J. B. Synthesis and characterization of the microporous titanosilicates ETS-4 and ETS-10. *Microporous Mesoporous Mater.* 56(2002) : 227.
- [9] Kunichi, S. M.; US patent 4853302, ETS-10 synthesis, 1989.
- [10] Valtchev, V.; Mintova, S. Synthesis of titanium silicate ETS-10: The effect of tetramethylammonium on the crystallization kinetics. *Zeolite* 14(1994) : 697.
- [11] Das, T. S.; Chandwadkar, A. J.; Sivasanker, S. A rapid method of synthesizing titanium silicate ETS-10. *Chem. Commun.* (1996) : 1105.

- [12] Rocha, J.; Ferreira, A.; Lin, Z.; Anderson, M. W. Synthesis of microporous titanosilicate ETS-10 from TiCl_3 and TiO_2 : a comprehensive study. *Microporous Mesoporous Mater.* 23(1998) : 253.
- [13] Yang, X.; Paillaud, J. L.; Van Breukelen, H. F. W. J.; Kessler, H.; Duprey, E. Synthesis of microporous titanosilicate ETS-10 with TiF_4 or TiO_2 . *Microporous Mesoporous Mater.* 46(2001) : 1.
- [14] Lu, L.; Su, F.; Zhao, X. S. A reinforce study on the synthesis of microporous titanosilicate ETS-10. *Microporous Mesoporous Mater.* 76(2004) : 113.
- [15] Anderson, M. W.; Philippou, A. Aldol-Type reactions over basic microporous titanosilicate ETS-10 Type catalysts. *Catal.* 189(2000) : 395.
- [16] Waghmode, S. B.; Wagholikar, S. G.; Sivasanker, S. Heck Reaction over Pd-loaded ETS-10 Molecular Sieve. *Bull. Chem. Soc. Jap.* 76(2003) : 1989.
- [17] Dorskocil, E. J. Ion-exchanged ETS-10 catalysts for the cycloaddition of carbon dioxide to propylene oxide. *Microporous Mesoporous Mater.* 76(2004) : 177.
- [18] Tatsumi, T.; Gao, Y.; Yoshitake, H.; Wu, P. Controlled detitanation of ETS-10 materials through the post-synthetic treatment and their applications to the liquid-phase epoxidation of alkenes. *Microporous Mesoporous Mater.* 70(2004) : 93.
- [19] Tatsumi, T.; Gao, Y.; Wu, P. Liquid-phase Knoevenagel reactions over modified basic microporous titanosilicate ETS-10. *Catal.* 224(2004) : 107.
- [20] Anson, A.; Kuznicki, S. M.; Kuznicki, T.; Hastrup, T.; Wang, Y.; Lin, C. C. H.; Sawada, J. A.; Eyring, E. M.; Hunter, D. Adsorption of argon, oxygen and nitrogen on silver exchanged ETS-10 molecular sieve. *Microporous Mesoporous Mater.* 109(2008) : 577.

- [21] Ramadhas, A. S.; Jayaraj, S.; Muraleedharan, C. Use of vegetable oils as I.C. engine fuel-a review. *Renew. Ener.* 29(2004) : 727.
- [22] Warabi, Y.; Kusdiana, D.; Saka, S. Reactivity of triglycerides and fatty acids of rapeseed oil in supercritical alcohols. *Biores. Tech.* 91(2004) : 283.
- [23] Demirbas, A. Biodiesel production via non-catalytic SCF method and biodiesel fuel characteristics. *Ener. Conser. Manage.* 47(2006) : 2271.
- [24] Di, S. M.; Tesser, R.; Dimicoli, M.; Cammarota, F.; Nastasi, M.; Santacesaria, E.: Synthesis biodiesel via homogeneous Lewis acid catalyst. *J. Mol. Catal. A* 239(2005) : 111.
- [25] Chongkhong, S.; Tongurai, C.; Chetpattananondh, P.; Bunyakan, C. Biodiesel production by esterification of palm fatty acid distillate. *Biomass and Bioenergy* 31(2007) : 563.
- [26] Lee, K. Y.; Kim, H. J.; Kang, B. S.; Kim, M. J.; Park, Y. M.; Kim, D. K.; Lee, J. S. Transesterification of vegetable oil to biodiesel using heterogeneous base catalyst. *Catal. Today* 93(2004) : 315.
- [27] Juan, J. C.; Zhang, J.; Yarmo, M. A. Structure and reactivity of silica-supported zirconium sulfate for esterification of fatty acid under solvent-free condition. *Appl. Catal. A* 287(2005) : 209.
- [28] Ni, J.; Meunier, F. C. Esterification of free fatty acids in sunflower oil over solid acid catalysts using batch and fixed bed-reactors. *Appl. Catal. A* 333(2007) : 122.
- [29] Marchetti, J. M.; Miguel, V. U.; Errazu, A. F. Heterogeneous esterification of oil with high amount of free fatty acids. *Fuel* 86(2007) : 906.

- [30] Suppes, G.; Dasari, M. A.; Daskocil, E. J.; Mankidy, P. J.; Goff, M. J. Transesterification of soybean oil with zeolite and metal catalysts. *Appl. Catal. A* 257(2004) : 213.
- [31] Bond, G. C. Heterogeneous Catalysis: Principles and Applications, Clarendon, Oxford, 1974.
- [32] Lepage, J. F.; Cosyns, J.; Courty, P. Applied Heterogeneous catalysis: Design Manufacture and Use of solid catalysts, Technip, Paris, 1987.
- [33] Analysis software user's manual, BELSORP, BEL JAPAN, INC, 57.
- [34] Szostak, R. Zeolite Molecular Sieves: Principles of Synthesis and Identification, Van Nostrand Reinhold, New York, 1989.
- [35] Dyer, A. An Introduction to Zeolite Molecular Sieve, John Wiley & Sons, 1988.
- [36] Available from: Wikipedia, the free encyclopedia, <http://en.wikipedia.org/wiki/Zeolite>
- [37] Dobelin, N.; Armbruster, T. Microporous titanasilicate AM-2: Ion-exchange and thermal stability. *Microporous Mesoporous Mater.* 99(2007) : 279.
- [38] Rizzo, C.; Carati, A.; Millini, R.; Bellussi, G.; Parker Jr. W. O.; Zanardi, S. Synthesis, characterization and adsorption capacities of microporous titanasilicate EMS-3. *Microporous Mesoporous Mater.* 90(2006) : 153.
- [39] Zecchina, A.; Xamena, F.X.; Paze, C.; Palomino, G.T.; Bordiga, S.; Area, C.O. Alkyne polymerization on the titanasilicate molecular sieve ETS-10. *Phys. Chem. Chem. Phys.* 3(2001) : 1228.
- [40] Rocha, J.; Lin, Z. Microporous mixed octahedral-pentahedral-tetrahedral framework silicates. *Reviews in Mineralogy & Geochemistry* 57(2005) : 173.
- [41] Mihailova, B.; Valtchev, V.; Mintova, S.; Konstantinov, L. Vibrational spectra of ETS-4 and ETS-10, *Zeolite* 16(1996) : 22.

- [42] Yang, X; Blosser, P.W. Location and bonding of cations in ETS-10 titanasilicate molecular sieve: A multinuclear n.m.r. investigation. *Zeolites* 17(1996) : 237.
- [43] Philippou, A.; Naderi, M.; Pervaiz, N.; Rocha, J.; Anderson, M. W. *n*-Hexane reforming reactions over basic Pt-ETS-10 and Pt-ETAS-10. *J. Catal.* 178(1998) : 174.
- [44] Philippou, A.; Anderson M. W. Aldol-type reactions over basic microporous titanasilicate ETS-10 type catalysts. *J. Catal.* 189(1999) : 395.
- [45] Robert, R.; Rajamohanan, P. R.; Hegde, S. G.; Chandwadkar, A. J.; Ratnasamy, P. NMR spectroscopic study of the interaction of 1-butene with the titanosilicates TS-1 and ETS-10. *J. Catal.* 155(1995) : 345.
- [46] Borello, E.; Lamberti, C. S.; Zecchina, B. A. Quantum-size effects in the titanasilicate molecular sieve. *Appl. Phys. Lett.* 71(1997) : 2319.
- [47] Lamberti, C. Electron-hole reduced effective mass in monoatomic...-O-Ti-O-Ti-O-Ti quantum wires embedded in the siliceous crystalline matrix of ETS-10. *Microporous Mesoporous Mater.* 30(1999) : 155.
- [48] Bordiga, S.; Palomino, G. T.; Zecchina, A.; Raghino, G.; Giamello, E.; Lamberti, C. Stoichiometric and sodium-doped titanium silicate molecular sieve containing atomically defined -OTiOTiO- chains: Quantum *ab initio* calculations, spectroscopic properties, and reactivity. *J. Chem. Phys.* 112(2000) : 3859.
- [49] Choi, J. H.; Kim, S. D.; Noh, S. H.; Oh, S. J.; Kim, W. J. Adsorption behaviors of nano-sized ETS-10 and Al-substituted-ETAS-10 in removing heavy metal ions, Pb^{2+} and Cd^{2+} . *Microporous Mesoporous Mater.* 87(2006) : 163.

- [50] Breck, D.W. Zeolite Molecular Sieves, John Wiley & Sons, New York, 1973.
- [51] Available from: Wikipedia, the free encyclopedia,
http://en.wikipedia.org/wiki/Ion_exchange
- [52] Abd El-Wahab, M. M. M.; Said, A. A. Phosphomolybdic acid supported on silica gel and promoted with alkali metal ions as catalyst for the esterification of acetic acid by ethanol. *J. Mol. Catal. A* 240(2005) : 109.
- [53] Nesaretnam, K.; Muhammad, B.; Chong, C. L.; Tan, Y. A. Selected readings on palm oil and its uses, Kuala Lumpur, Palm Oil Research Institute of Malaysia, 1994.
- [54] Available from: Wikipedia, the free encyclopedia,
http://en.wikipedia.org/wiki/Fatty_acid
- [55] Song, C.; Hsu, C. S.; Mochida, I. Chemistry of Diesel Fuels, New York, Taylor & Francis, 2000.
- [56] Naik, S.N.; Meher, L.C.; Vidya Sagar, D. Technical aspects of biodiesel production by transesterification: a review. *Renew. Sustain. E. Rev.* 10(2004) : 1.
- [57] Barnwal, B. K.; Sharma, M. P. Prospects of biodiesel production from vegetable oils in India. *Renew. Sustain. E. Rev.* 9(2005) : 363.
- [58] Robson, H. Verified synthesis of zeolitic materials, 2nd Edition, Elsevier Science, Amsterdam, 2001.
- [59] Analysis software user's manual, BELSORP, BEL JAPAN, INC., 73-83.
- [60] Corma, A.; Martín-Aranda, R. M.; Sánchez, F. Zeolites as base catalysts: Condensation of benzaldehyde derivatives with activated methylenic compounds on germanium-substituted faujasite. *J. Catal.* 126(1990) : 192.

[61] Available from: PTT Public Company Limited,

<http://www.pttplc.com/TH/Default.aspx>

[62] Barnwal, B. K.; Sharma, M. P. Prospects of biodiesel production from vegetable oils in India. *Renew. Sustain. E. Rev.* 9(2005) : 363.



สถาบันวิทยบริการ
จุฬาลงกรณ์มหาวิทยาลัย



Appendices

สถาบันวิทยบริการ
จุฬาลงกรณ์มหาวิทยาลัย

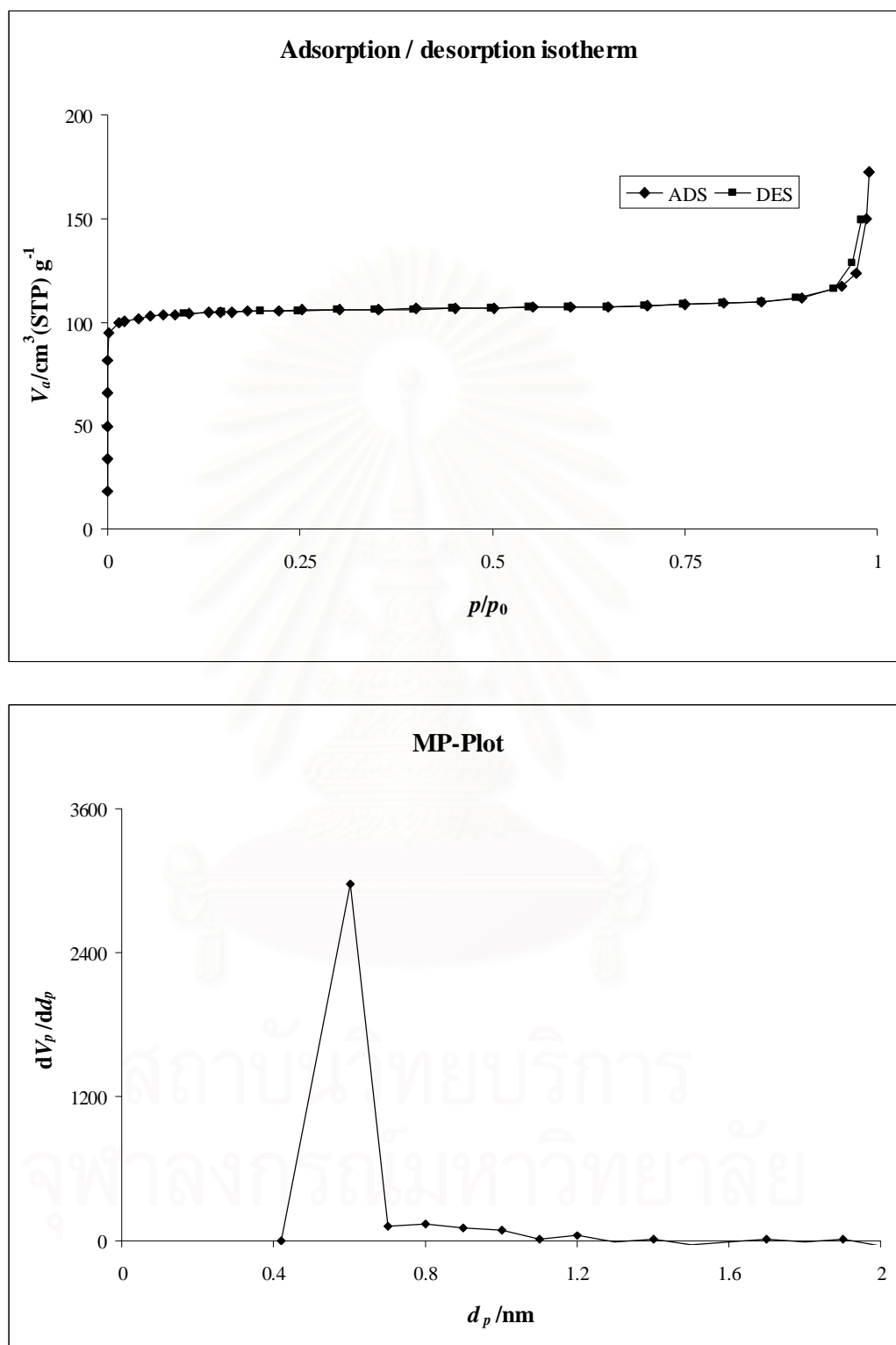


Figure A-1 N_2 adsorption-desorption isotherm and pore size distribution of ETS-10 catalyst

1. Calculation of methyl oleate, methyl palmitate and methyl linoleate yield

$$\% \text{ Methyl oleate yield} = \frac{\text{Mole of methyl oleate}}{\text{Mole of starting oleic acid}} \times 100 \dots\dots(A-1)$$

$$\text{Where ; Mole of starting oleic acid} = \frac{\text{Weight of atarting oleic acid (g)}}{\text{Molecular weight of oleic acid (g/mole)}}$$

$$\text{Mole of methyl oleate} = \text{Mole of methyl oleate for GC analyze} \times \text{sampling factor}$$

$$\text{Mole of methyl oleate for for GC analyze} = \frac{\text{Weight of methyl oleate calculated from standard curve (g)}}{\text{Molecular weight of methyl oleate (g/mole)}}$$

Yield of methyl palmitate and methyl linoleate were calculated similarly to methyl oleate.

สถาบันวิทยบริการ
จุฬาลงกรณ์มหาวิทยาลัย

2. Scanning electron microscopy-energy dispersive X-ray

Table A-1 Sodium contents in fresh and after reaction Na-ETS-10 catalyst

Sample	Na contents (wt%)			
	1	2	3	Average
Na-ETS-10	9.28	8.52	8.66	8.82
Na-ETS-10 after rxn.	7.52	7.40	7.52	7.48

Table A-2 Potassium contents in fresh and after reaction K-ETS-10 catalyst

Sample	K contents (wt%)			
	1	2	3	Average
K-ETS-10	5.55	4.76	5.87	5.39
K-ETS-10 after rxn.	3.67	3.54	3.92	3.71

Table A-3 Rubidium contents in fresh, after reaction and regenerated Rb-ETS-10 catalyst

Sample	Rb contents (wt%)			
	1	2	3	Average
Rb-ETS-10	7.98	7.85	7.79	7.87
Rb-ETS-10 after rxn. #1	5.98	6.09	7.33	6.47
Rb-ETS-10 after rxn. #2	5.47	6.41	4.13	5.34
Regenerated Rb-ETS-10	10.65	11.93	11.48	11.35

Table A-4 Cesium contents in fresh and after reaction Cs-ETS-10 catalyst

Sample	Cs contents (wt%)			
	1	2	3	Average
Cs-ETS-10	11.23	10.78	14.51	12.17
Cs-ETS-10 after rxn.	7.71	7.30	13.39	9.47

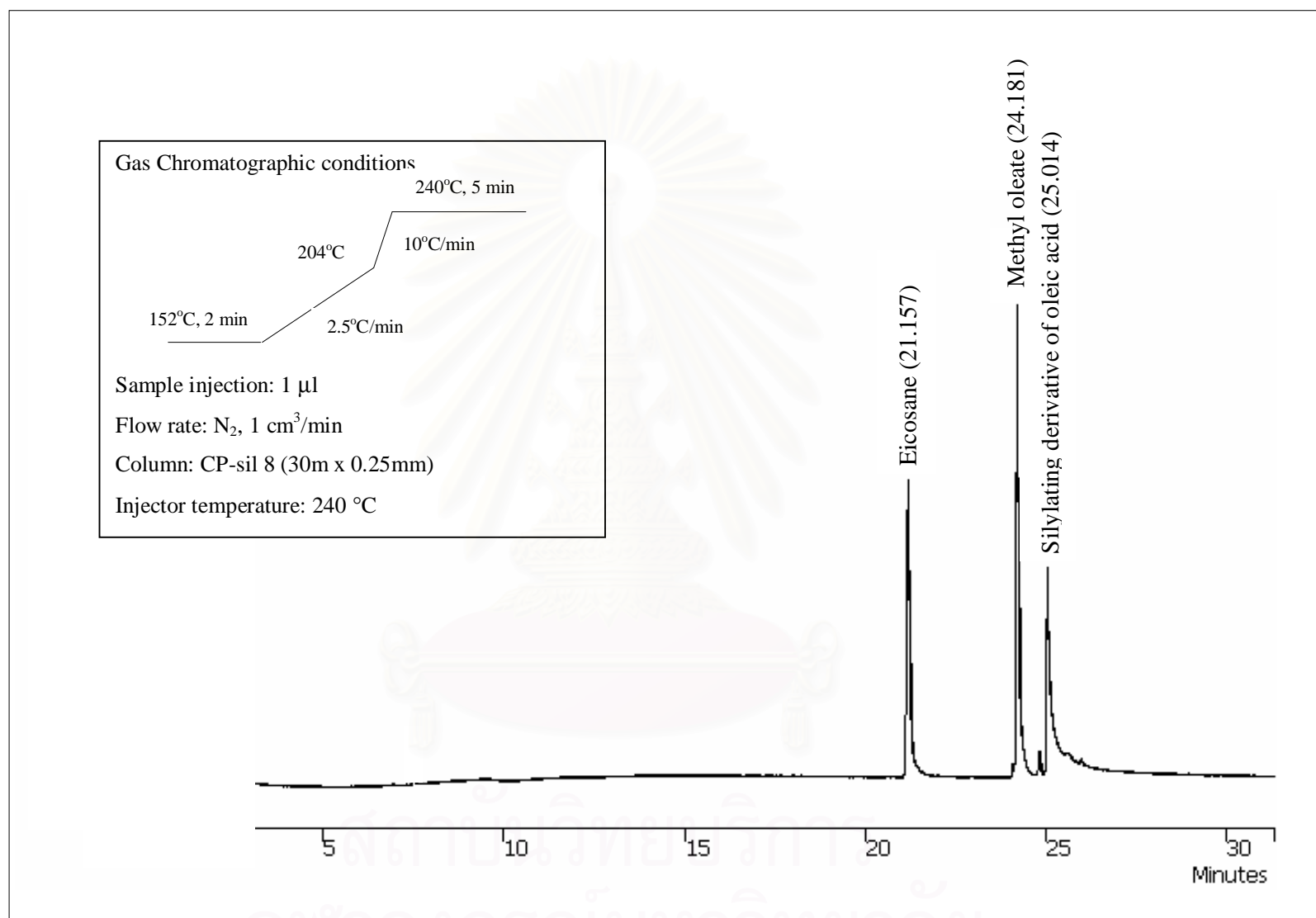


Figure A-2 GC chromatogram of methyl oleate product from esterification reaction

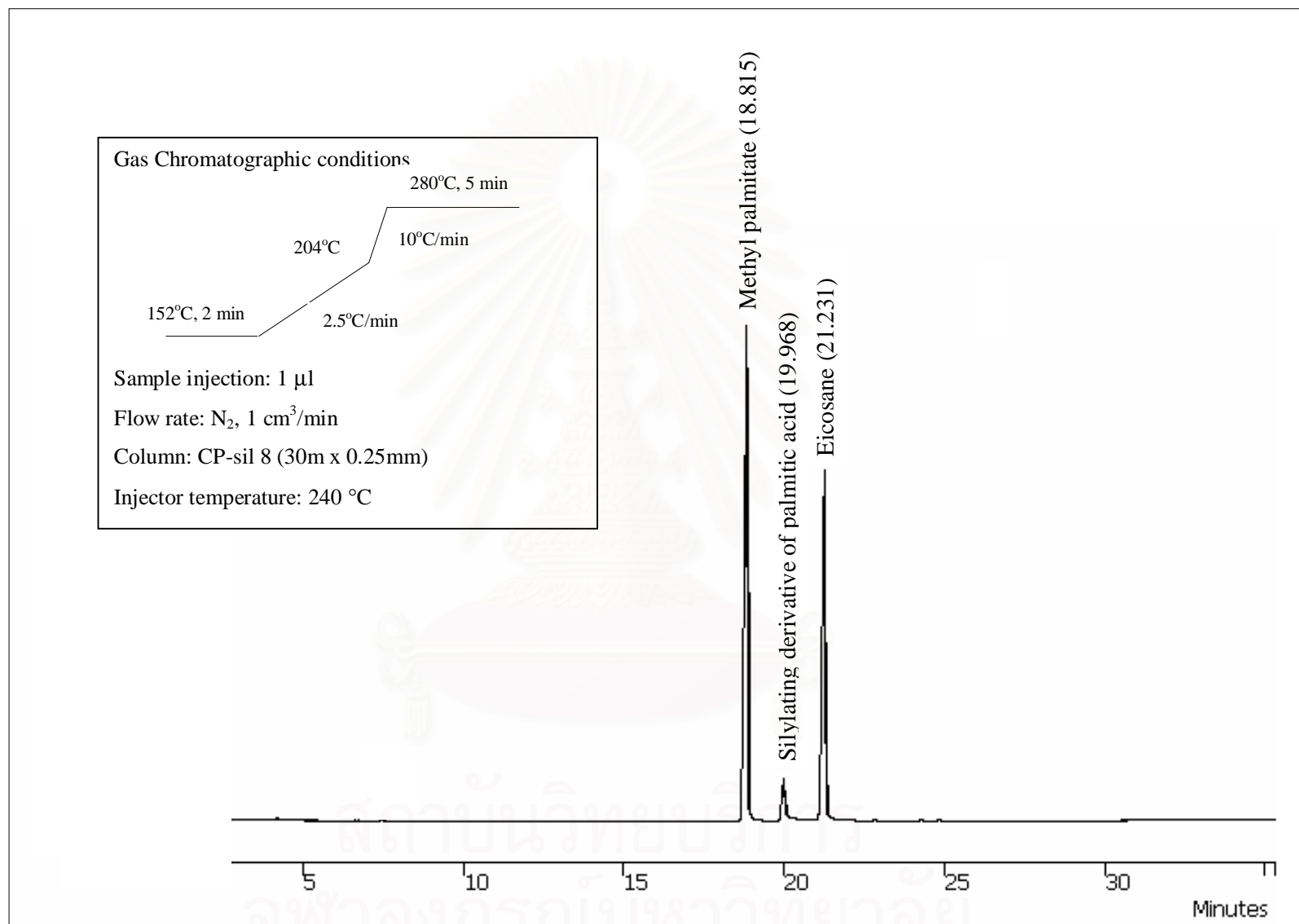


Figure A-3 GC chromatogram of methyl palmitate product from esterification reaction

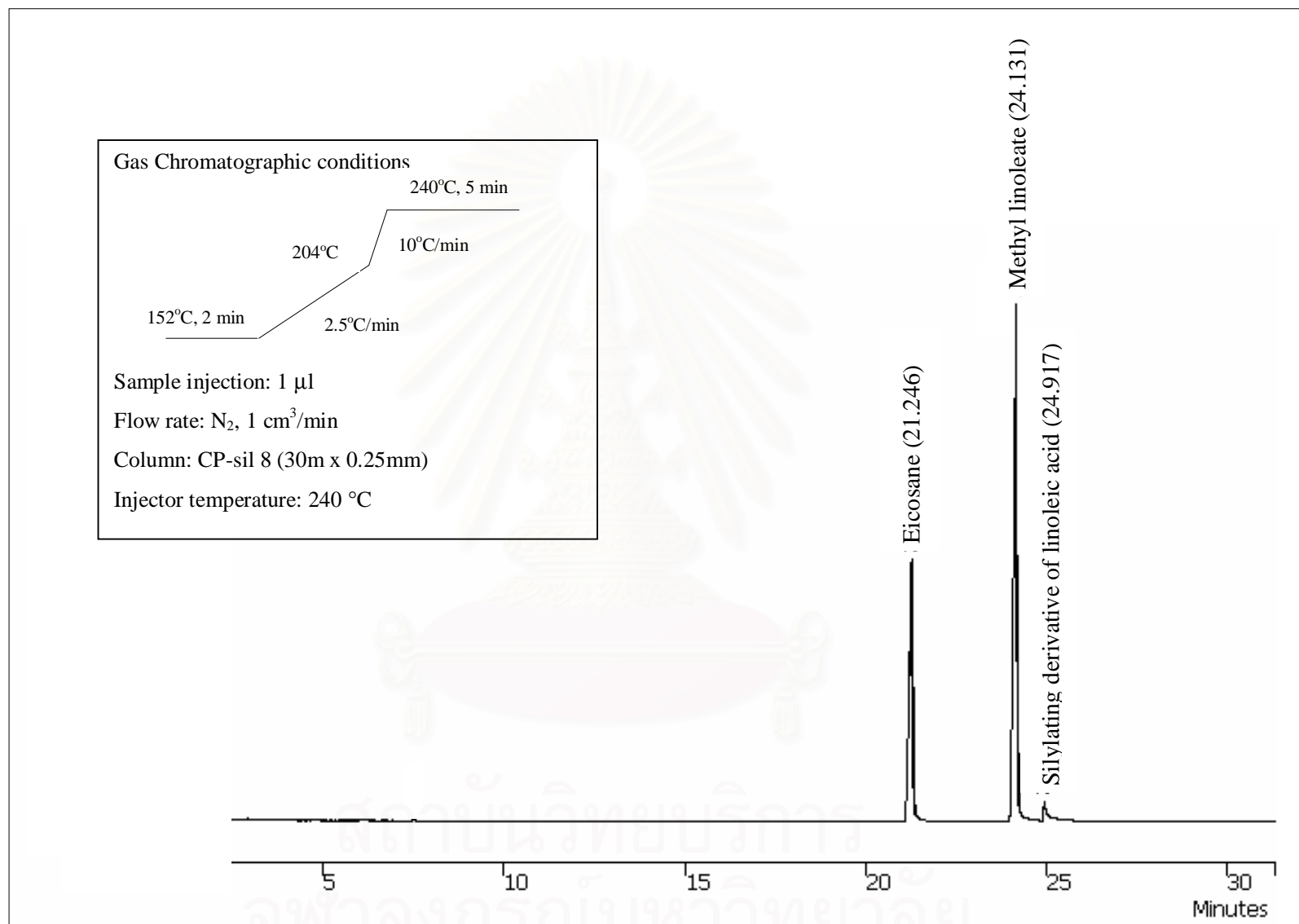


Figure A-4 GC chromatogram of methyl linoleate product from esterification reaction

Table A-5 EU Specification for automotive diesel [60]

Specification	Units	Year 2000 Limits	Possible Future Limits
Cetane number		51 (min)	55 (min)
Cetane index		No spec	52 (min)
Density@15°C	g/cm ³	0.845 (max)	0.84
Distillation			
90% boiling point	°F	No spec	608 (max)
95% boiling point	°F	680 (max)	644 (max)
Final boiling point	°F	No spec	662 (max)
90% boiling point	°C	No spec	320 (max)
95% boiling point	°C	360 (max)	340 (max)
Final boiling point	°C	No spec	350 (max)
Polyaromatic hydrocarbons (PAH)	wt%	11 (max)	2 (max)
Total aromatic	wt%	No spec	15 (max)
Sulfur	wppm	350 (max)*	10 (max)

* As discussed elsewhere, diesel sulfur will be limited to 50 wppm in 2005

สถาบันวิทยบริการ
จุฬาลงกรณ์มหาวิทยาลัย

Table A-6 Chemical and physical properties of diesel and biodiesel [61]

Properties	MOC SPEC.	Diesel	Biodiesel
Specific gravity @ 15.6/15.6 °C	0.81-0.87	0.8302	0.8342
Cetane index	Min. 47	58.2	57.2
Viscosity @ 40 °C cSt	1.8-4.1	3.34	3.725
Pour point °C	Max. 10	0	-3
Sulfur content % wt.	Max 0.05	0.037	0.032
Copper strip corrosion (number)	Max. 1	1a	1a
Carbon residue % wt.	Max 0.05	< 0.001	< 0.001
Water and sediment % vol.	Max 0.05	Traces	Traces
Ash % wt.	Max 0.01	0.001	0.001
Flash point °C	Min 52	69	70
Distillation	-	-	-
90% recovered °C	Max. 357	352.0	356.2
Colour	Max. 40	0.5	0.5
Lubricity by HFRR	Max.460	465	204
Gross heating value (J/g)	-	45906	45387
TAN (mgKOH/g)	-	-	-
Total insoluble mg/100 ml	-	-	-
Total aromatics g/100 ml	-	23.2	22.7

Table A-7 Properties of biodiesel from different oils [62]

Vegetable oil methyl esters (biodiesel)	Cetane No.	Kinematic Viscosity at 38°C (mm ² /s)	Lower heating value (MJ/kg)	Cloud point (°C)	Pour point (°C)	Flash point (°C)	Density (kg/l)
Peanut	4.9	54	33.6	5	-	176	0.883
Soya bean	4.5	45	33.5	1	-7	178	0.885
Babassu	3.6	63	31.8	4	-	127	0.875
Palm	5.7	62	33.5	13	-	164	0.880
Sunflower	4.6	49	33.5	1	-	183	0.860
Tallow	-	-	-	12	9	96	-
Diesel	3.06	50	43.8	-	-19	76	0.855
20% biodiesel blend	3.2	51	43.2	-	-16	128	0.859

VITAE

Miss Sirima Jeenpatiphat was born on May 12, 1983 in Bangkok, Thailand. She graduated with Bachelor's Degree in General Science from Faculty of Liberal Arts & Science, Kasetsart University in 2005. She continued her study in Petrochemistry and Polymer Science Program, Faculty of Science, Chulalongkorn University in 2006. During her graduate study, she also received a research scholarship from PTT Public Company Limited. She has completed her study leading to a Master of Science Degree in Petrochemistry and Polymer Science Program in 2007.

Her present in 1/116, Nontnaburi 1 Rd., Suanyai, Nonthaburi, Thailand, 11000, Tel 08-1776-5875.



สถาบันวิทยบริการ
จุฬาลงกรณ์มหาวิทยาลัย